

X-ray absorption spectroscopy



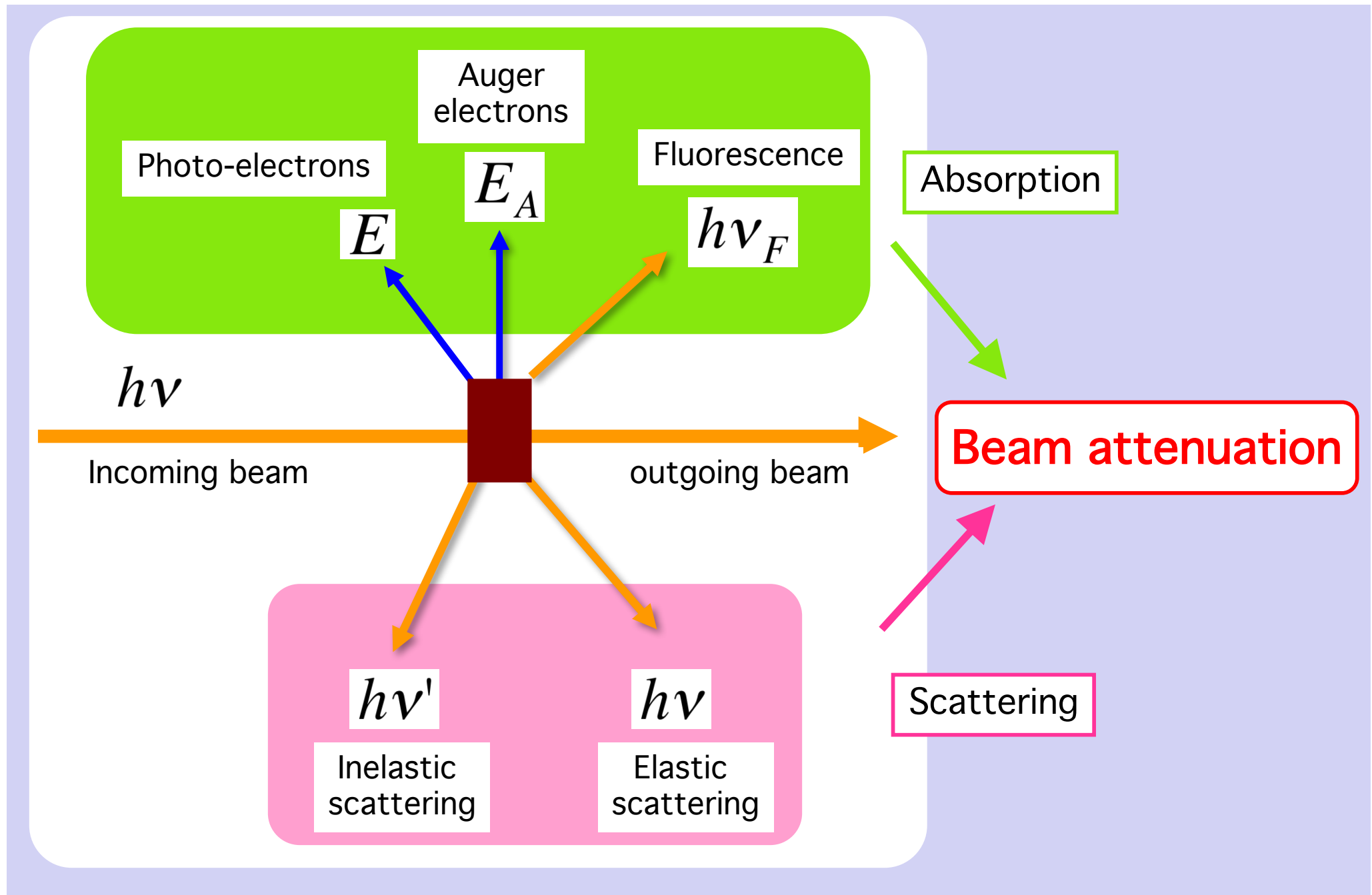
Paolo Fornasini

University of Trento
Department of Physics

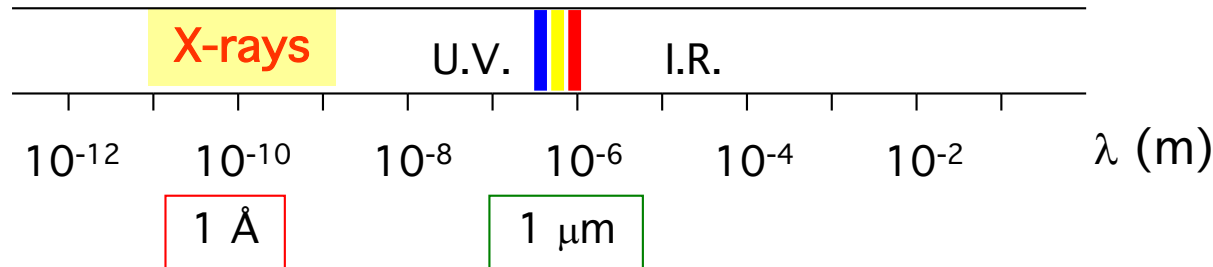
paolo.fornasini@unitn.it

http://alpha.science.unitn.it/~rx/raggi_x/fornasini/paolo_home.html

Attenuation mechanisms for X-rays

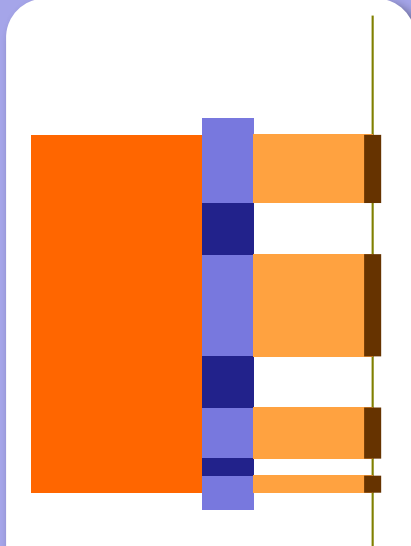


Basic X-ray techniques

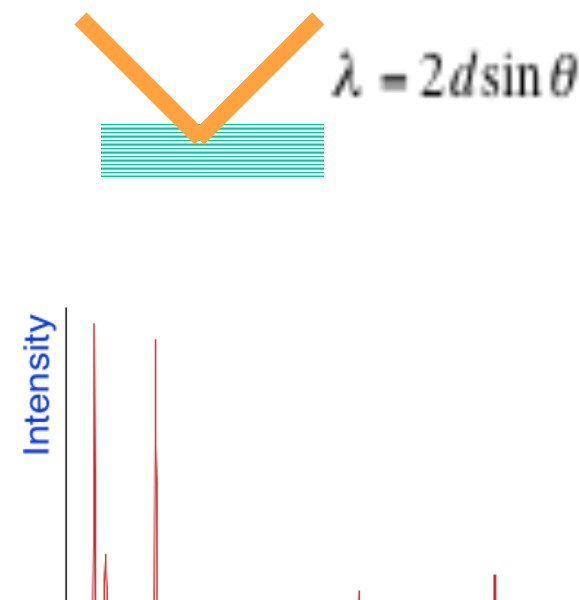


$$E[\text{keV}] = \frac{12.4}{\lambda[\text{\AA}]}$$

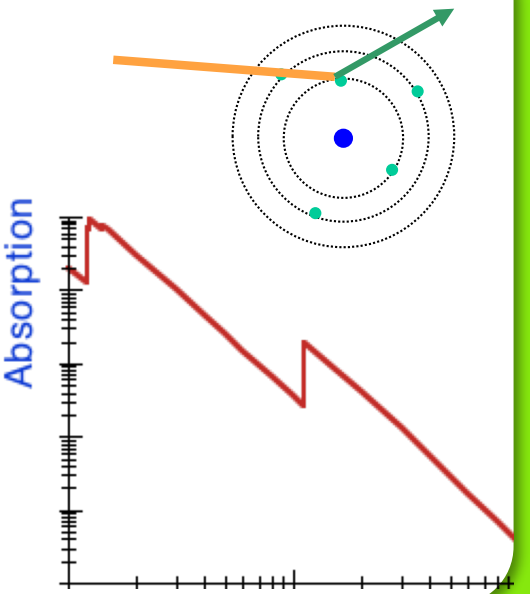
Imaging



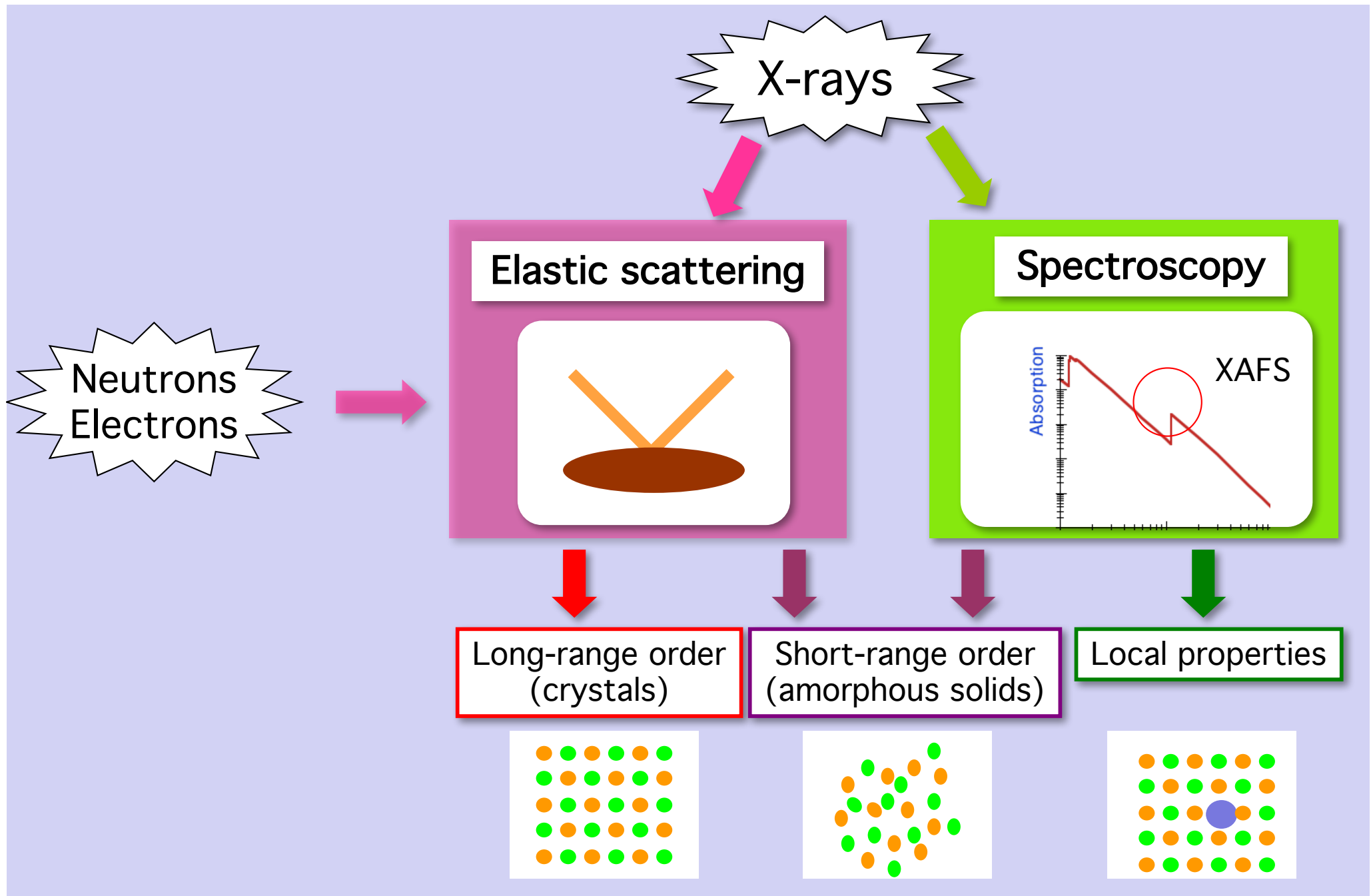
Scattering



Spectroscopy



Structural techniques



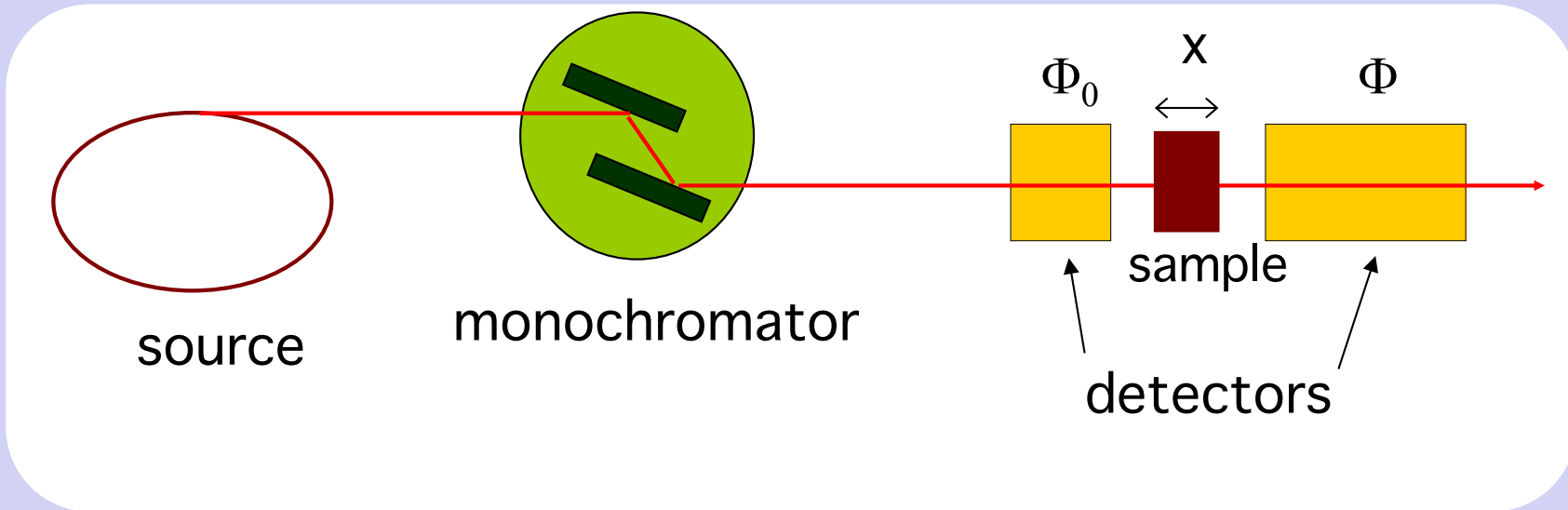
Summary

- X-rays absorption – phenomenology
- X-rays absorption - theory
- EXAFS: theoretical background
- EXAFS experiments
- EXAFS: data analysis, examples

X-rays absorption - phenomenology

The attenuation coefficient

The attenuation depends on X-ray energy and on sample composition



Exponential attenuation $\Phi = \Phi_0 \exp [-\mu(\omega) x]$

Attenuation coefficient

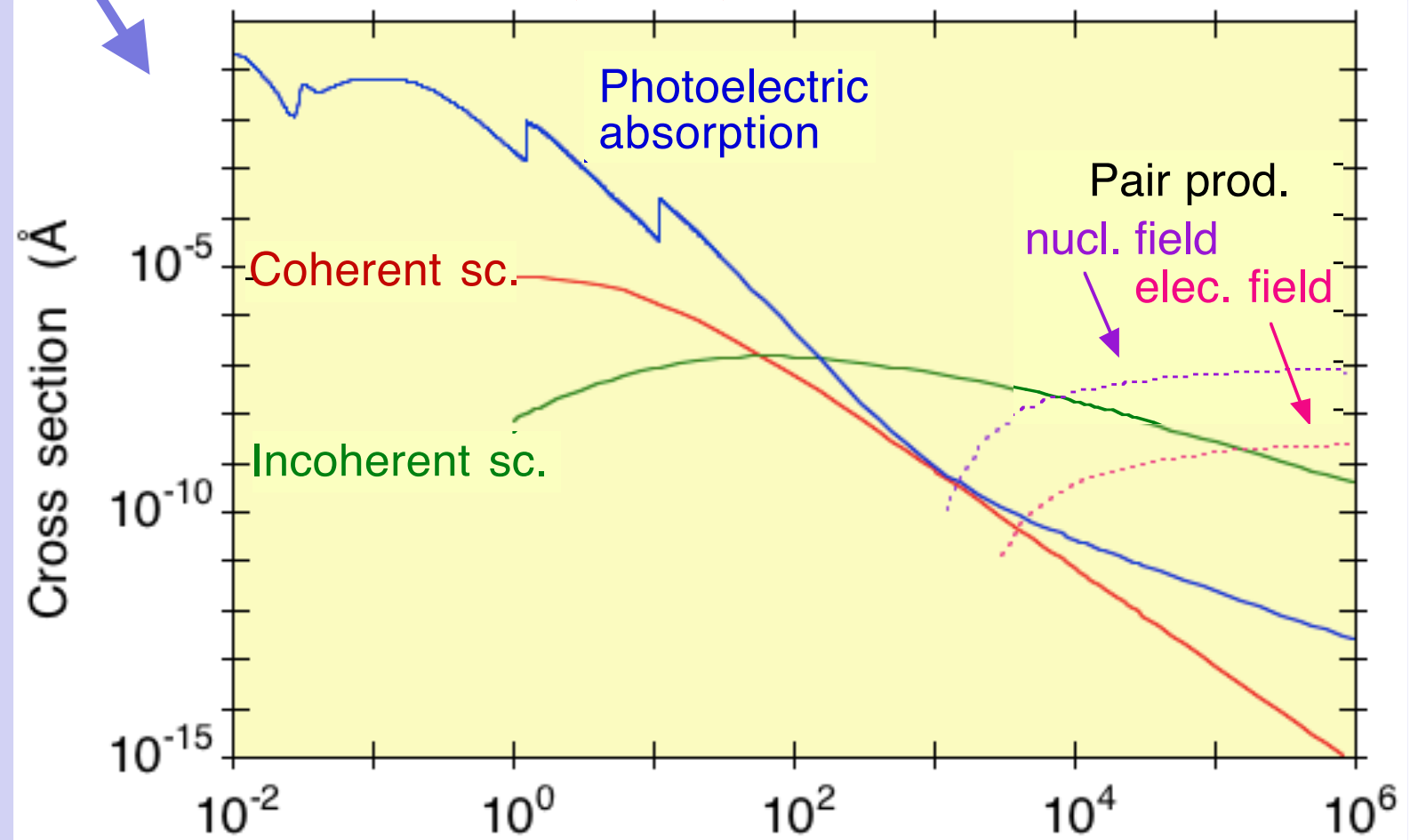
$$\mu(\omega) = \frac{1}{x} \ln \frac{\Phi_0}{\Phi}$$

Atomic cross sections – different contributions

$$\mu(\omega) = \frac{N_A \rho}{A} \sigma_a(\omega)$$

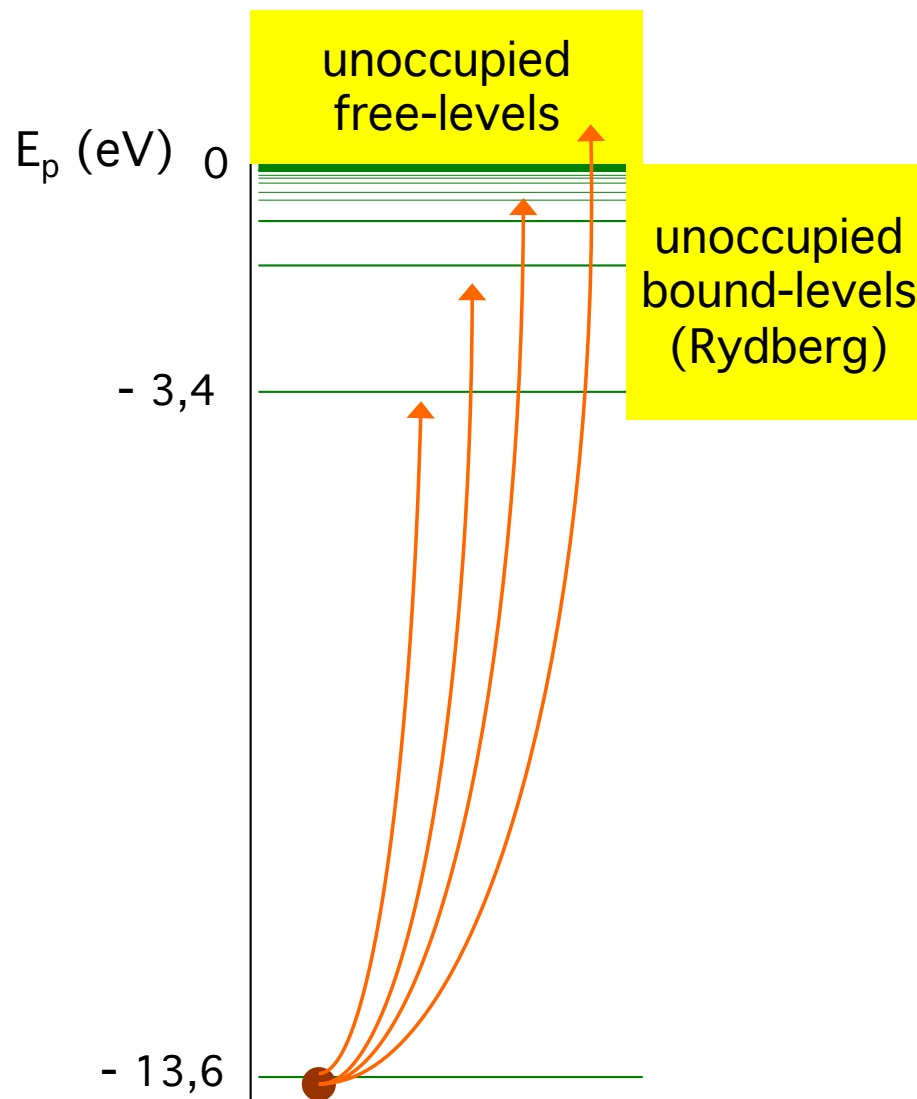
Range of interest

ρ = density
 N_A = Avogardo nr
 A = atomic mass

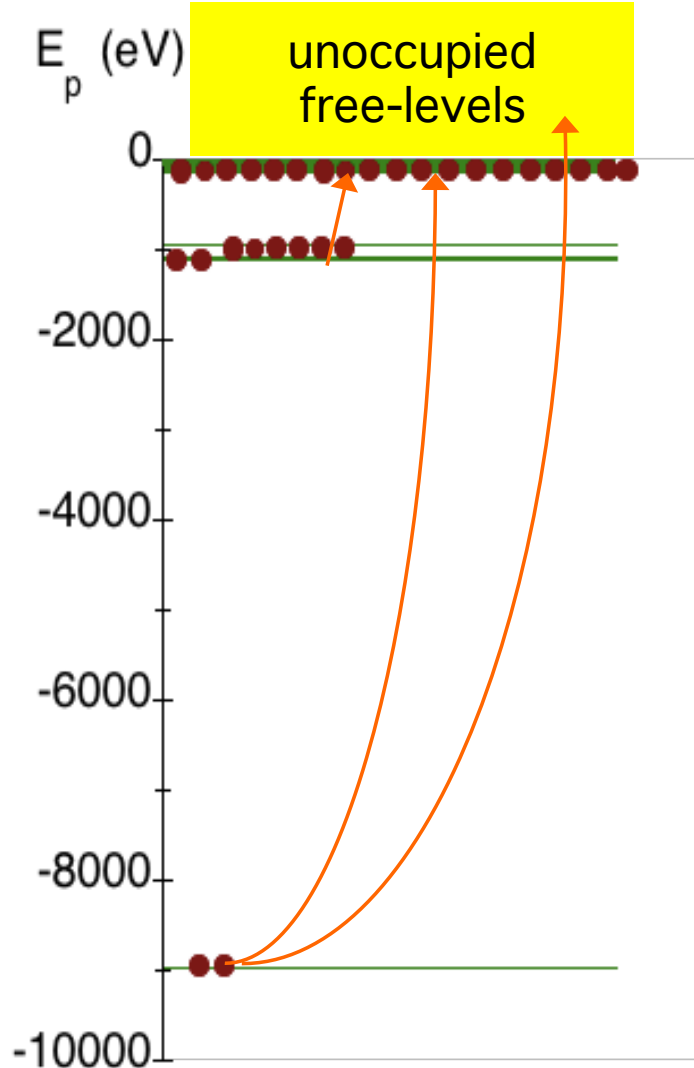


Excitation and ionization

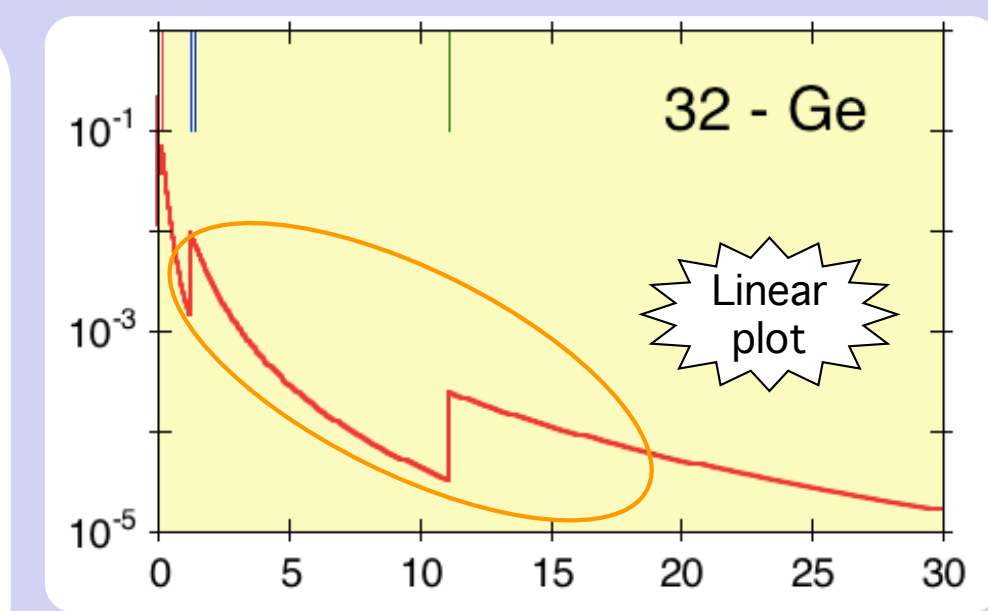
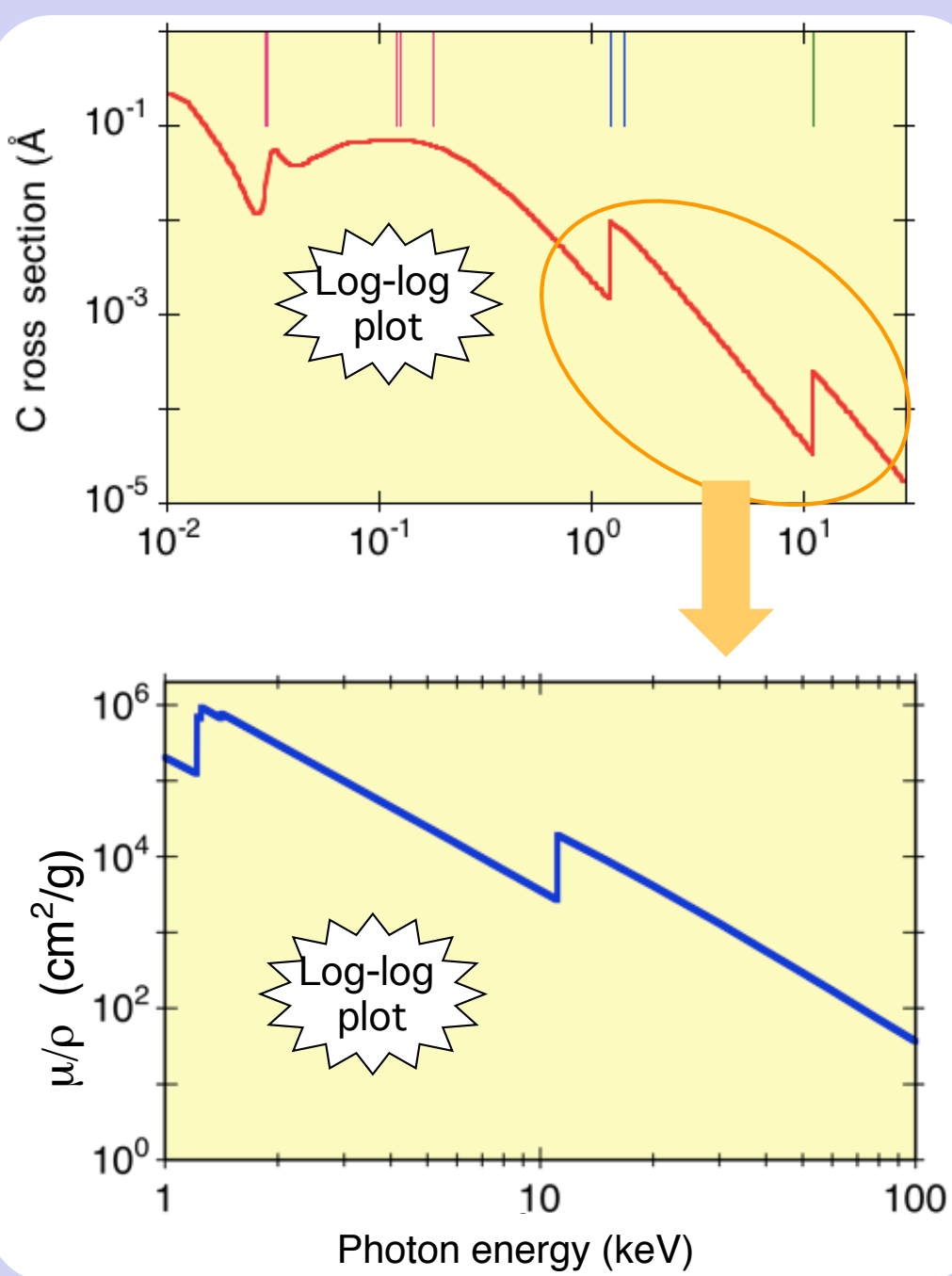
1- Hydrogen



29 - Copper

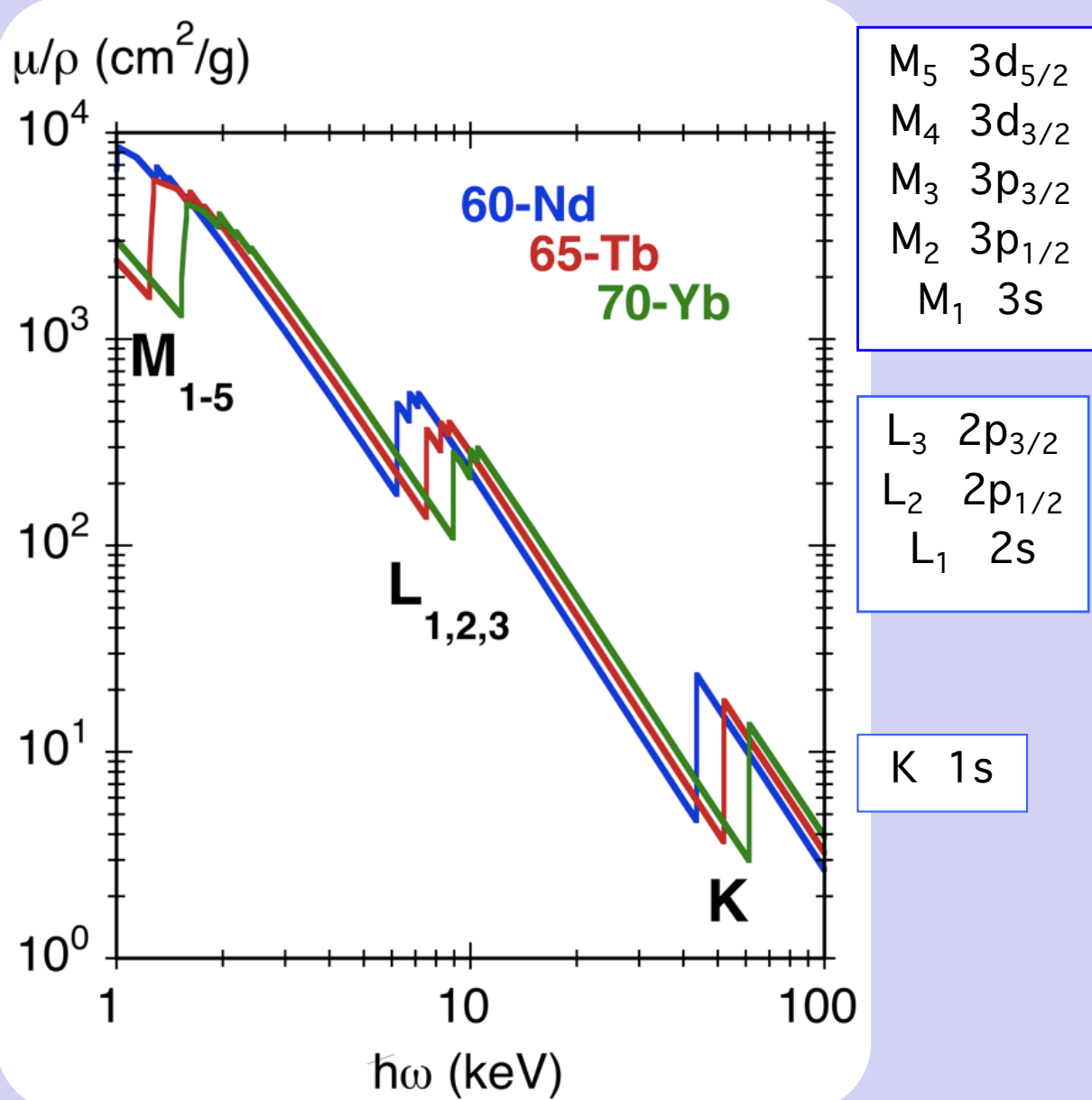


X-ray absorption



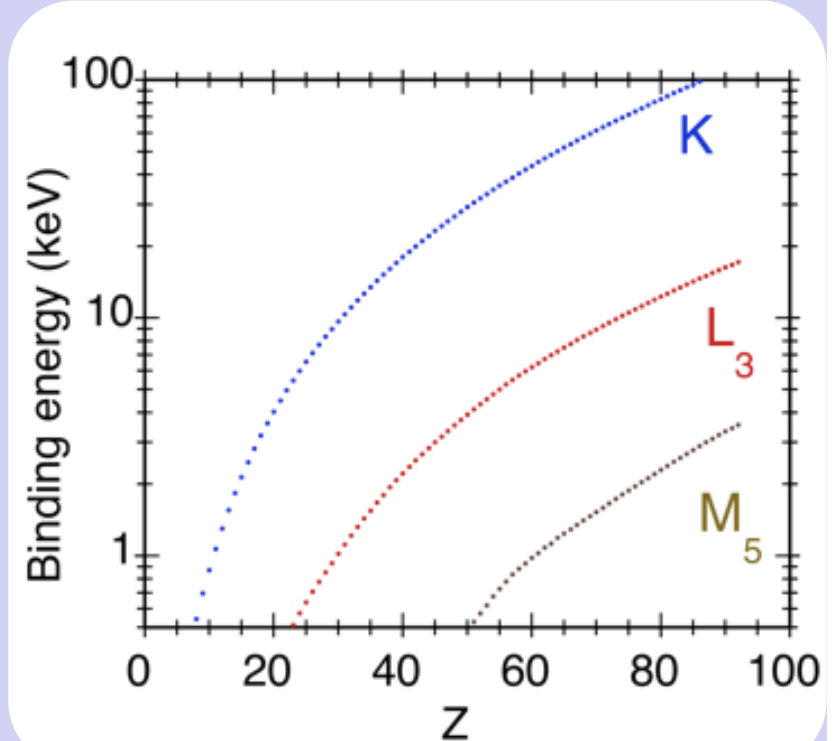
$$\mu(\hbar\omega) \simeq \frac{Z^4}{(\hbar\omega)^3} + \text{edges}$$

X-rays absorption edges

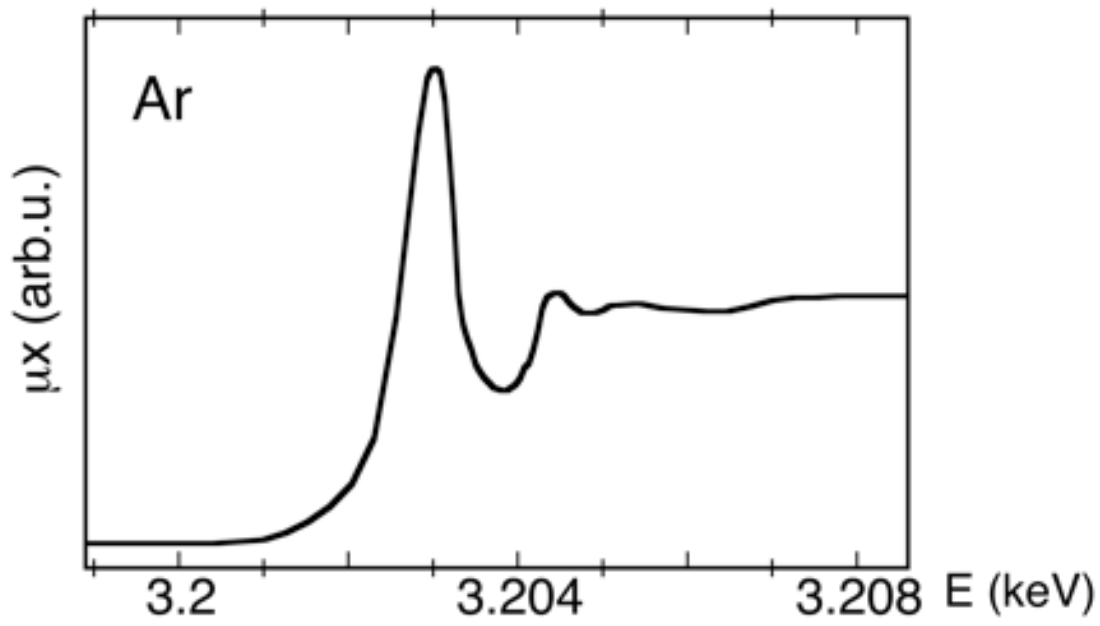


Nomenclature

Z - dependence



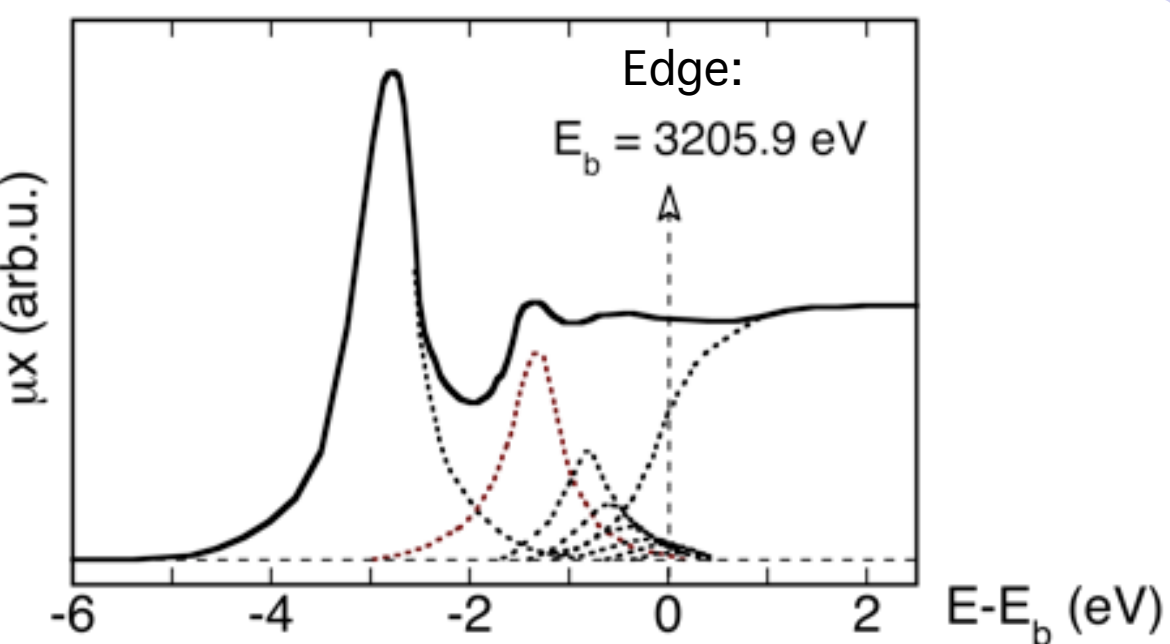
Atomic gases: edge fine structure



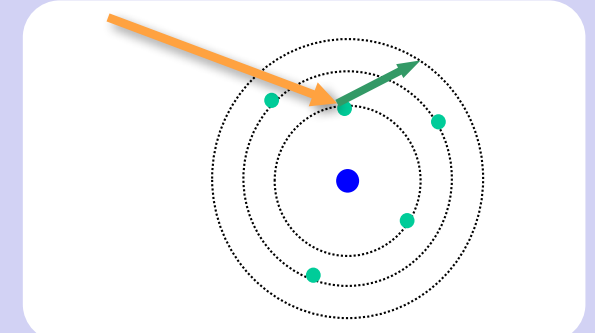
Experiment

L. G. Parratt,
Phys. Rev. 56, 295 (1939)

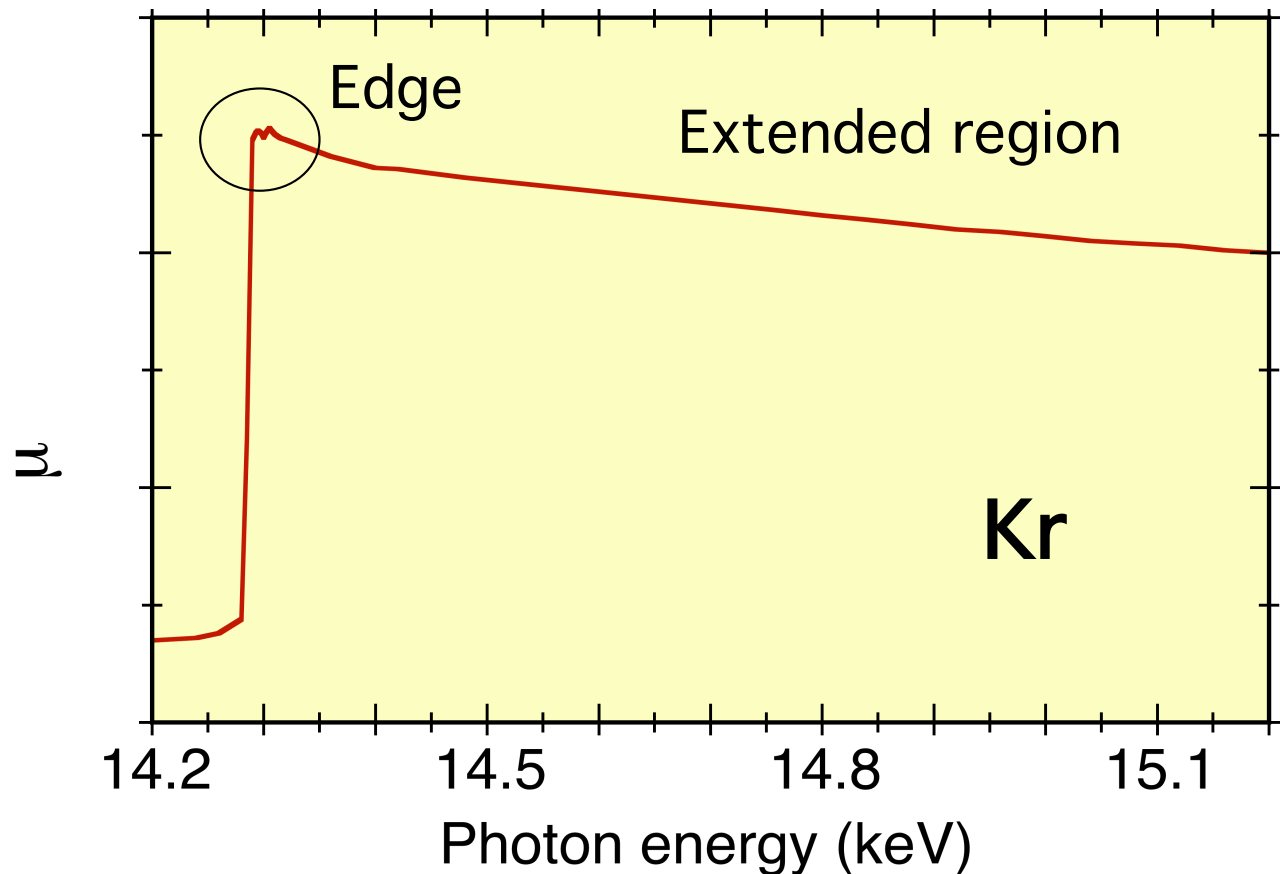
Energy resolution ~ 0.6 eV



Interpretation:
- Rydberg levels
- edge to continuum



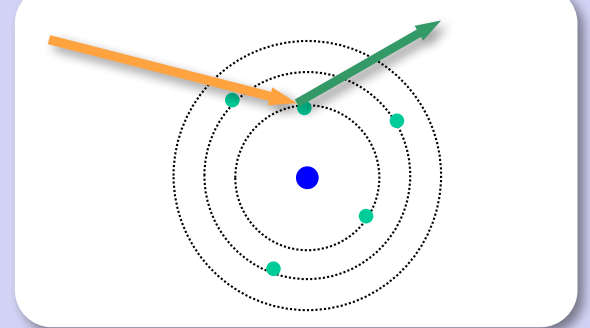
Atomic gases: smooth absorption coefficient



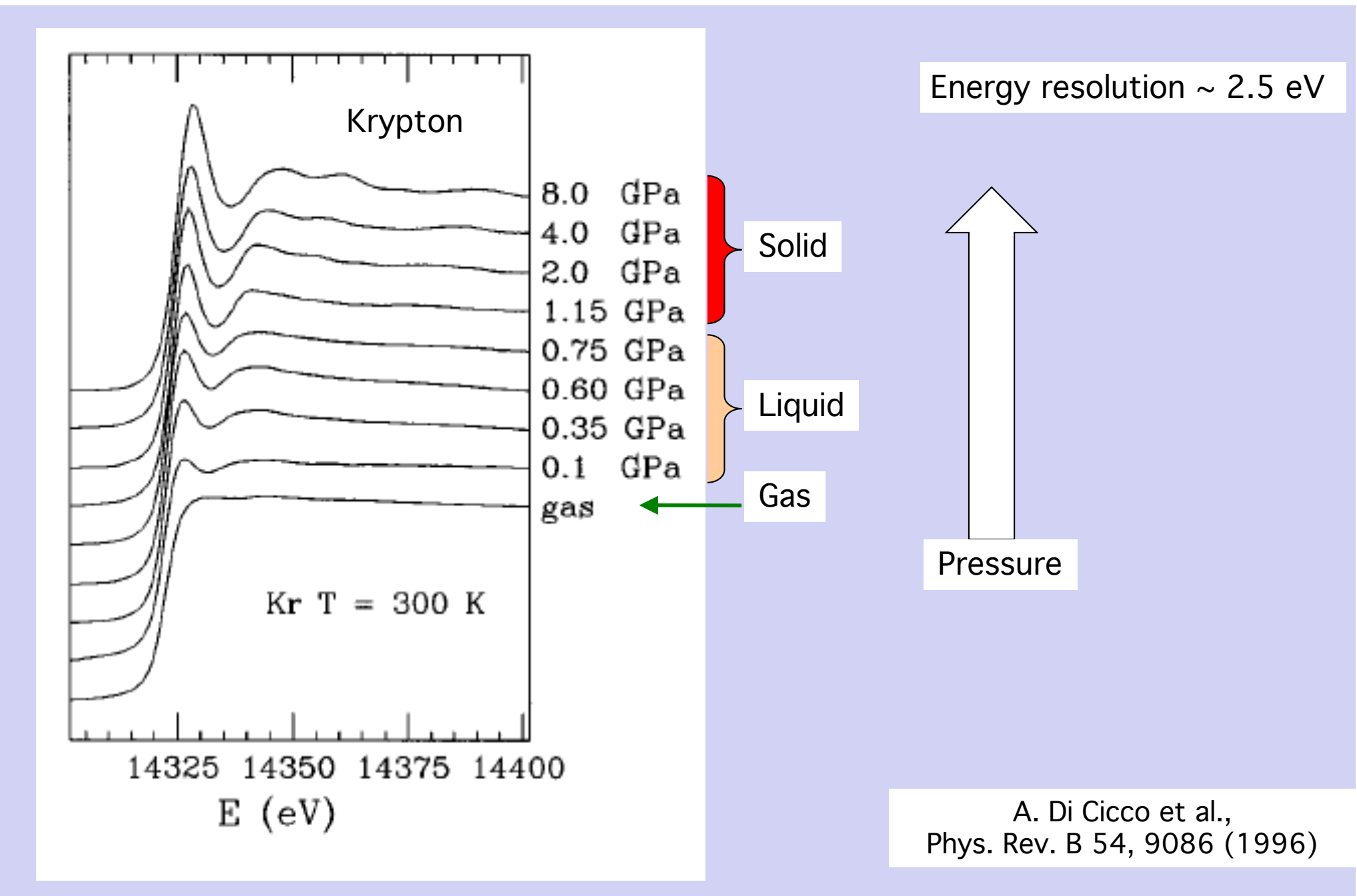
Core level



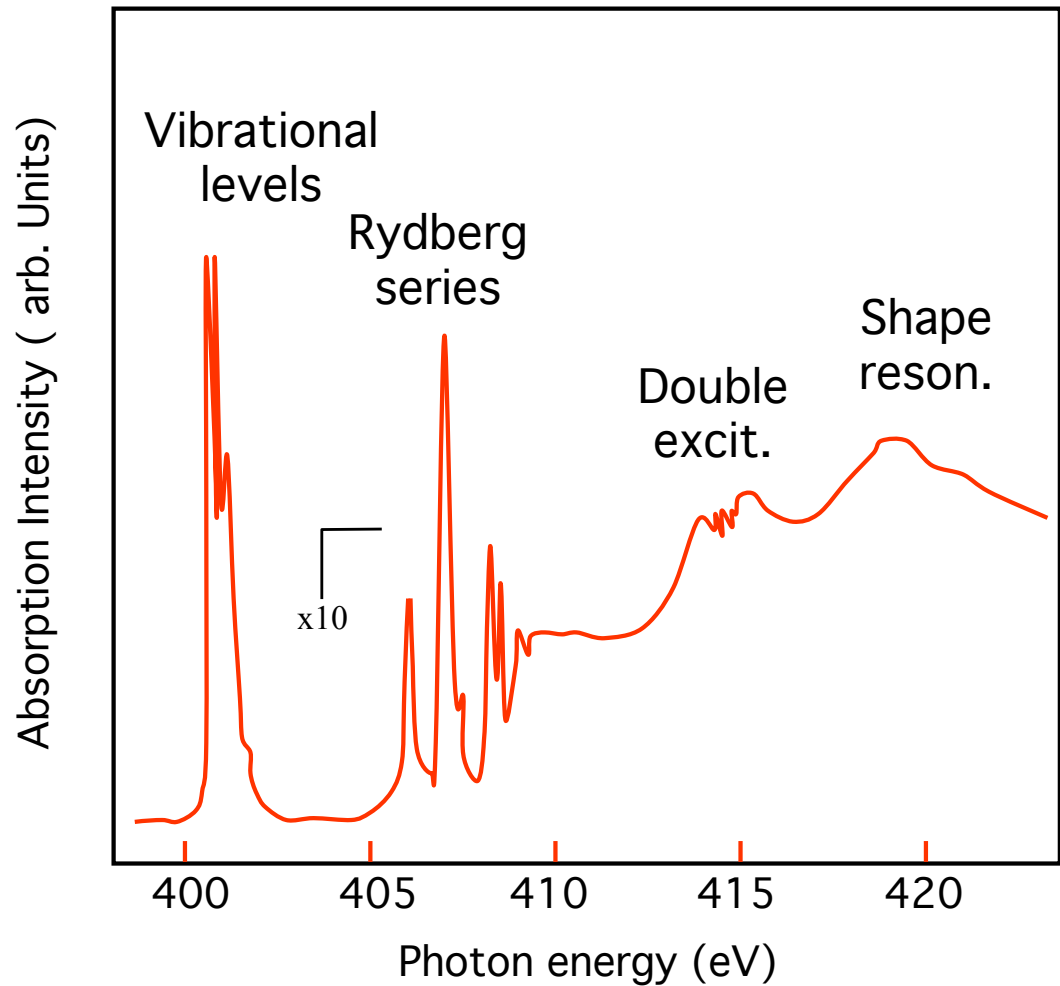
- Unoccupied bound levels
(poor resolution)
- Continuum (smooth)



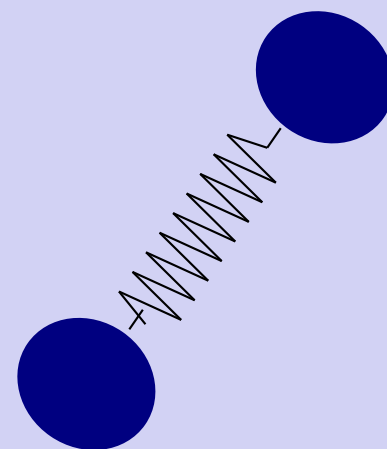
Atomic gases and condensed states



Molecular gases: Fine structure



Gas-phase N_2
K-edge



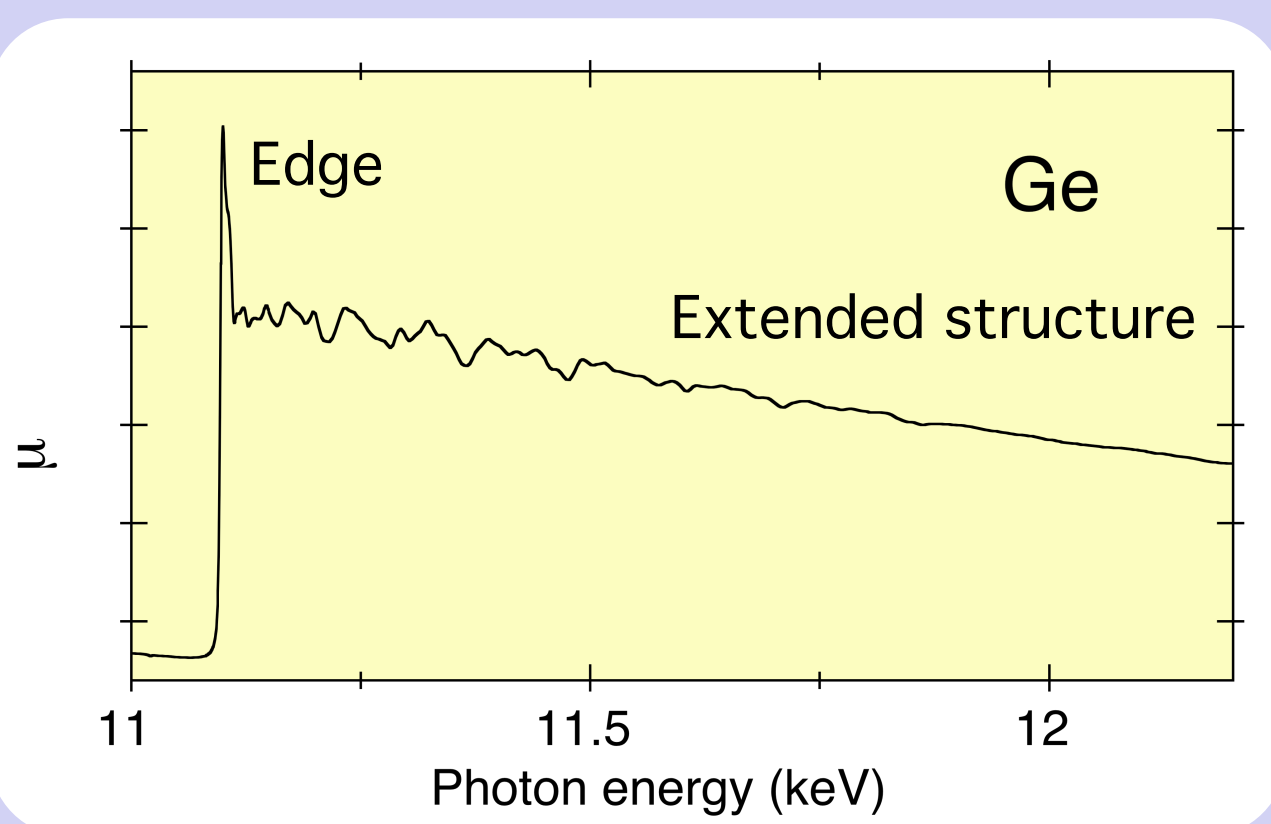
Core level



Unoccupied bound levels
Unoccupied free levels

C.T. Chen and F. Sette,
Phys. Rev. A 40 (1989)

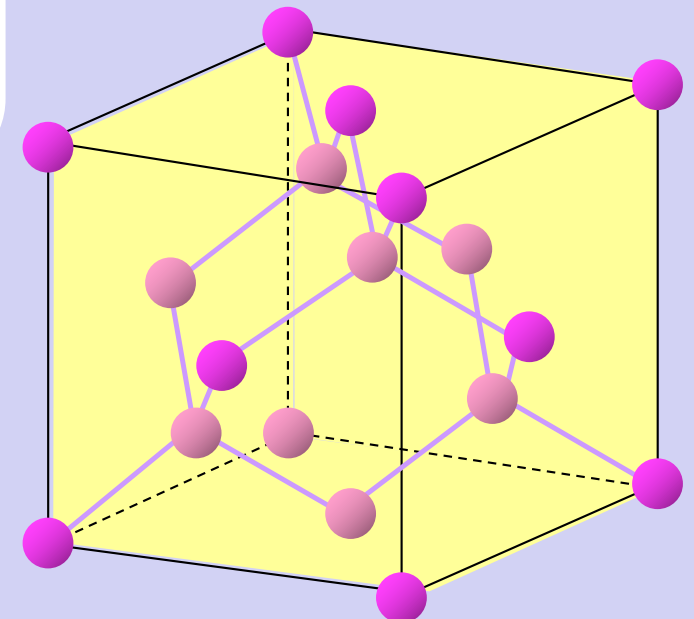
Condensed systems: Fine structure



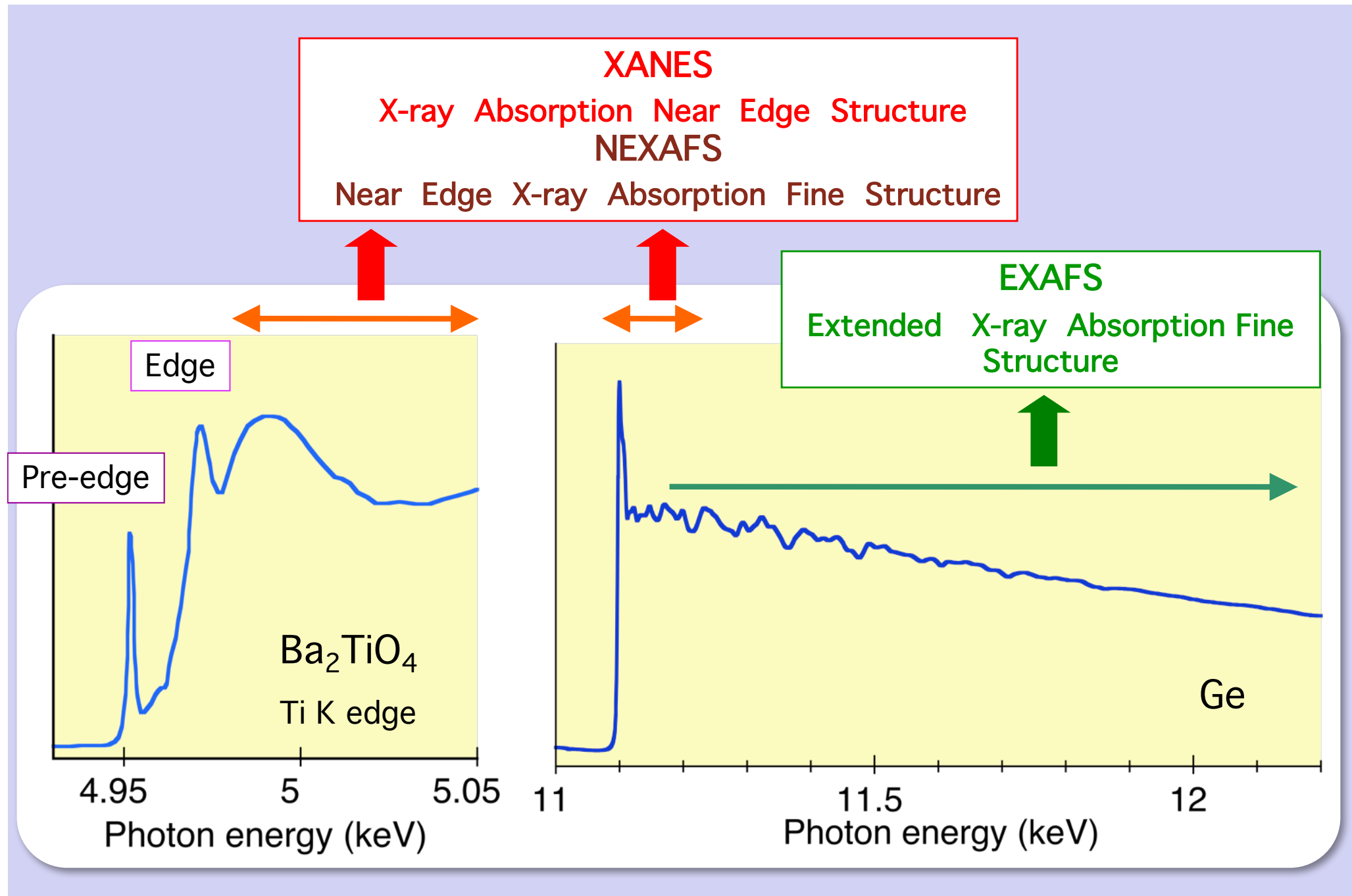
Core level



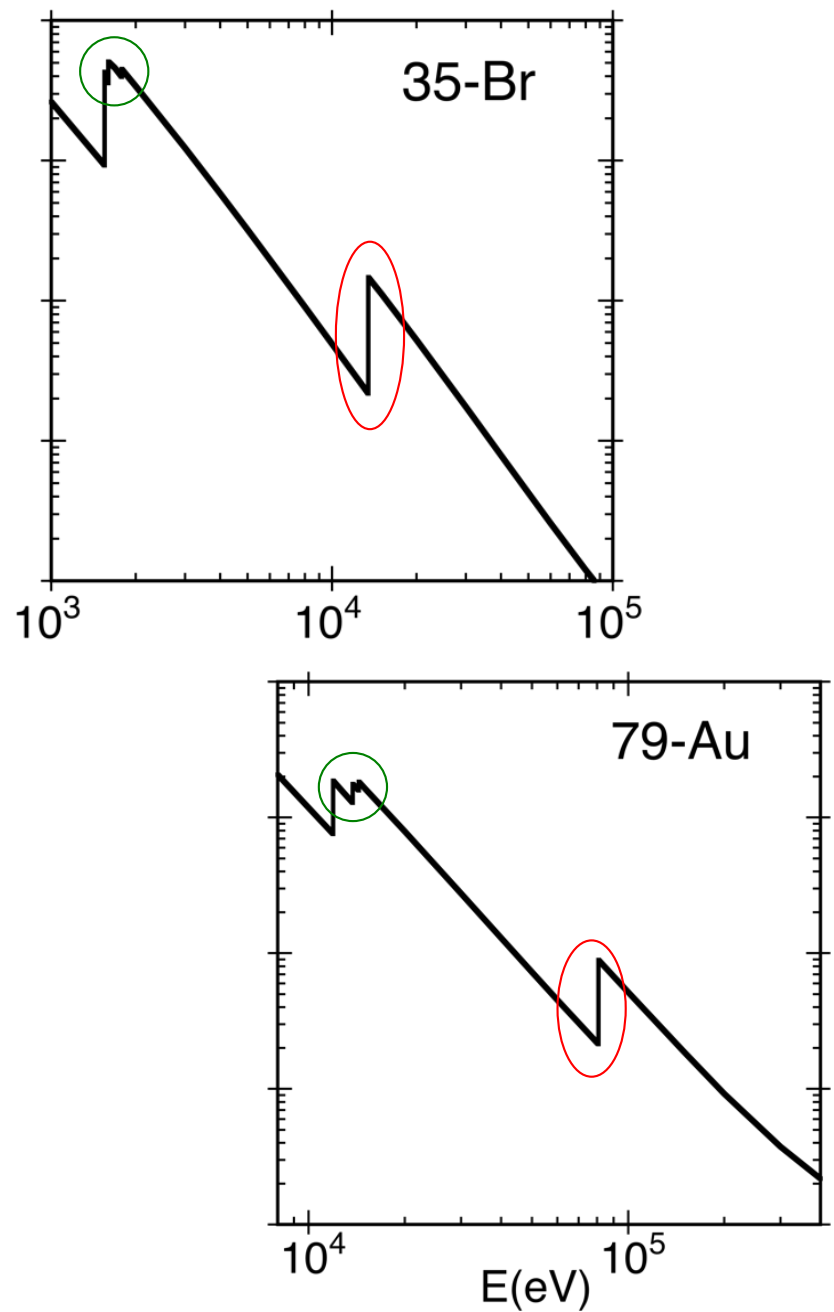
Unoccupied bound levels
Unoccupied free levels



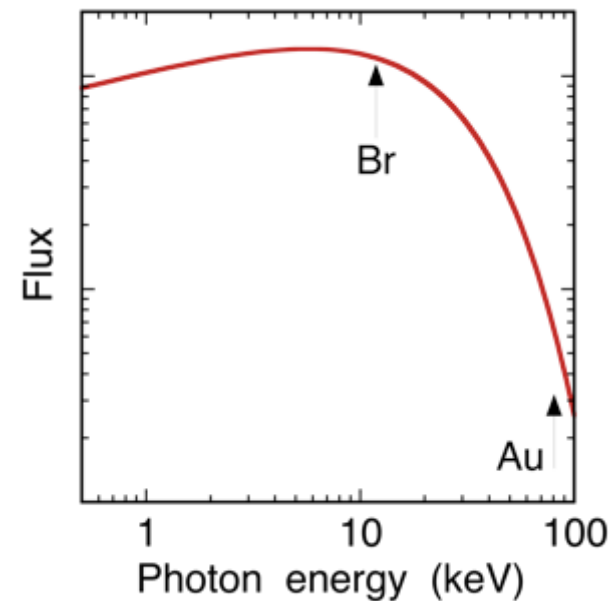
XAFS: Nomenclature



L edges .vs. K edge



S.R. flux at the K edge



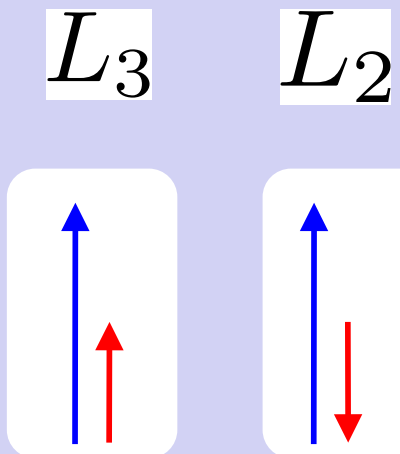
Energy resolution at the K edge

$^{35}\text{-Br}$ $\Delta E \sim 2.5$ eV

$^{79}\text{-Au}$ $\Delta E \sim 52$ eV

K edges unsuited for heavy elements
L edges ?

L_2 and L_3 edges: Spin-orbit splitting



Spin-orbit splitting:

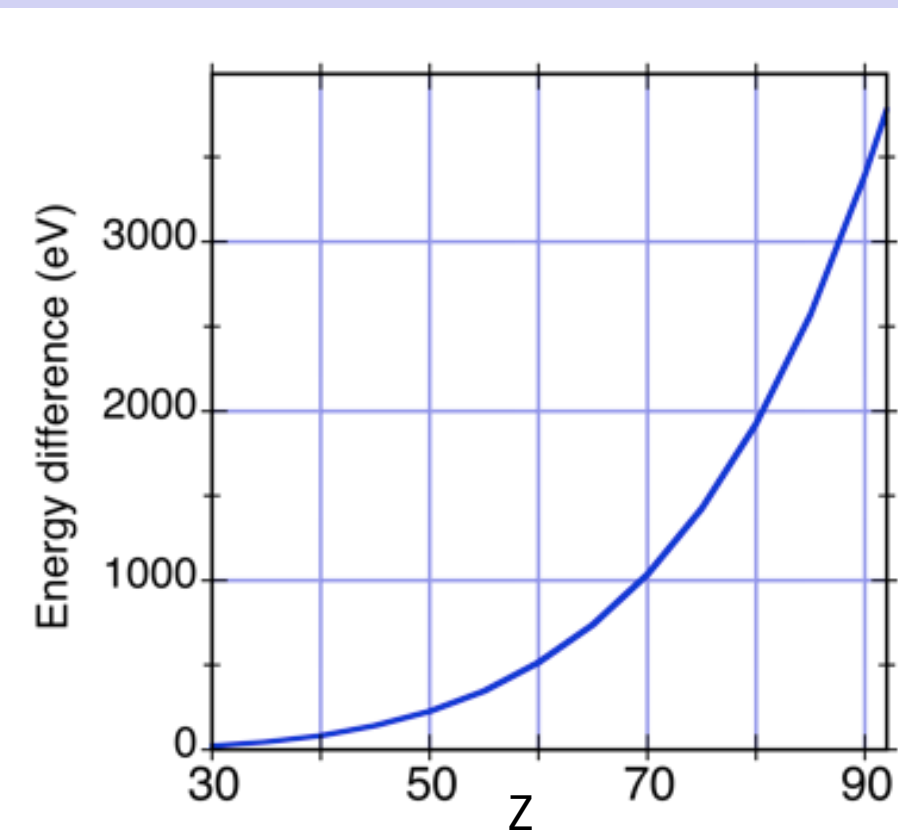
$$\Delta E_{SL} = \frac{|E_{n\ell}| Z^2 \alpha^2}{n\ell(\ell+1)} \simeq 5.32 \times 10^{-5} \frac{|E_{n\ell}| Z^2}{n\ell(\ell+1)}$$

$$\alpha = \frac{1}{4\pi\epsilon_0} \frac{e^2}{\hbar c} = \frac{1}{137}$$

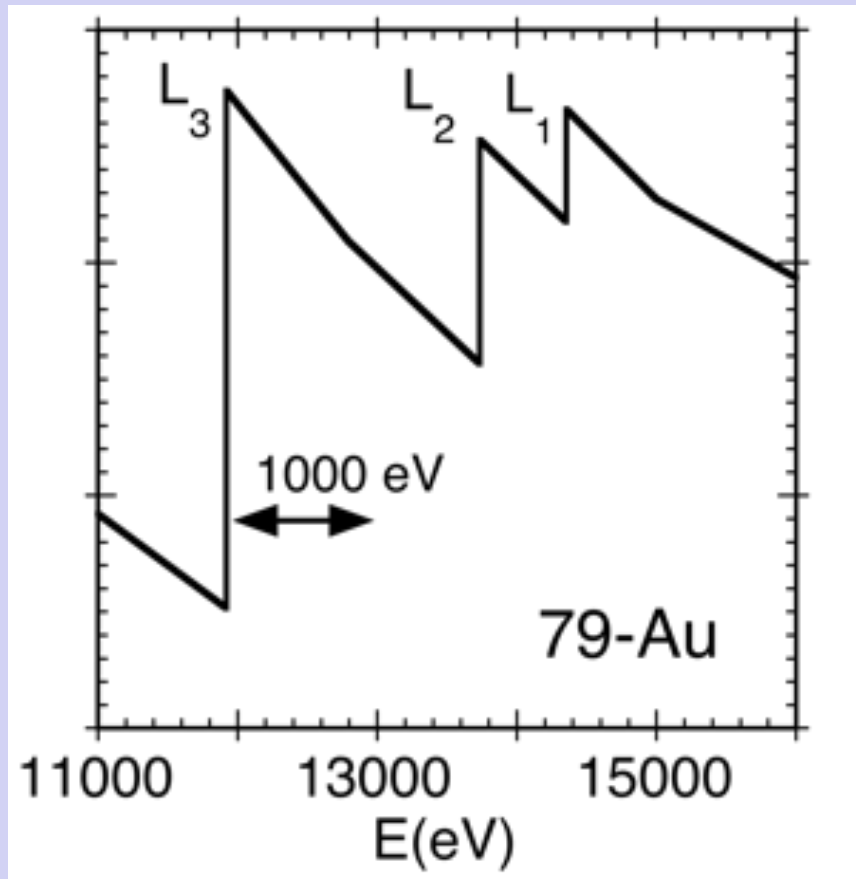
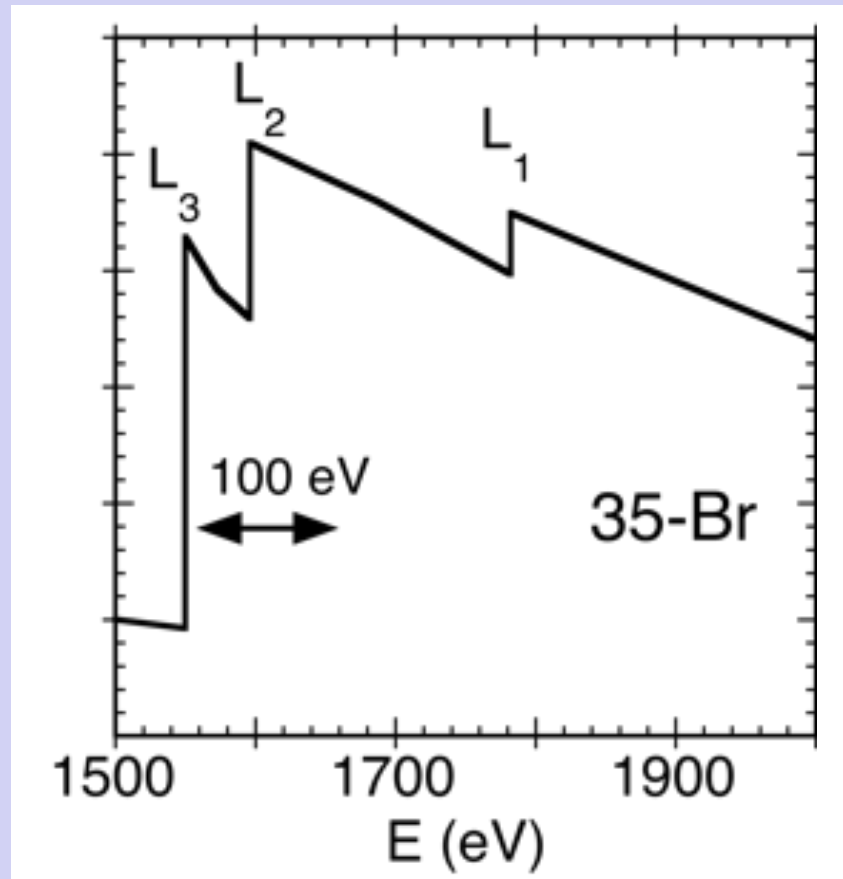
$\ell_z=1$
 $s_z=1/2$
 $2p_{3/2}$

$\ell_z=1$
 $s_z=-1/2$
 $2p_{1/2}$

$$\Delta E_{L_2 - L_3} \simeq 1.33 \times 10^{-5} |E_{n\ell}| Z^2$$



L edges XAFS



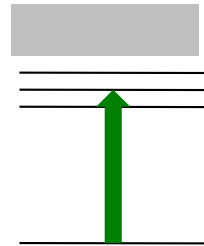
Edge & XANES: all L edges

EXAFS: L_2 and L_1 edges EXAFS polluted by L_3 EXAFS
 L_3 EXAFS sufficiently extended only for heavy elements

Fine Structure: Molecules and Condensed systems

$h\nu \leq \text{binding energy}$

Unoccupied
free levels

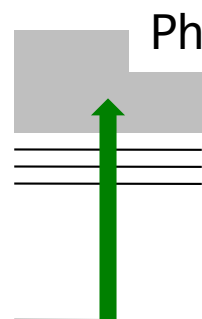


Core level

Pre-edge structures
Edge structures

$h\nu > \text{binding energy}$

Continuum
levels



Core level

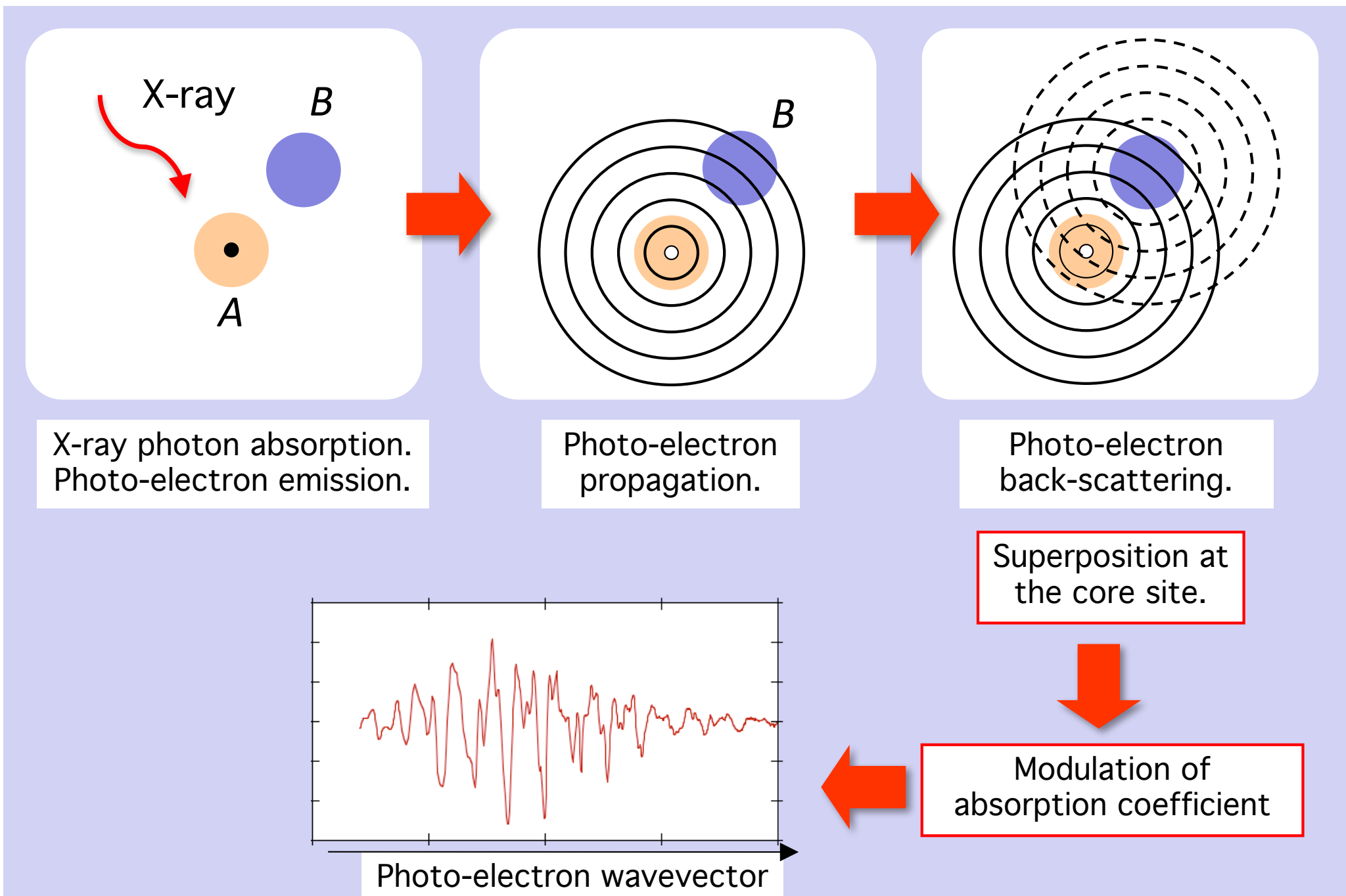
Back-scattering
from
neighbouring atoms

Single scattering
Multiple scattering

EXAFS
XANES

EXAFS: phenomenological mechanism

Paolo
Fornasini
Univ. Trento



Lectures on XAFS

EXAFS

- introduction
- basic theory
- experiments
- data analysis

P. Fornasini

XANES

M. Benfatto
C. Meneghini

Data analysis

C. Meneghini
M. Merlini

Applications

XAFS in nanostructures & materials science
F. Boscherini

SR & Matter in extreme conditions
G. Aquilanti

SR & Environmental science
P. Lattanzi

SR & Earth sciences
G. Artioli

SR & Chemistry
A. Martorana

SR & catalysts
C. Lamberti

X-rays absorption - theory

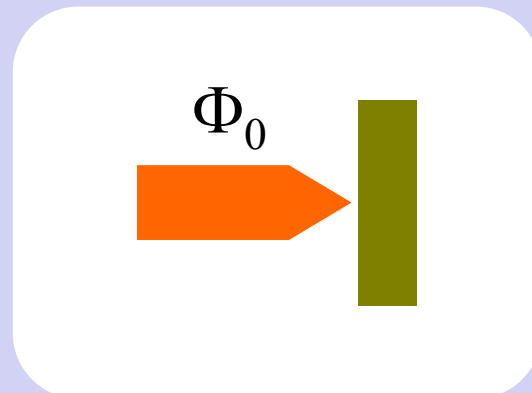
Photon flux

Vector potential

$$\begin{aligned}\vec{A}(\vec{r}) &= A_0 \hat{\eta} \cos(\vec{k} \cdot \vec{r} - \omega t) \\ &= A_0 \hat{\eta} \operatorname{Re} \left\{ e^{i(\vec{k} \cdot \vec{r} - \omega t)} \right\}\end{aligned}$$

Energy flux

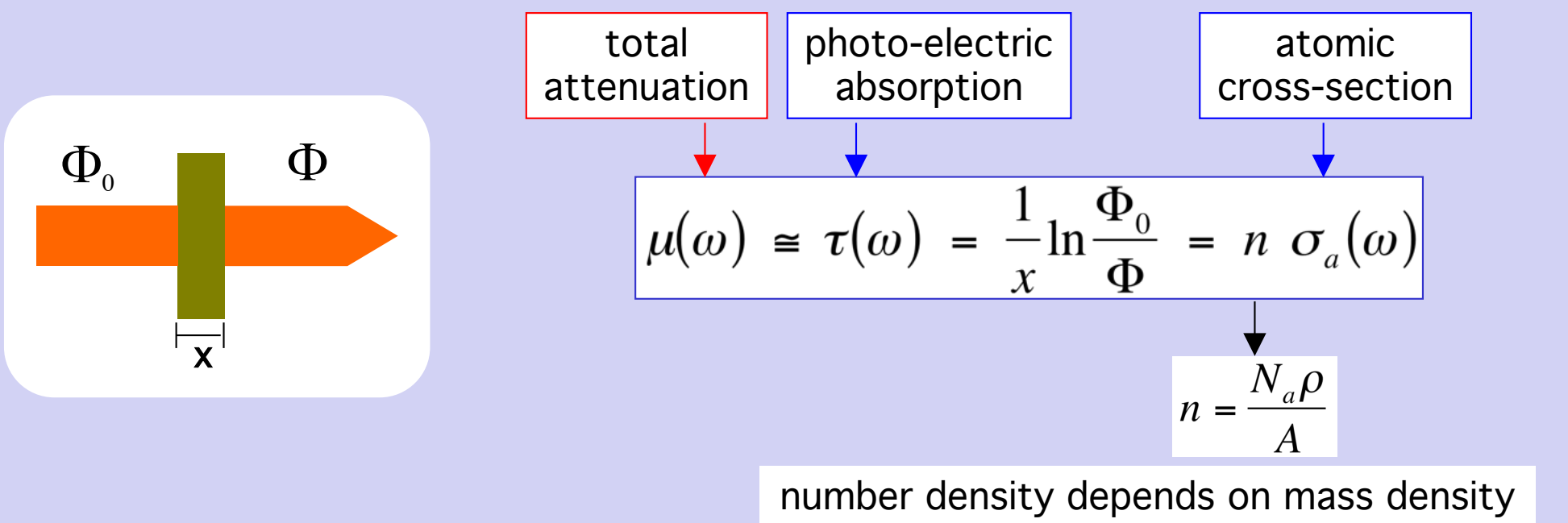
$$\Phi = \langle u \rangle c = \frac{\epsilon_0 \omega^2 A_0^2 c}{2} \quad \text{J m}^{-2} \text{s}^{-1}$$



Photon flux

$$\Phi = \frac{\text{energy flux}}{\text{photon energy}} = \frac{(\epsilon_0 \omega^2 A_0^2 / 2)c}{\hbar \omega} = \frac{\epsilon_0 \omega A_0^2 c}{2\hbar} \quad \text{m}^{-2} \text{s}^{-1}$$

Absorption coefficient



Mass attenuation coefficient (indep. of mass density)

Elements

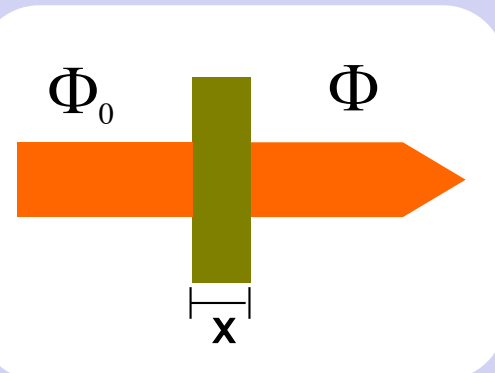
$$\frac{\mu}{\rho} = \frac{N_a}{m_{at}} \sigma_a$$

Compounds $P_x Q_y \dots$

$$\left(\frac{\mu}{\rho} \right)_{tot} = x \left(\frac{\mu}{\rho} \right)_P \frac{m_P}{M} + y \left(\frac{\mu}{\rho} \right)_Q \frac{m_Q}{M} + K$$

N_a = Avogadro number; m_{at} = atomic mass; M = molecular mass

Half-thickness



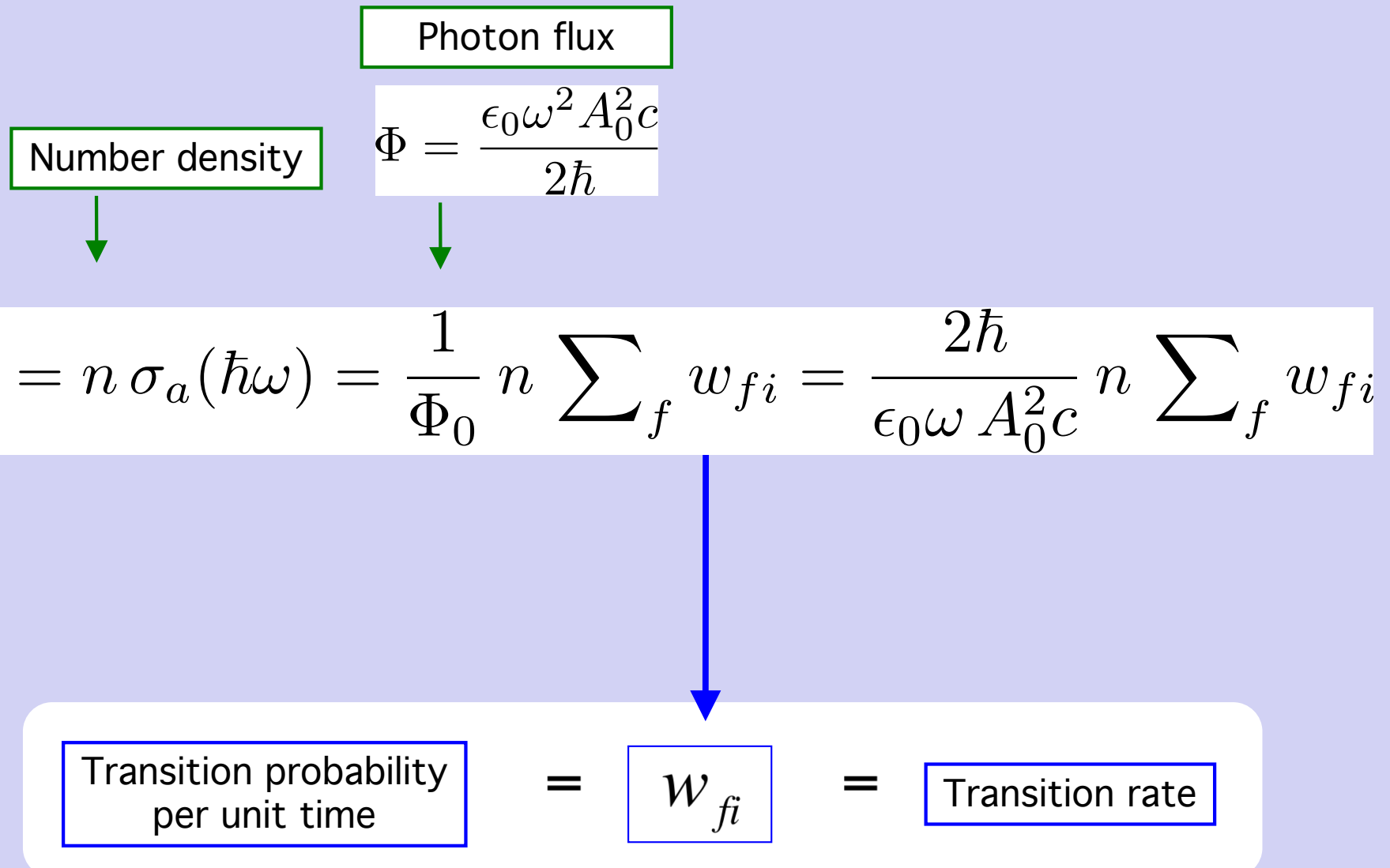
Thickness for which the flux is halved

$$\Phi = \frac{\Phi_0}{2} \quad \rightarrow \quad x_{1/2} = \frac{\ln 2}{\mu} = \frac{0.693}{\left(\frac{\mu}{\rho}\right)}$$

Table 2.1: Half-thickness (cm) for selected substances at selected X-ray wavelengths.

$\hbar\omega$ (keV)	Air	Mylar	Be	Al	Cu	Pb	density (g/cm ³)
0.0012	1.39	1.85	2.7	8.96	11.34	8.3e-5	
5	14.05	0.018	0.0085	0.001	0.0005	727.33	0.0007
20	2719.8	0.860	1.6641	0.075	0.0023	2.468	0.0076
50							

Cross section and transition rates

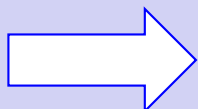
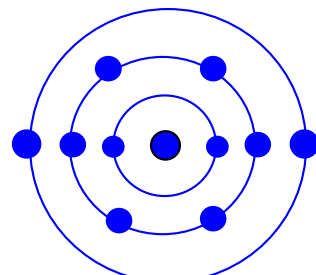


Semi-classical approximation

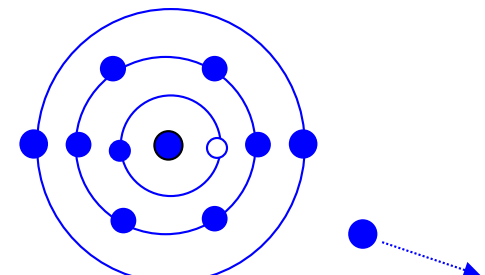
- Quantum treatment of atoms
- Classical treatment of field

$$w_{fi} = \text{Transition probability per unit time} = \text{Transition rate}$$

Initial state:
atom in ground state



Final state:
excited atom + photoelectron

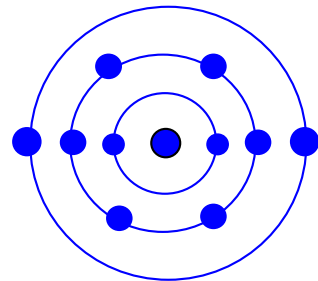


Energy conservation

$$E_f = E_i + \hbar\omega$$

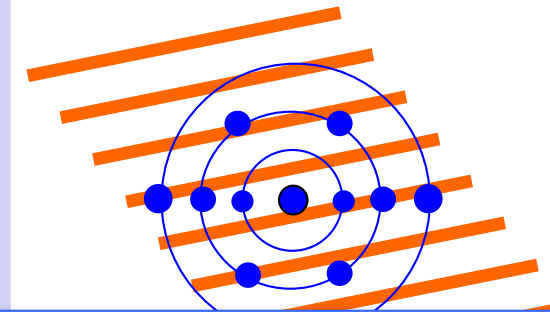
Radiation-matter interaction

Initial ground state



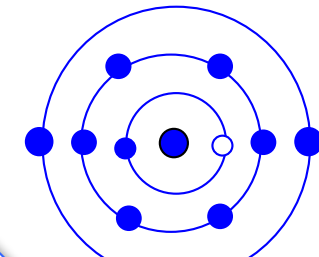
$|\Psi_i\rangle$

Interaction



$|\Psi(t)\rangle$

Final excited state

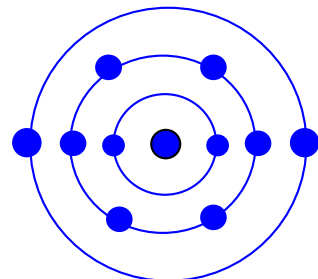


$|\Psi_f\rangle$

$$w_{fi} = ??$$

Fermi's Golden Rule

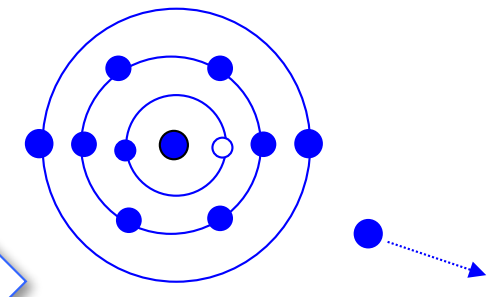
Initial ground state



$|\Psi_i\rangle$

Time-dependent
perturbation theory.
1st order

Final excited state



$|\Psi_f\rangle$

$$w_{fi} = \frac{\pi}{2\hbar} |\langle \Psi_f | H_I | \Psi_i \rangle|^2 \rho(E_f)$$

Interaction Hamiltonian



$$H_I(\vec{r}) = \frac{e}{m} \sum_f \vec{p}_j \cdot \vec{A}(\vec{r})$$

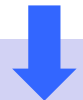
$$E_f = E_i + \hbar\omega$$

Coordinates representation

$$w_{fi} = \frac{\pi}{2\hbar} |\langle \Psi_f | H_I | \Psi_i \rangle|^2 \rho(E_f)$$



$$w_{fi} = \frac{\pi}{2\hbar} \left| \int \Psi_f(\vec{r}) H_I(\vec{r}) \Psi_i(\vec{r}) d\vec{r} \right|^2 \rho(E_f)$$



$$H_I(\vec{r}) = \frac{e}{m} \sum_f \vec{p}_j \cdot \vec{A}(\vec{r})$$

Transition rates and absorption coefficient

$$\begin{aligned} w_{fi} &= \frac{\pi}{2\hbar} |\langle \Psi_f | H_I | \Psi_i \rangle|^2 \rho(E_f) \\ &= \frac{\pi e^2 A_0^2}{2\hbar m^2} \left| \left\langle \Psi_f \left| \sum_j e^{i\vec{k} \cdot \vec{r}_j} \hat{\eta} \cdot \vec{p}_j \right| \Psi_i \right\rangle \right|^2 \rho(E_f) \end{aligned}$$

Sum over electrons

$$\begin{aligned} \mu(\hbar\omega) &= \frac{2\hbar}{\epsilon_0 \omega A_0^2 c} n \sum_f w_{fi} \\ &= \frac{\pi e^2}{\epsilon_0 \omega m^2 c} n \sum_f \left| \left\langle \Psi_f \left| \sum_j e^{i\vec{k} \cdot \vec{r}_j} \hat{\eta} \cdot \vec{p}_j \right| \Psi_i \right\rangle \right|^2 \rho(E_f) \end{aligned}$$

Sum over final states

Sum over electrons

$$E_f = E_i + \hbar\omega$$

A first summary

$$\mu(\hbar\omega) \propto \sum_f \left| \left\langle \Psi_f \left| \sum_j e^{i\vec{k} \cdot \vec{r}_j} \hat{\eta} \cdot \vec{p}_j \right| \Psi_i \right\rangle \right|^2 \rho(E_f)$$

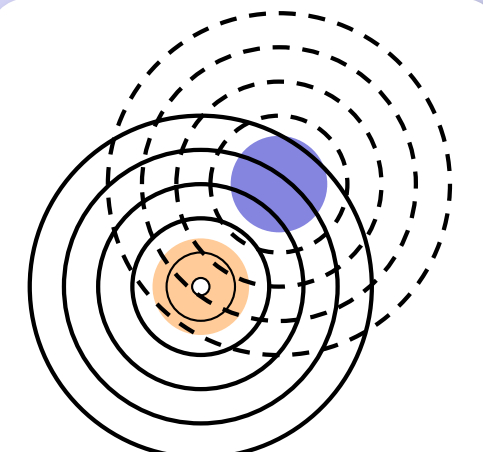
Sum over final states

Sum over electrons

Final atomic state

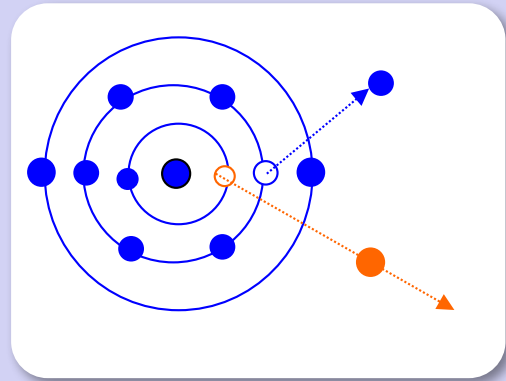
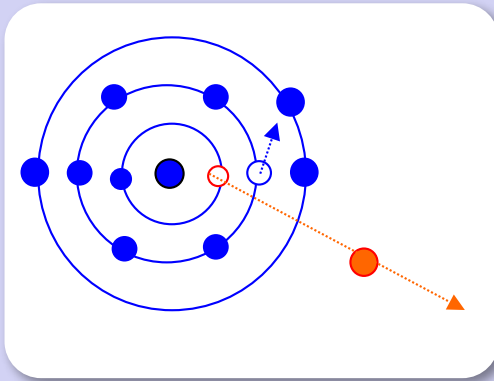
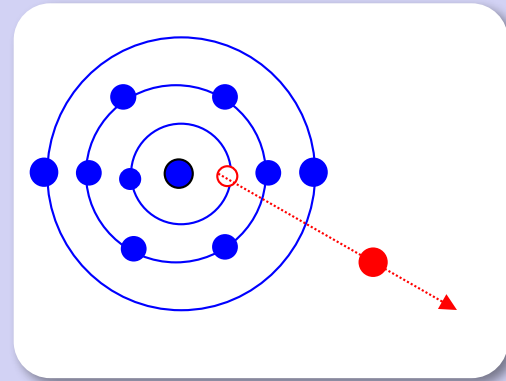
Oscillating e.m. field

?

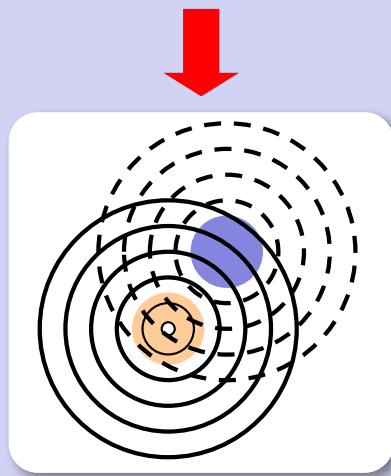


Further approximations

Final states



$$\mu_{\text{tot}}(\hbar\omega) = \mu_{\text{el}}(\hbar\omega) + \mu_{\text{inel}}(\hbar\omega)$$



EXAFS coherent signal

One-electron approximation

$$\begin{aligned}\mu_{\text{tot}}(\hbar\omega) &= \mu_{\text{el}}(\hbar\omega) + \mu_{\text{inel}}(\hbar\omega) \\ &\propto w_{\text{el}} + \sum w_{\text{inel}}\end{aligned}$$



- 1 core electron excited
- N-1 passive electrons relaxed



- 1 core electron excited
- Other electrons excited

see below

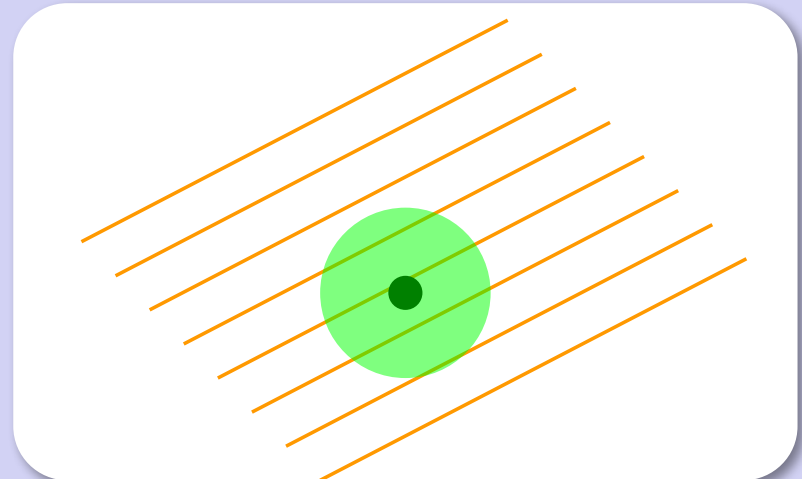
$$\mu_{\text{el}}(\hbar\omega) \propto \sum_f \left| \left\langle \Psi_f^{N-1} \psi_f \left| e^{i\vec{k} \cdot \vec{r}} \hat{\eta} \cdot \vec{p} \right| \psi_i \Psi_i^{N-1} \right\rangle \right|^2 \rho(E_f)$$



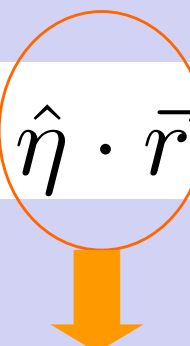
one-electron position

Electric dipole approximation

$$e^{i\vec{k} \cdot \vec{r}} = 1 + i\vec{k} \cdot \vec{r} - \dots \simeq 1$$



$$H_I \propto e^{i\vec{k} \cdot \vec{r}} \hat{\eta} \cdot \vec{p} \simeq \hat{\eta} \cdot \vec{p} = \omega^2 \hat{\eta} \cdot \vec{r}$$



$$\mu_{\text{el}}(\omega) \propto \left| \left\langle \Psi_f^{N-1} \psi_f | \hat{\eta} \cdot \vec{r} | \psi_i \Psi_i^{N-1} \right\rangle \right|^2$$

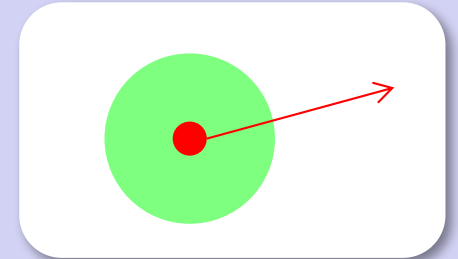
Dipole selection rules:

$$\begin{aligned} \Delta l &= \pm 1 & \Delta s &= 0 \\ \Delta j &= 0, \pm 1, & \Delta m &= 0, \pm 1 \end{aligned}$$

Sudden approximation

No interaction between **photoelectron** and **passive electrons**

$$|\Psi^{N-1}\psi\rangle = |\Psi^{N-1}\rangle|\psi\rangle$$



1 active electron

N-1 passive electrons

$$\mu_{\text{el}}(\omega) \propto |\langle \psi_f | \hat{\eta} \cdot \vec{r} | \psi_i \rangle|^2 \rho(E_f) \left| \langle \Psi_f^{N-1} | \Psi_i^{N-1} \rangle \right|^2$$

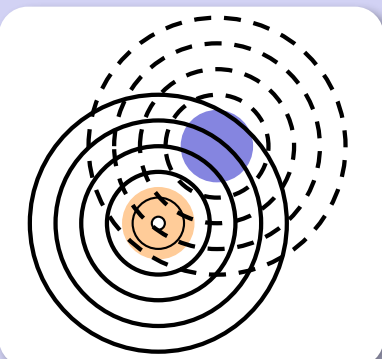


One-electron
final state

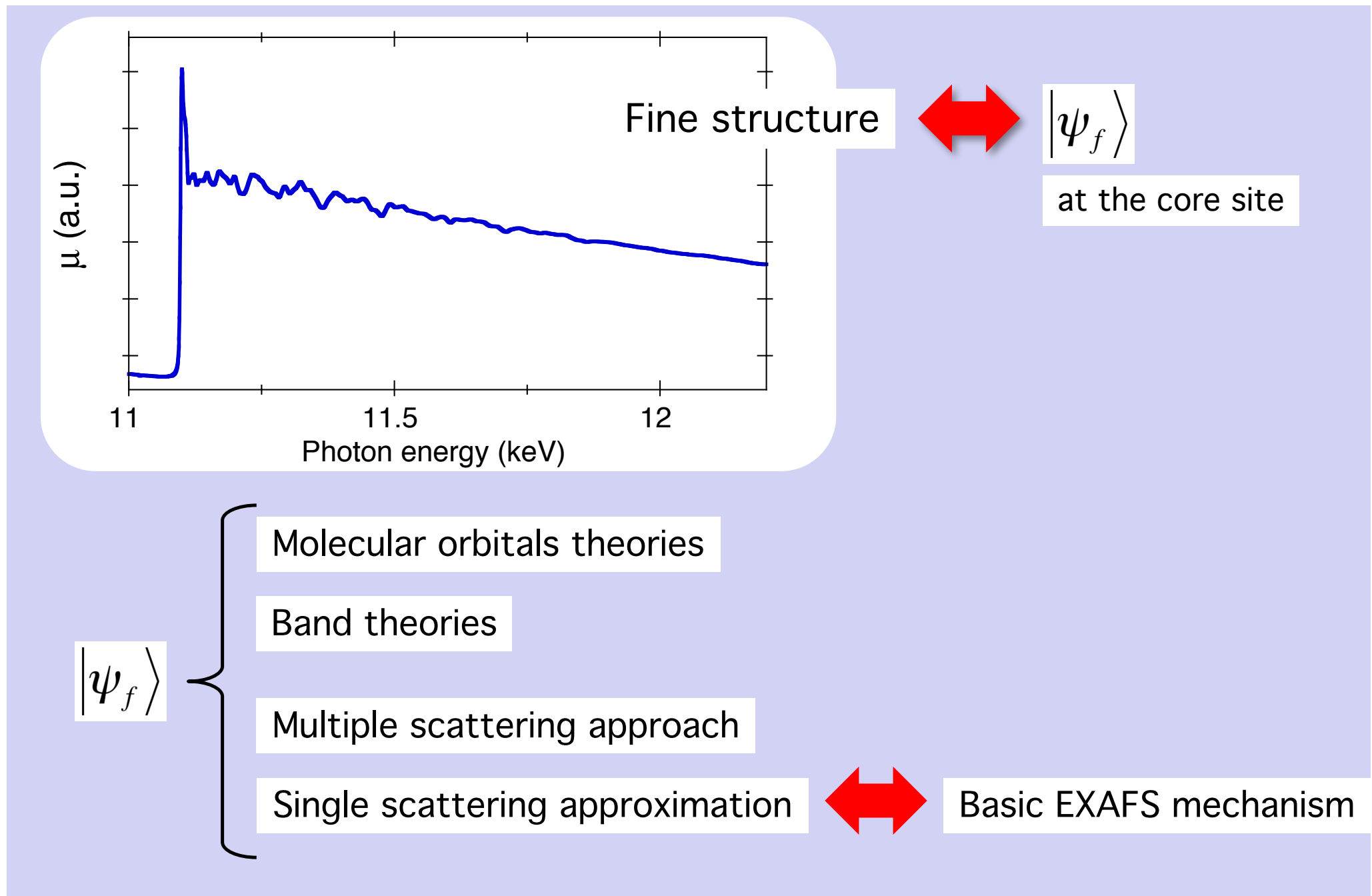
$$S_0^2 \simeq 0.6 - 0.9$$



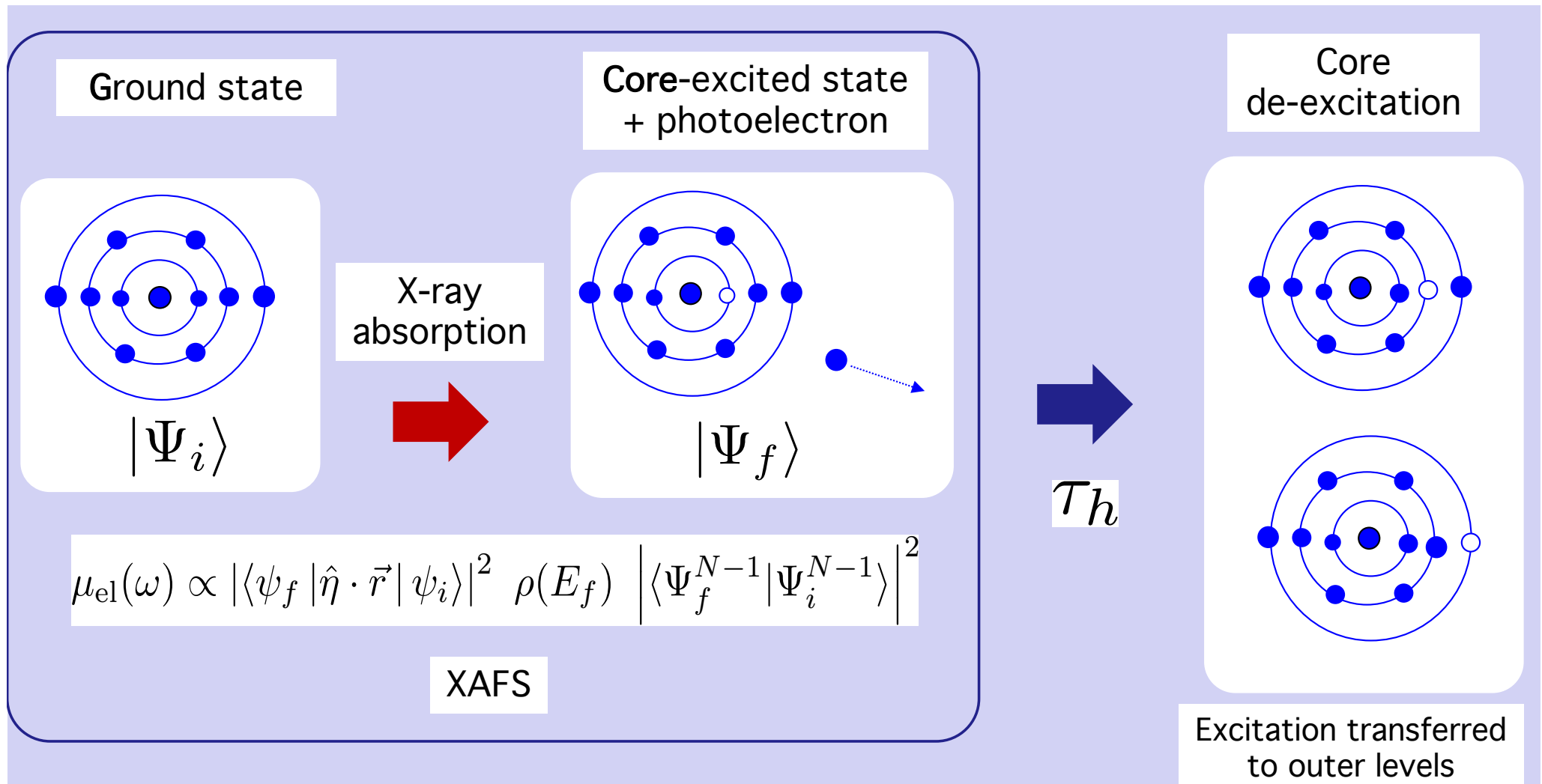
Structural
info



The final state



Atomic de-excitation



τ_h = lifetime of core excited

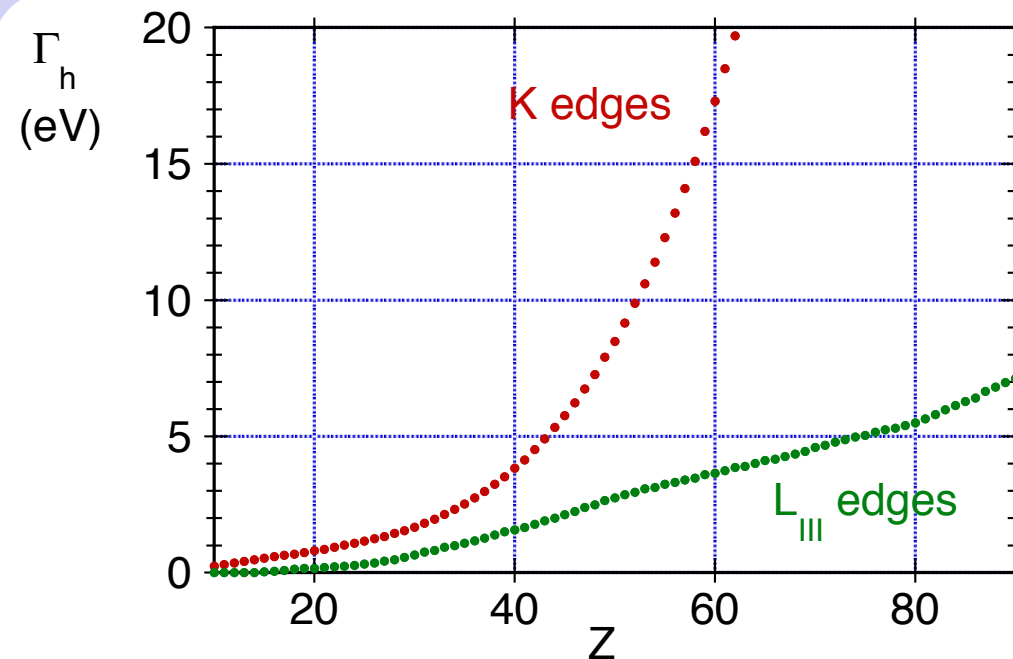
τ_h is shorter for higher atomic number Z

Core-hole lifetime and energy width

Lifetime
of the excited state
 $\tau_h \sim 10^{-16} - 10^{-15}$ s

$$\tau_h \propto \frac{1}{\Gamma_h}$$

Energy width
of the excited state
 Γ_h



Dependence on Z

τ_h

Contribution to
photo-electron life-time

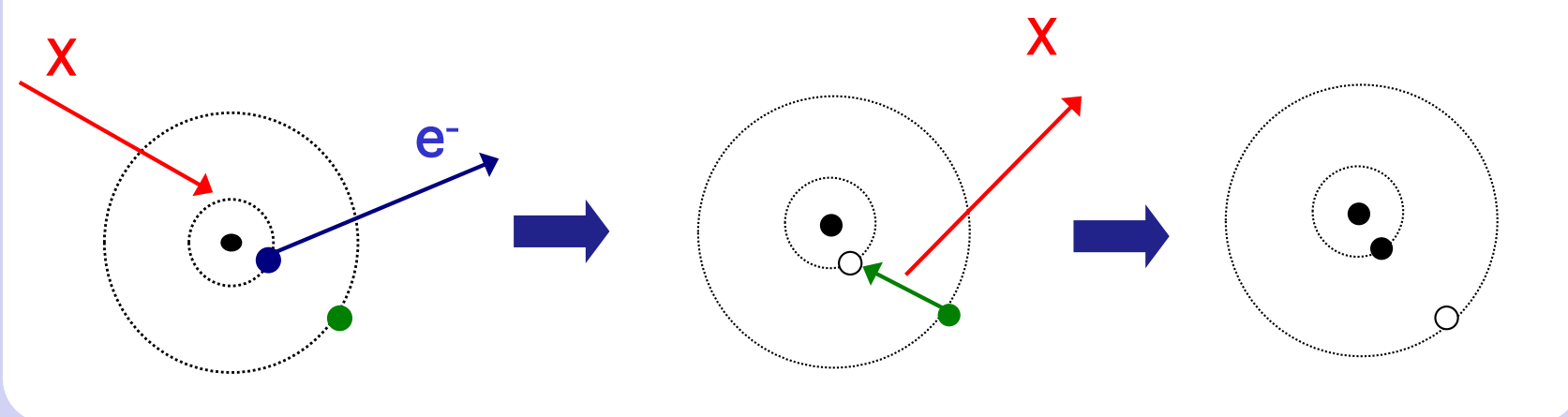
Γ_h

Energy resolution
of XAFS spectra

De-excitation mechanisms

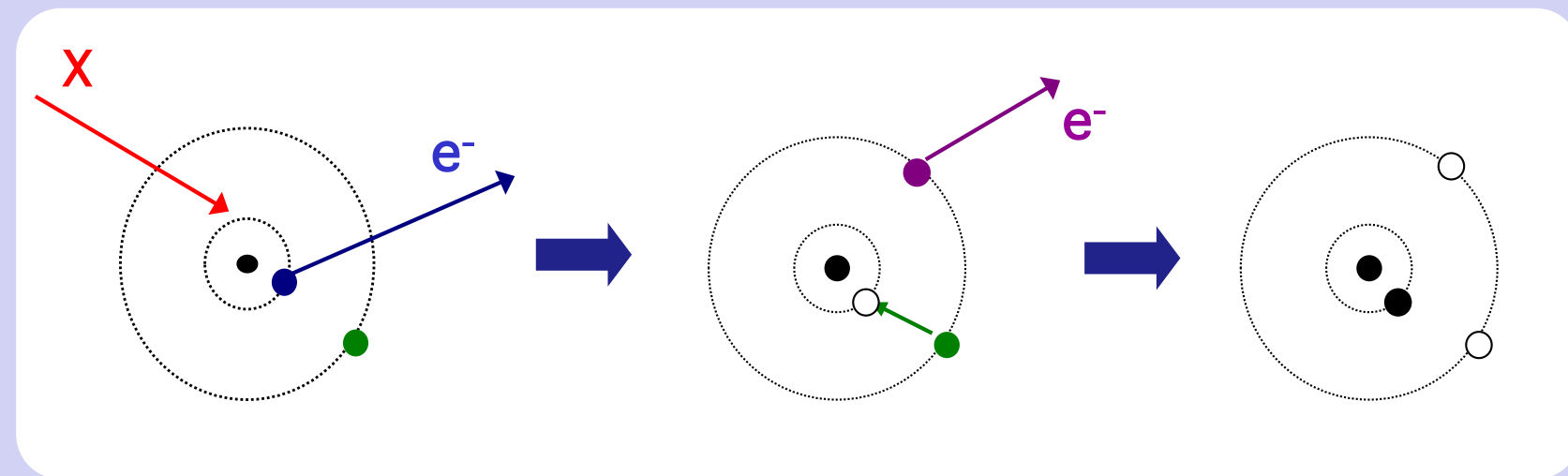
Radiative: fluorescence

X



Non-radiative: Auger

A

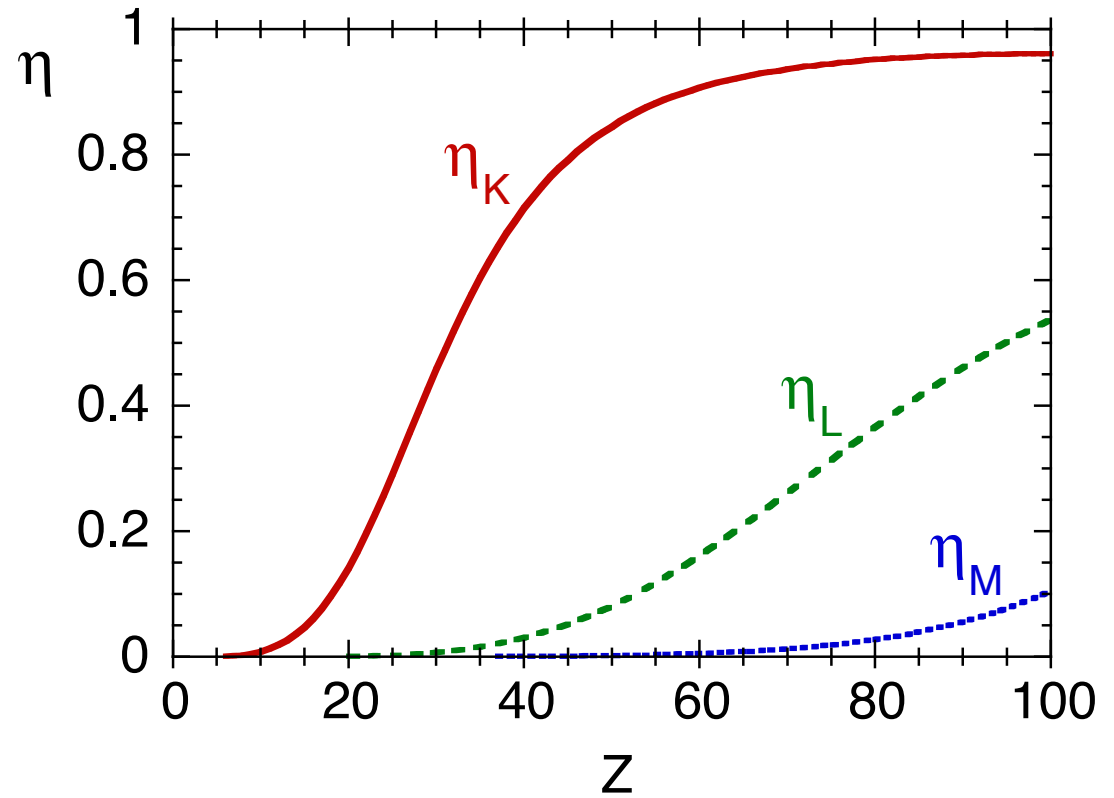


Fluorescence yield

Fluorescence versus Auger

Fluorescence yield

$$\eta = \frac{X}{X + A}$$



Both fluorescence and Auger yields intensities are proportional to the absorption coefficient



Alternative measurements of XAFS

EXAFS: theoretical background

Absorption coefficient

$$\mu(\hbar\omega) = \frac{2\hbar}{\epsilon_0\omega A_0^2 c} n \sum_f w_{fi}$$

Time-dep. perturbation theory

$$W_{if} \propto \left| \langle \Psi_f | \hat{H}_I | \Psi_i \rangle \right|^2 \rho(E_f)$$

- one-electron approx.
- sudden approx.
- electric dipole approx.

1 active electron

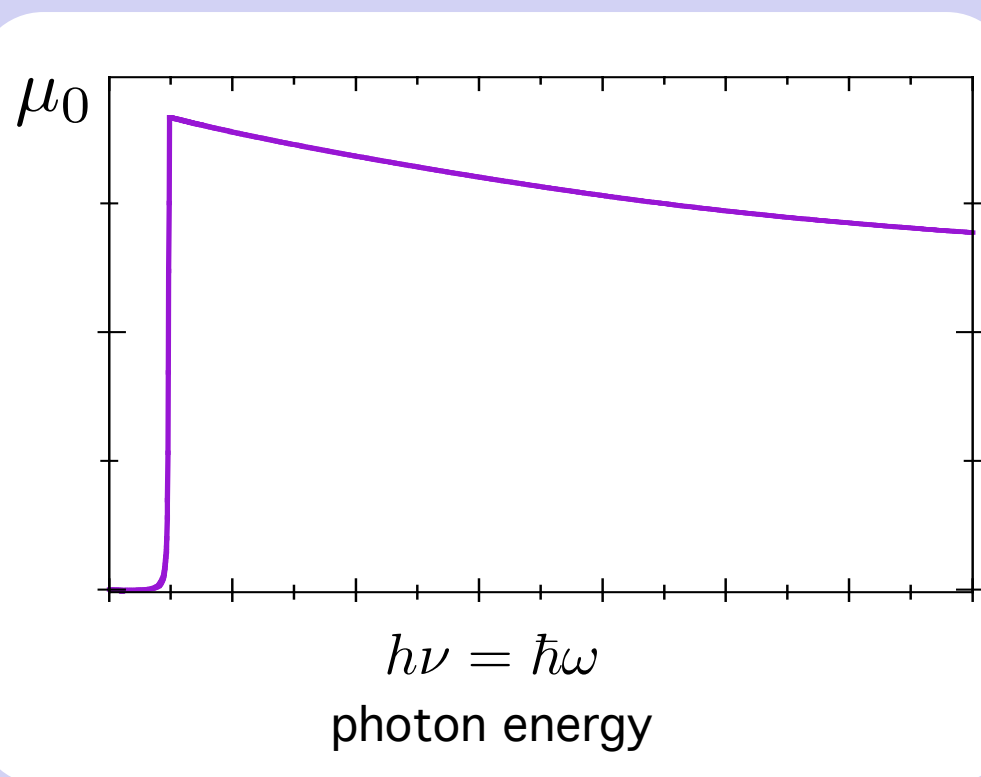
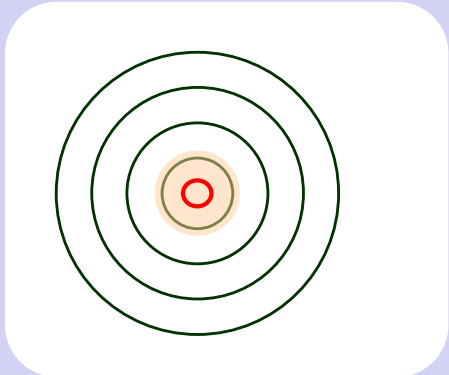
N-1 passive electrons

$$\mu_{el}(\omega) \propto |\langle \psi_f | \hat{\eta} \cdot \vec{r} | \psi_i \rangle|^2 \rho(E_f) \left| \langle \Psi_f^{N-1} | \Psi_i^{N-1} \rangle \right|^2$$

Structural
information

$$S_0^2 \simeq 0.6 - 0.9$$

A: isolated atom



$$\mu_0(\omega) \propto |\langle \psi_f^0 | \hat{\eta} \cdot \vec{r} | \psi_i \rangle|^2$$

outgoing electron core state

Photon → photo-electron

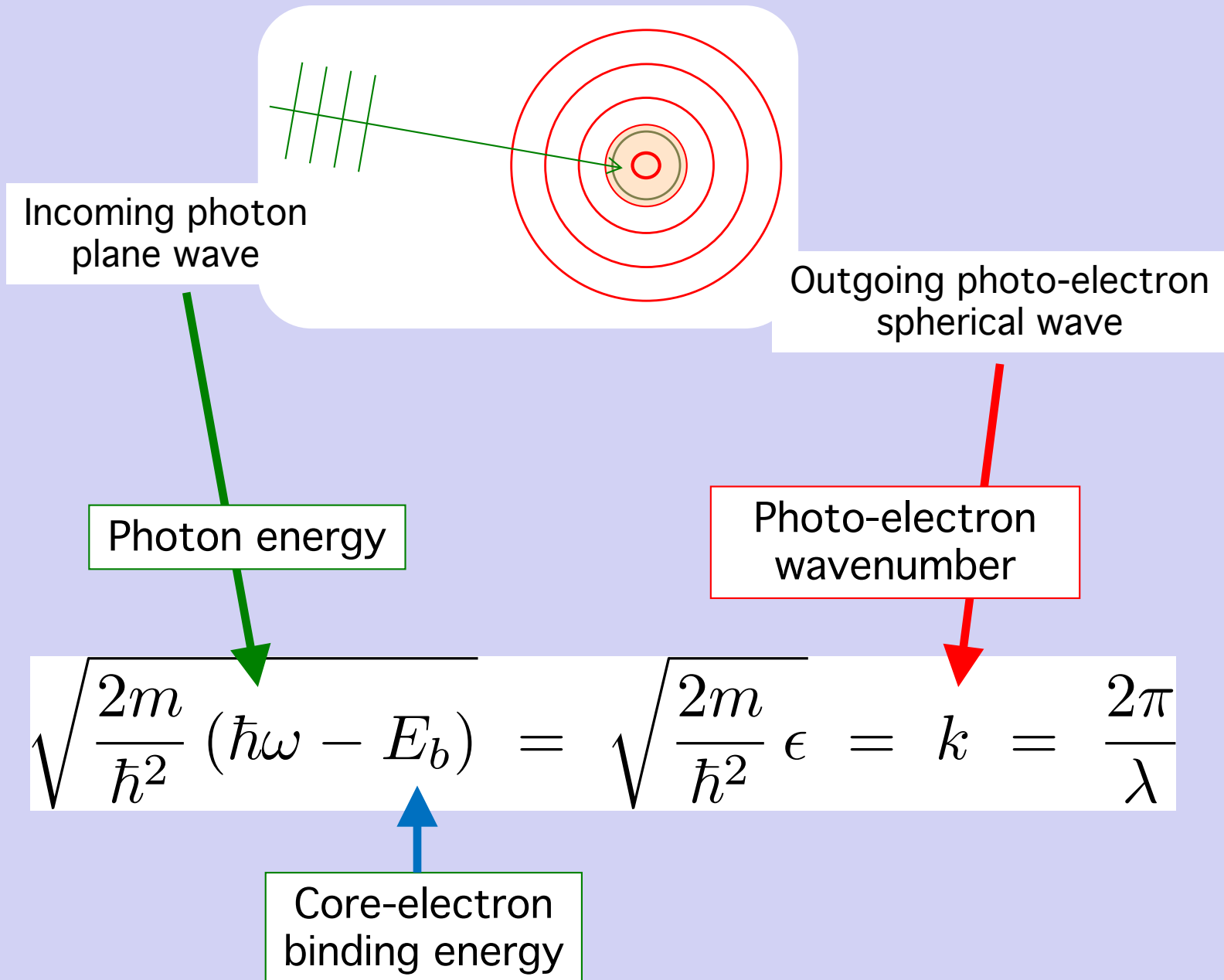
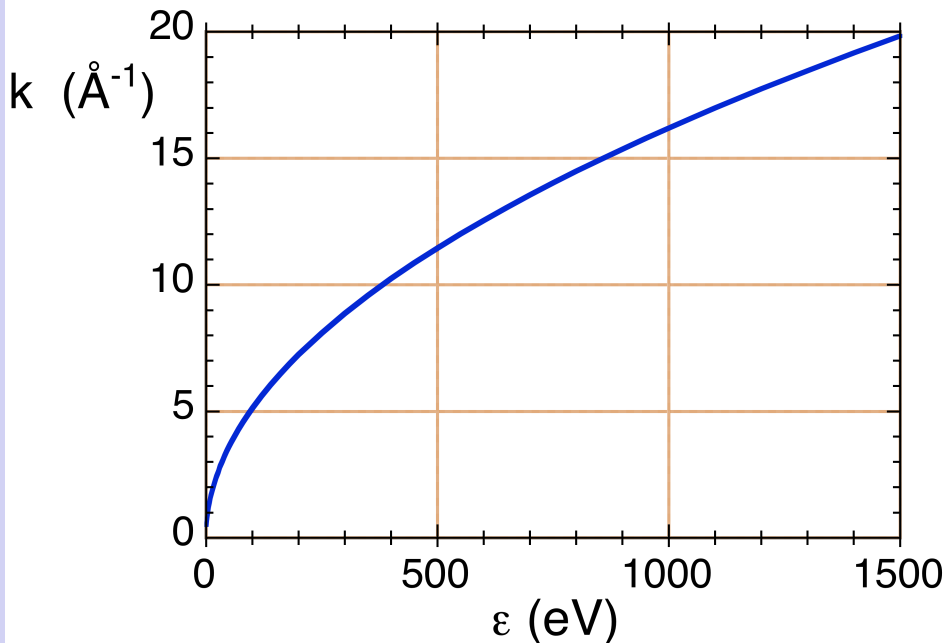


Photo-electron parameters

Wave-number



Wave-length

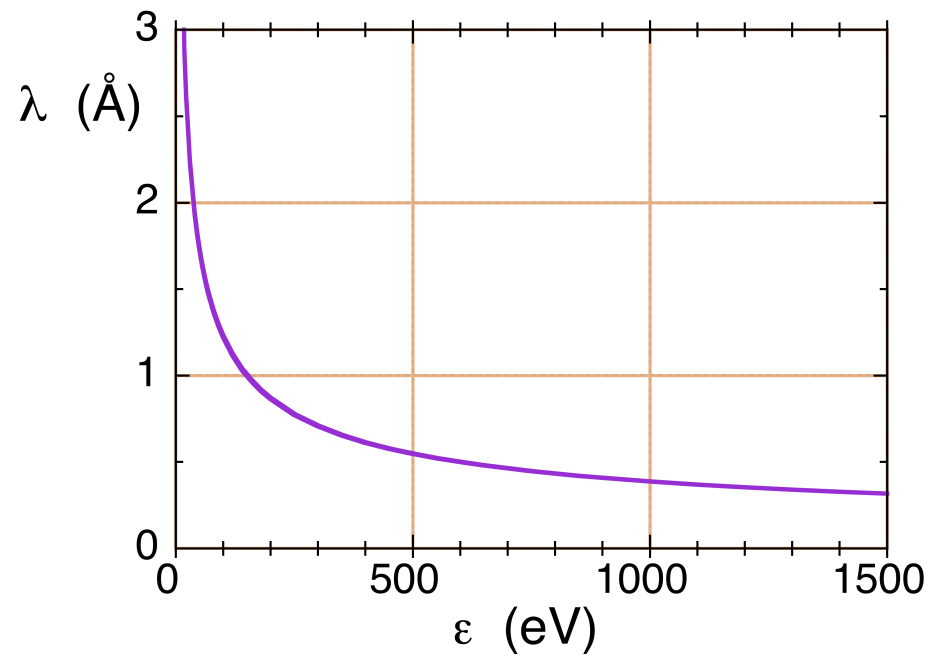
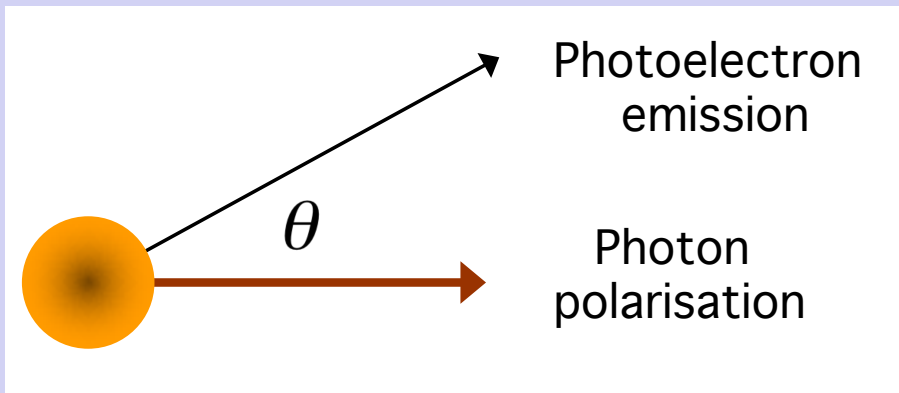


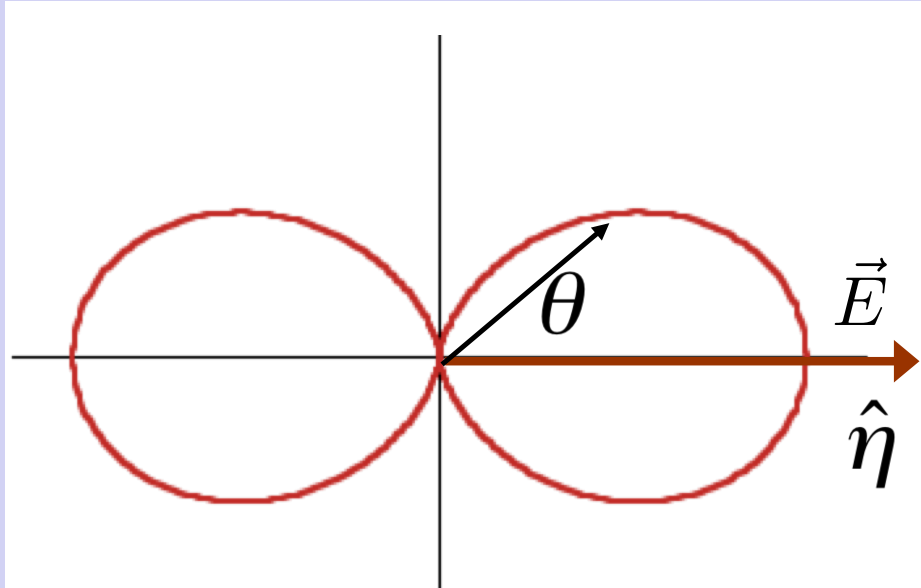
Photo-electron Energy

Angular emission of photo-electron



asimmetry parameter

$$N(\theta) \propto 1 + \frac{\beta}{2} (3 \cos^2 \theta - 1)$$

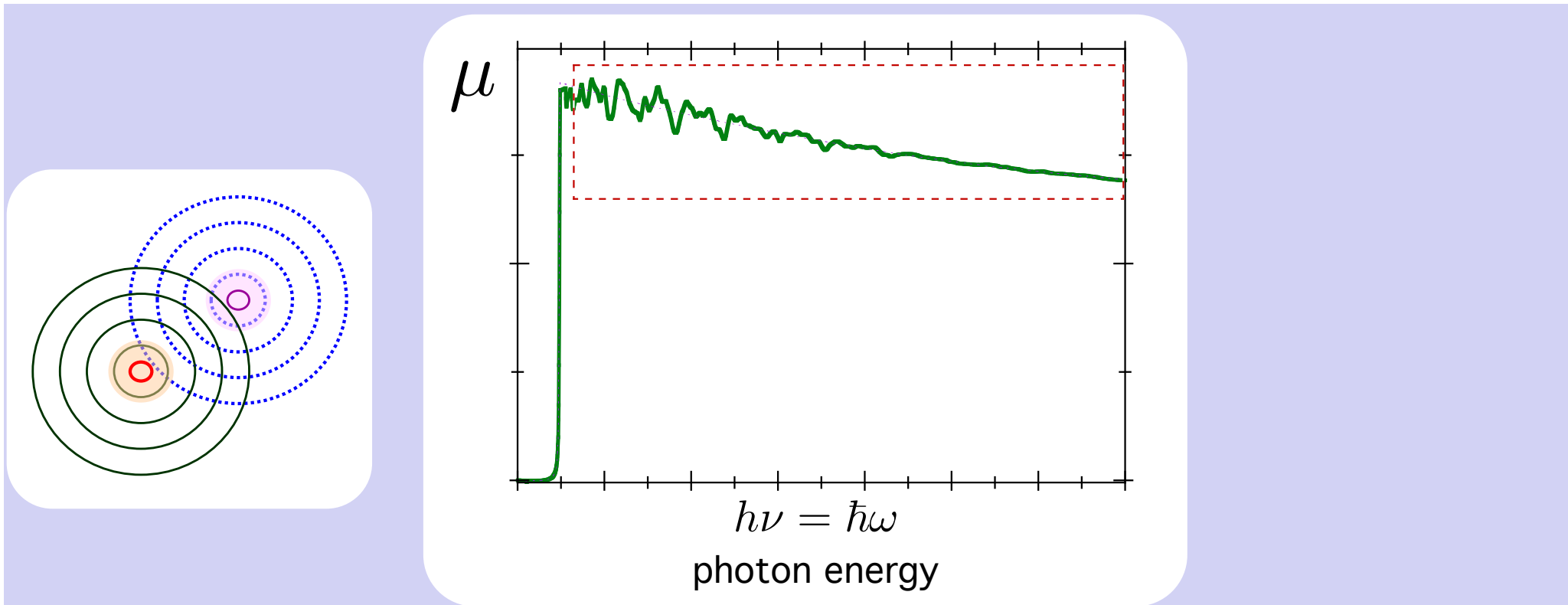


$$\beta = 2$$

Emission from s orbitals

$$N(\theta) \propto 3 \cos^2 \theta = 3 |\hat{r} \cdot \hat{r}|^2$$

B: non-isolated atom



$$\mu(\omega) \propto |\langle \psi_f | \hat{\eta} \cdot \vec{r} | \psi_i \rangle|^2$$

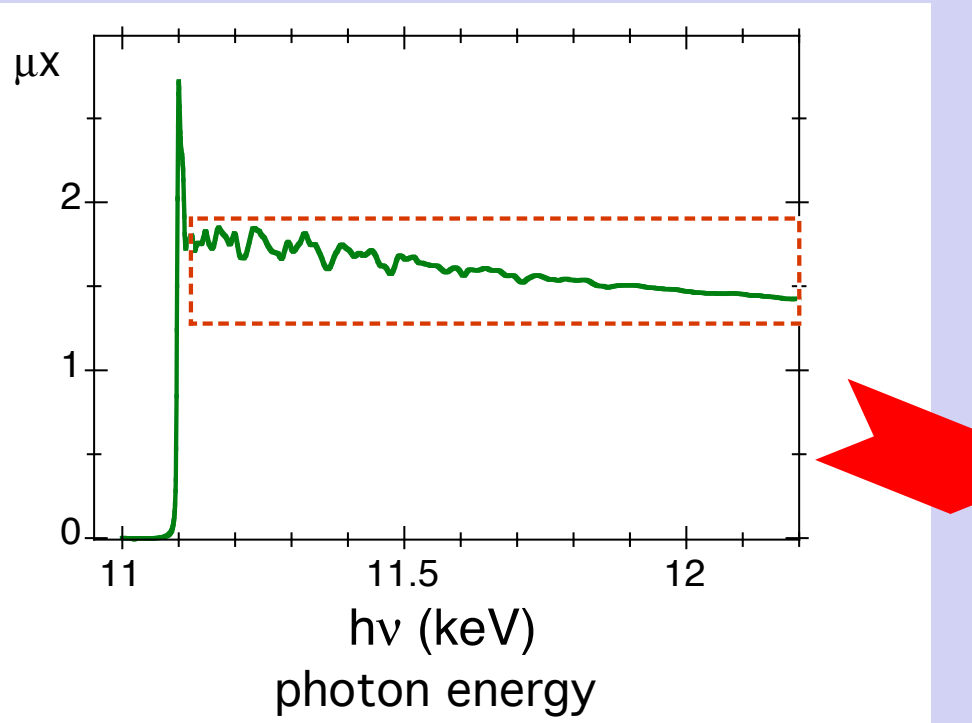


Outgoing + scattered
electron



core state

The EXAFS normalized signal $\chi(k)$



$$\chi(k) = \frac{\mu - \mu_0}{\mu_0}$$

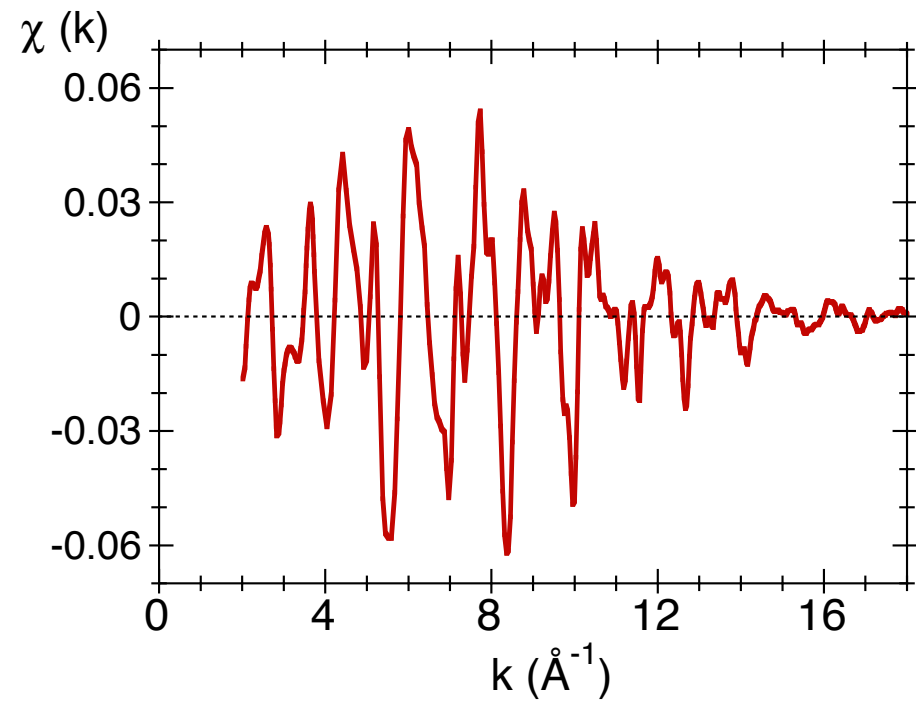
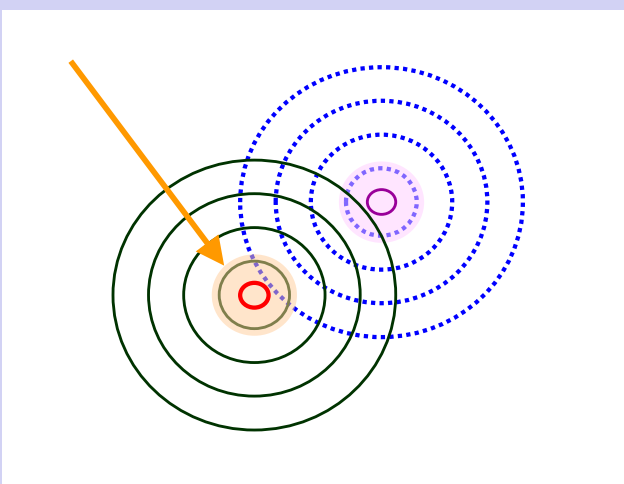
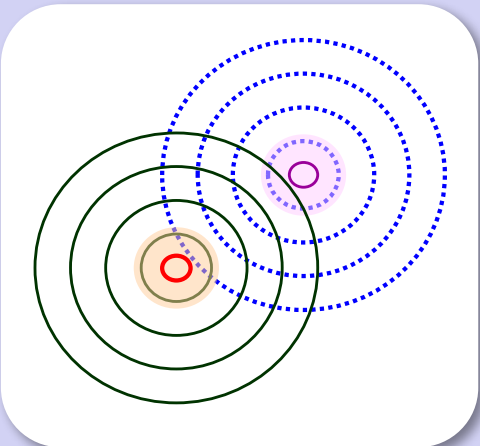


photo-electron wave-number



The absorption coefficient



Final state

$$|\psi_f\rangle = |\psi_f^0 + \delta\psi_f\rangle$$



Perturbation
due to photoelectron scattering



Structural
info

$$\mu(\omega) \propto |\langle \psi_f^0 + \delta\psi_f | \hat{\eta} \cdot \vec{r} | \psi_i \rangle|^2$$

$$\mu(\omega) \propto |\langle \psi_f^0 | \hat{\eta} \cdot \vec{r} | \psi_i \rangle|^2$$



μ_0

$$+ 2\text{Re} \{ \langle \psi_f^0 | \hat{\eta} \cdot \vec{r} | \psi_i \rangle \langle \delta\psi_f | \hat{\eta} \cdot \vec{r} | \psi_i \rangle \}$$



EXAFS oscill.

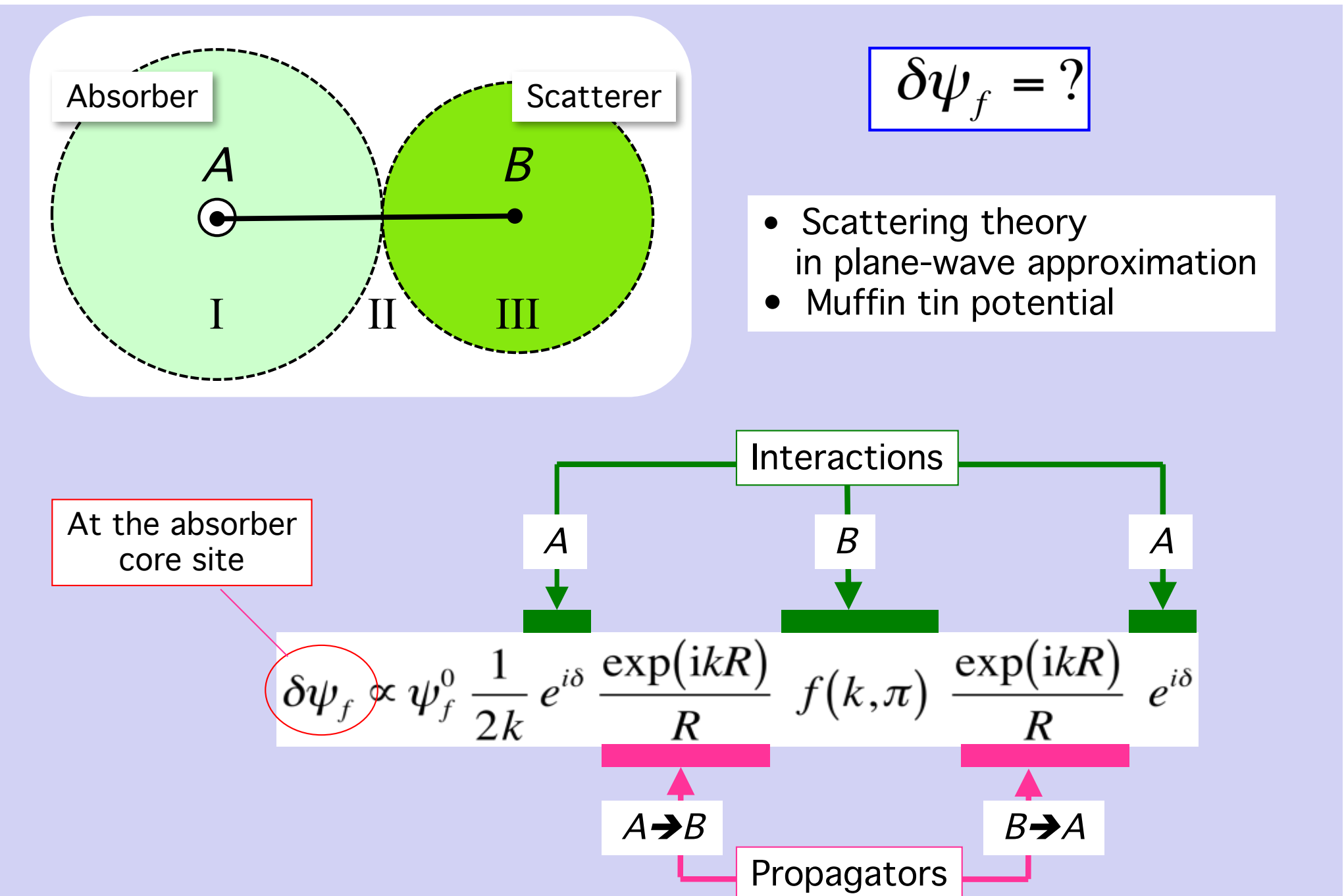
$$+ |\langle \delta\psi_f | \hat{\eta} \cdot \vec{r} | \psi_i \rangle|^2$$



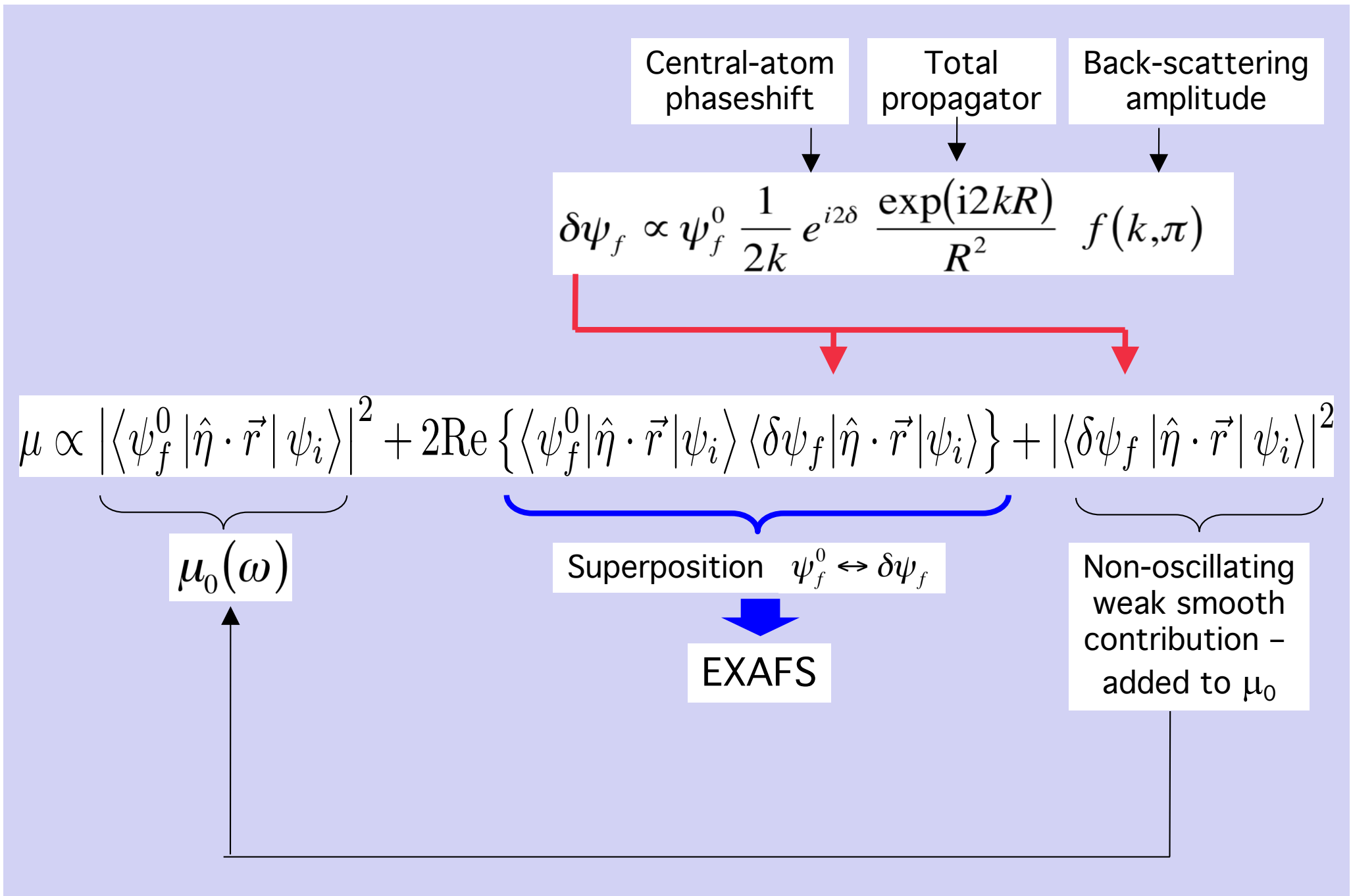
?

$\delta\psi_f = ?$

Two-atomic system: $\delta\psi_f$

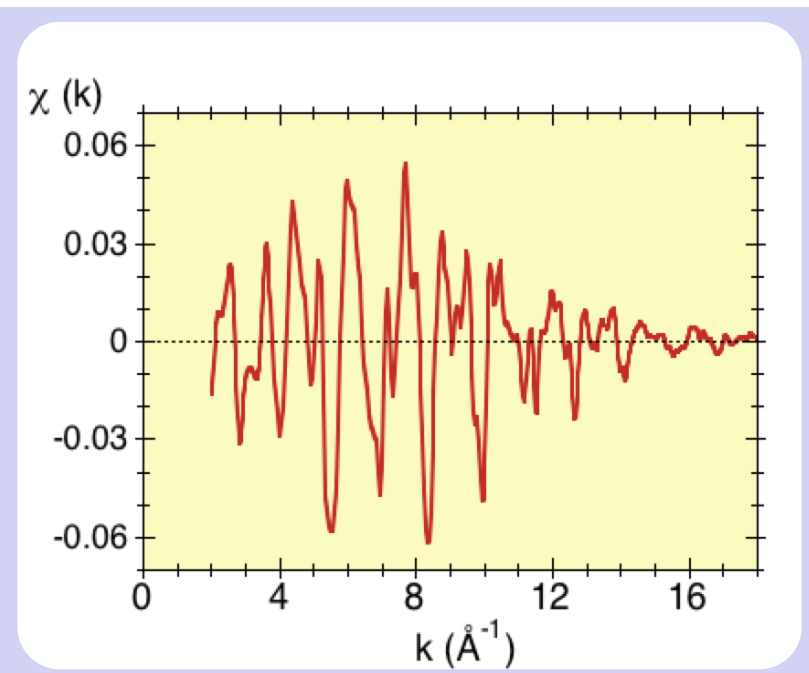
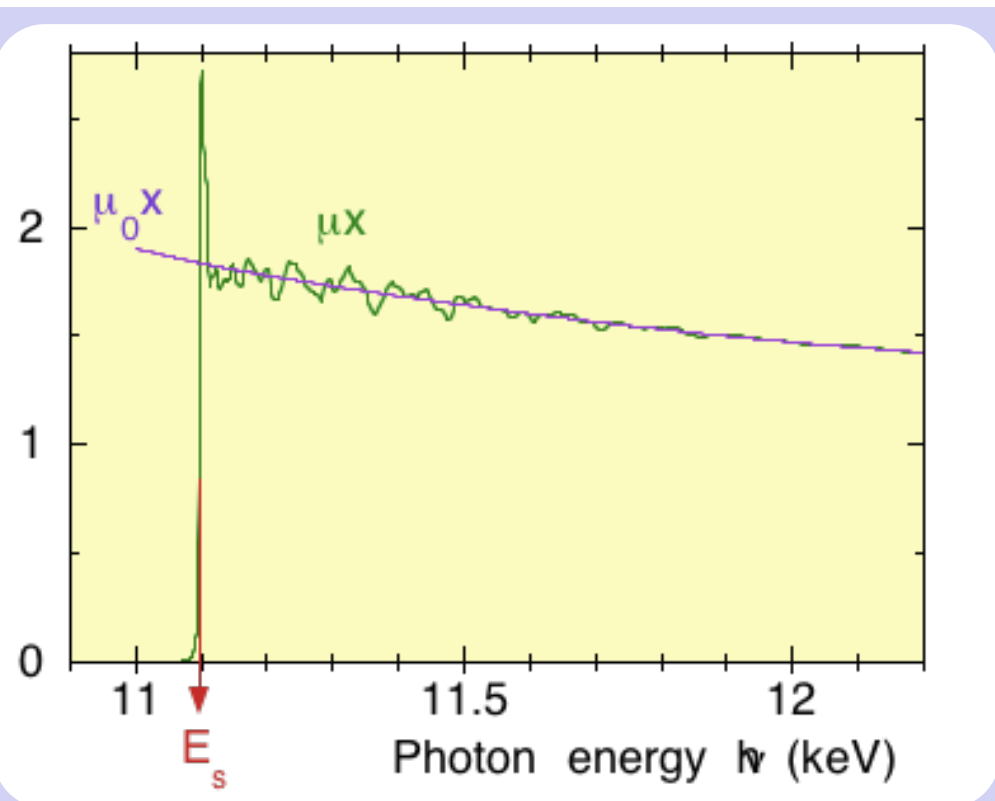


Two-atomic system: absorption coefficient



Normalized EXAFS function

Paolo
Fornasini
Univ. Trento



$$\chi(k) = \frac{\mu - \mu_0}{\mu_0}$$

$$\mu - \mu_0 = 2\text{Re} \left\{ \langle \psi_f^0 | \hat{\eta} \cdot \vec{r} | \psi_i \rangle \langle \delta \psi_f | \hat{\eta} \cdot \vec{r} | \psi_i \rangle \right\}$$

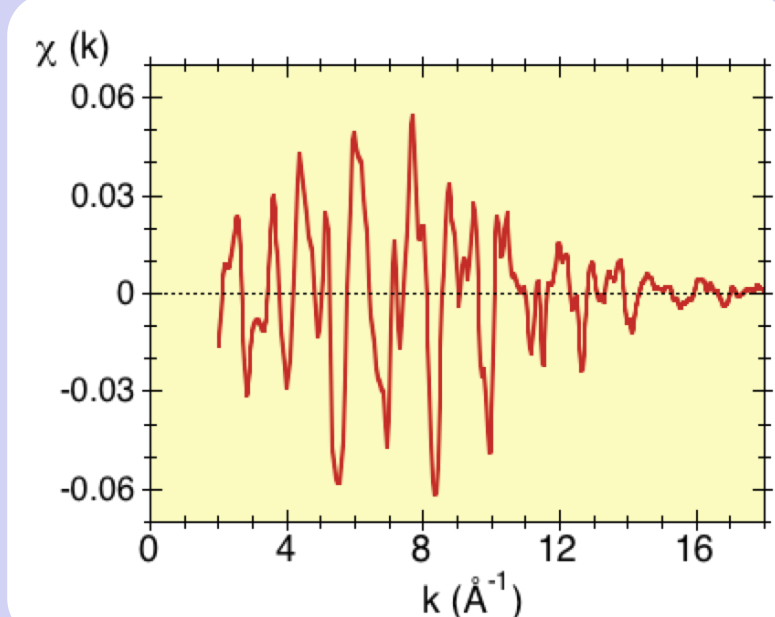
$$\mu_0 \propto \left| \langle \psi_f^0 | \hat{\eta} \cdot \vec{r} | \psi_i \rangle \right|^2$$



EXAFS function in coordinate representation

$$\chi(k) = \frac{\mu - \mu_0}{\mu_0}$$

Quantum states → wavefunctions



$$\chi(k) = \frac{2\text{Re} \int d\vec{r} (\psi_f^{0*} \hat{\eta} \cdot \vec{r} \psi_i)(\delta\psi_f^* \hat{\eta} \cdot \vec{r} \psi_i)}{\int d\vec{r} (\psi_f^{0*} \hat{\eta} \cdot \vec{r} \psi_i)}$$

Core orbital = source & detector

EXAFS for a two-atomic system

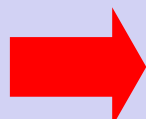
$$\delta\psi_f \propto \psi_f^0 i e^{2i\delta} \frac{\exp(i2kR)}{2kR^2} f(k,\pi)$$

$$\chi(k) = \frac{2\text{Re} \int d\vec{r} (\psi_f^{0*} \hat{\eta} \cdot \vec{r} \psi_i) (\delta\psi_f^* \hat{\eta} \cdot \vec{r} \psi_i)}{\int d\vec{r} (\psi_f^{0*} \hat{\eta} \cdot \vec{r} \psi_i)}$$

polarisation

back-scattering
amplitude

central atom
phase-shift



$$\chi(k) = 3 |\hat{\eta} \cdot \hat{R}|^2 \frac{1}{kR^2} \text{Im} [f(k,\pi) \exp(2i\delta_1) \exp(2ikR)]$$

spherical wave
attenuation

back & forth path

Basic interference effect

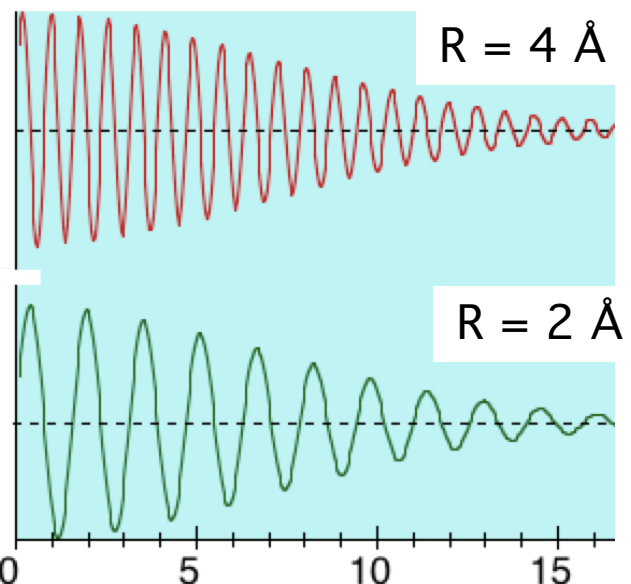
Complex form

$$\chi(k) = 3 |\hat{\eta} \cdot \hat{R}|^2 \frac{1}{kR^2} \operatorname{Im} \{ f(k, \pi) e^{2i\delta_1} e^{2ikR} \}$$

$$f(k, \pi) e^{2i\delta} = |f(k, \pi)| e^{i\phi}$$

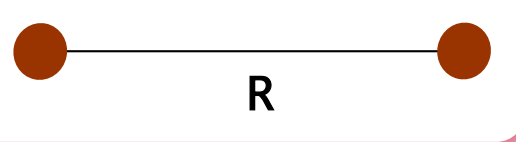
Real form

$$\chi(k) = 3 |\hat{\eta} \cdot \hat{R}|^2 \frac{1}{kR^2} |f(k, \pi)| \sin\{2kR + \phi(k)\}$$



EXAFS
frequency

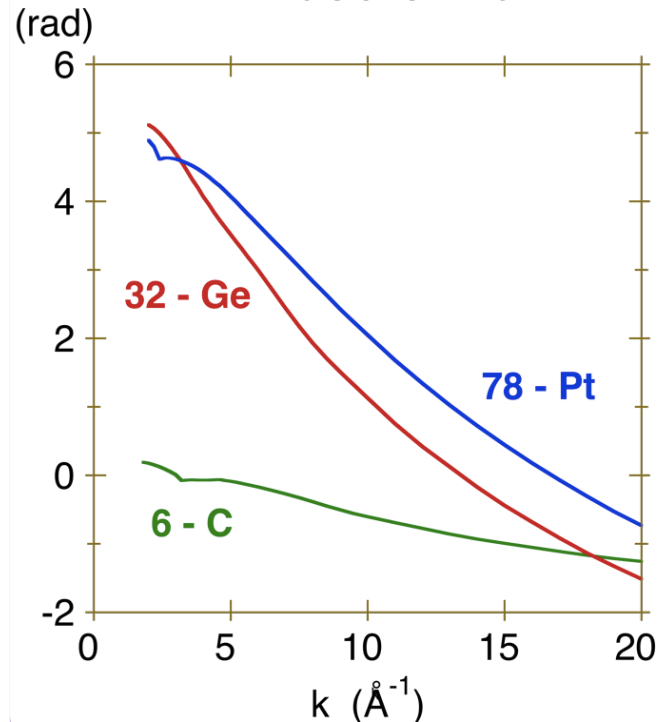
Inter-atomic
distance



Amplitudes and phase-shifts

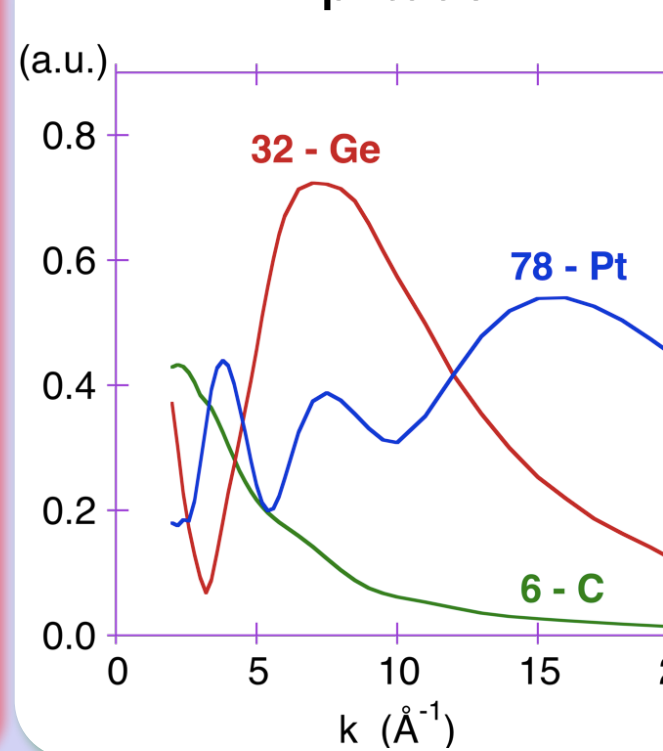
Central-atom

Phase-shift

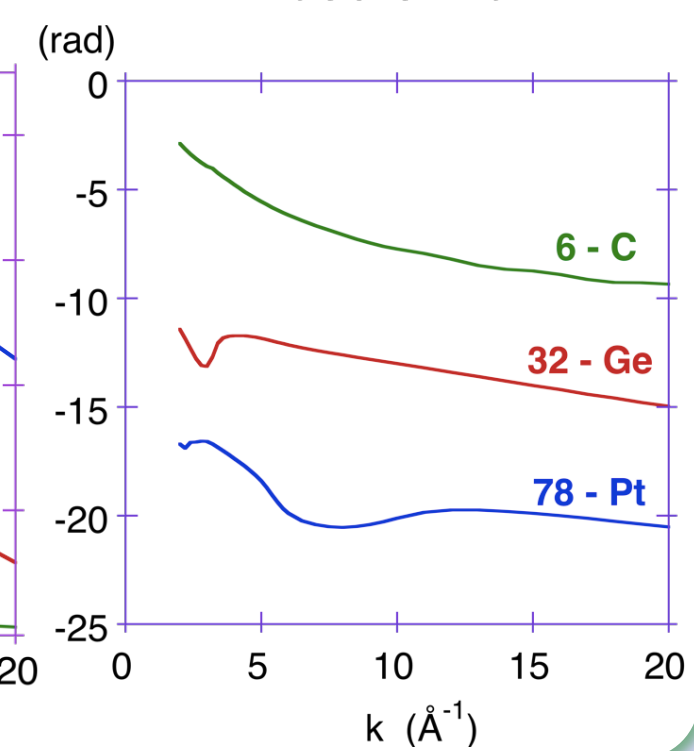


Back-scattering atom

Amplitude



Phase-shift



[Calculated by FEFF 6.01]

Z dependence

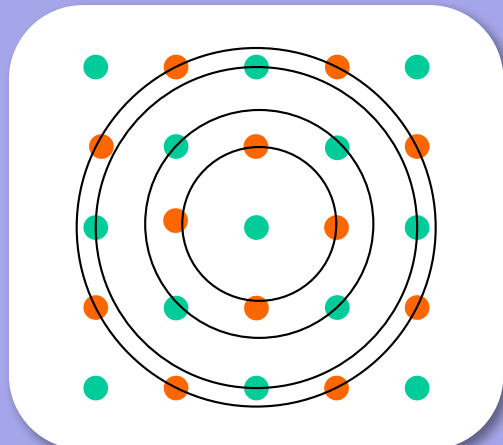
sensitivity to
atomic species



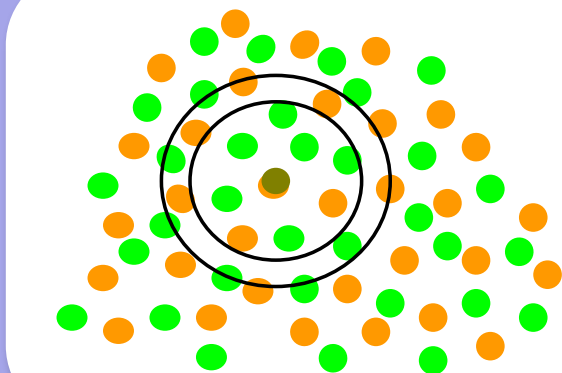
Many-atomic systems

Paolo
Fornasini
Univ. Trento

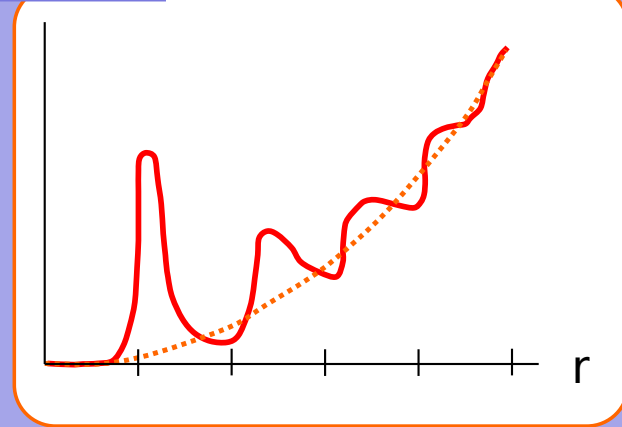
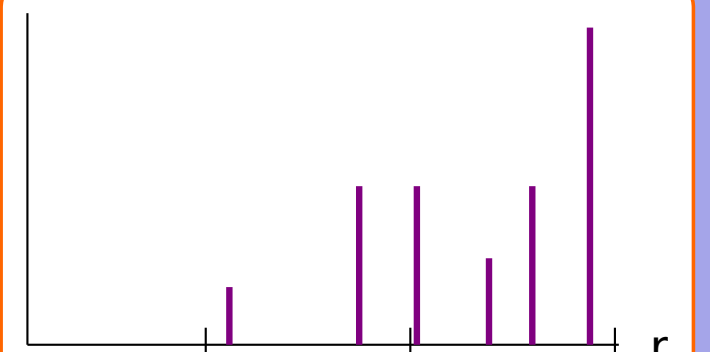
Crystals



Amorphous systems

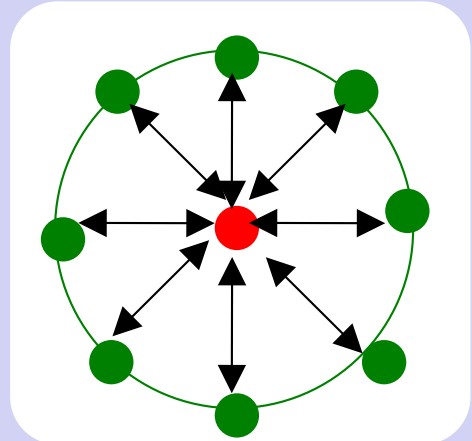


Radial Distribution Functions



Coordination shells

N atoms at the same distance



Final state

$$|\psi_f\rangle = |\psi_f^0 + N \delta\psi\rangle$$

Scattering from N neighbours

Absorption coefficient

$$\mu(\omega) \propto |\langle \psi_f^0 + N \delta\psi_f | \hat{\eta} \cdot \vec{r} | \psi_i \rangle|^2$$

$$\mu(\omega) \propto |\langle \psi_f^0 | \hat{\eta} \cdot \vec{r} | \psi_i \rangle|^2 + 2N \text{Re} \{ \langle \psi_f^0 | \hat{\eta} \cdot \vec{r} | \psi_i \rangle \langle \delta\psi_f | \hat{\eta} \cdot \vec{r} | \psi_i \rangle \} + N^2 |\langle \delta\psi_f | \hat{\eta} \cdot \vec{r} | \psi_i \rangle|^2$$

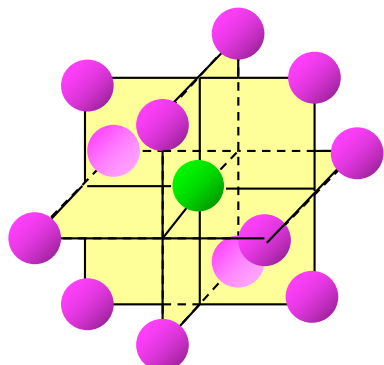
$$\mu_0(\omega)$$

N EXAFS terms

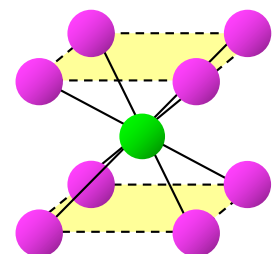
Non-oscillating
weak smooth
contribution –
added to μ_0

Coordination number

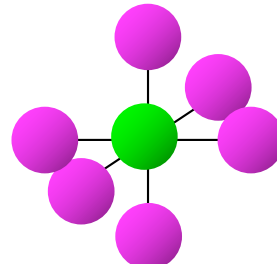
Number of atoms in the first coordination shell (nearest-neighbours)



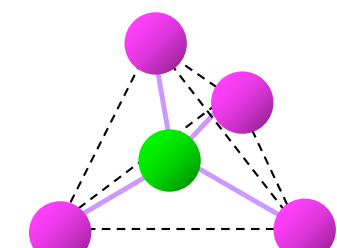
$N=12$ (e.g. fcc)



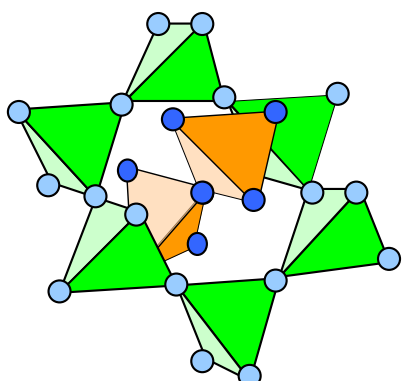
$N=8$ (e.g. bcc)



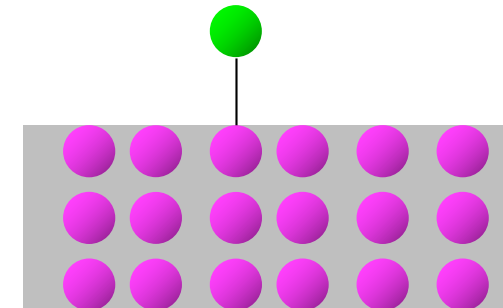
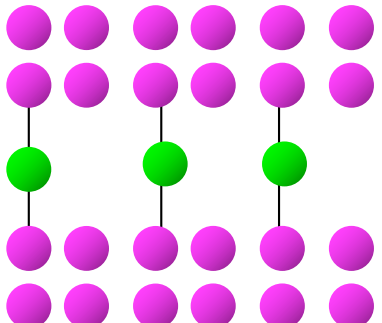
$N=6$ (e.g. NaCl)



$N=4$ (e.g. diamond)

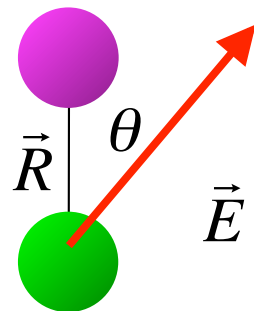


$N=2$



$N=1$ (e.g. adsorbates)

Polarisation effect



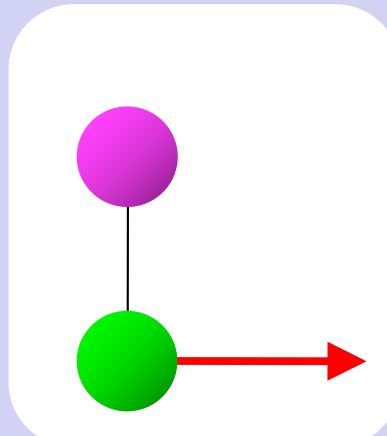
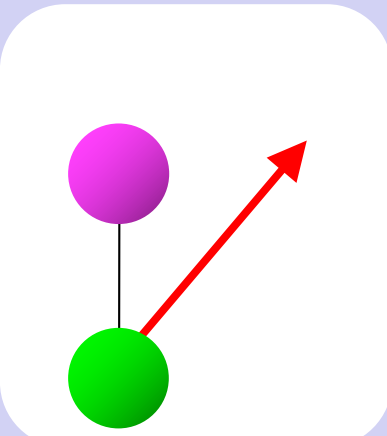
Sum over atoms

$$\chi(k) = \frac{1}{k} \sum_j 3 |\hat{\eta} \cdot \hat{R}|^2 \text{Im} \left\{ f_j(k, \pi) e^{2i\delta_1} \frac{1}{R_j^2} e^{2ikR_j} \right\}$$

$\underbrace{3 \cos^2 \theta_j}_{\boxed{3 \cos^2 \theta_j}}$

Effective coordination number

$$N^* = 3 \sum_j \cos^2 \theta_j$$



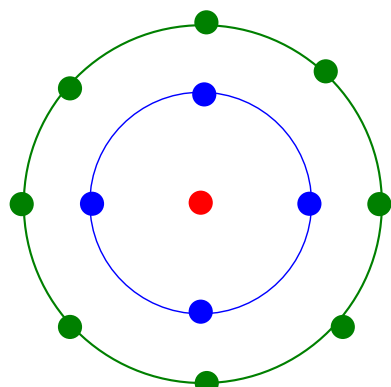
Coordination shells

Sum over atoms

$$\chi(k) = \frac{1}{k} \sum_j 3 |\hat{\eta} \cdot \hat{R}|^2 \operatorname{Im} \left\{ f_j(k, \pi) e^{2i\delta_1} \frac{1}{R_j^2} e^{2ikR_j} \right\}$$

Isotropic samples: $\langle |\hat{\eta} \cdot \hat{R}|^2 \rangle = 1/3$
 $\langle 3|\hat{\eta} \cdot \hat{R}|^2 \rangle = 1$

Coordination shells



Sum over shells

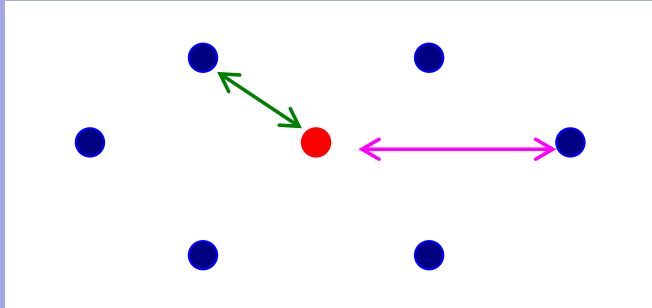
$$\chi(k) = \frac{1}{k} \sum_{\text{shell}} N_s \operatorname{Im} \left[f_s(k, \pi) e^{2i\delta_1} \frac{1}{R_s^2} \exp(2ikR_s) \right]$$

Nr of atoms in the shell

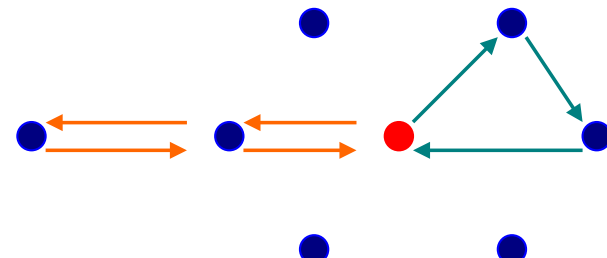
Single and multiple scattering

Scattering paths

SS = Single scattering

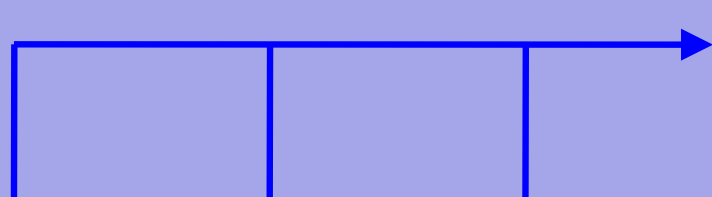


MS = Multiple scattering



Multiple scattering series

Multiple
Scattering



$$\chi_n(k) = n - \text{legs paths}$$

$$\frac{\mu - \mu_0}{\mu_0} = \sum \chi_2(k) + \sum \chi_3(k) + \sum \chi_4(k) + \dots$$

$$\mu(k) = \mu_0(k) \left\{ 1 + \sum \chi_2(k) + \sum \chi_3(k) + \sum \chi_4(k) + \dots \right\}$$

Single
Scattering



$$\mu(k) = \mu_0(k) [1 + \chi(k)]$$

$$\frac{\mu - \mu_0}{\mu_0} = \chi(k)$$

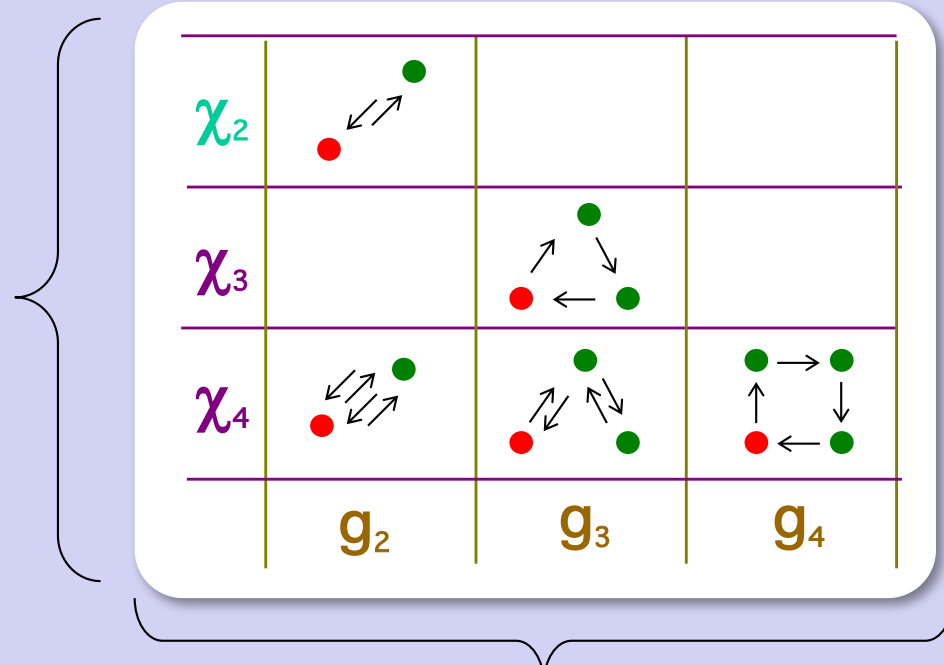
only 2-legs paths
→ coordination shells

Sum over paths and over correlations

$$\mu(k) = \mu_0(k) \left\{ 1 + \sum \chi_2(k) + \sum \chi_3(k) + \sum \chi_4(k) + \dots \right\}$$



Contribution from
all n-order paths



$$\mu(k) = \mu_0(k) \left\{ 1 + \sum \mu^{(2)}(k) + \sum \mu^{(3)}(k) + \sum \mu^{(4)}(k) + \dots \right\}$$

Multiple scattering series

Paolo
Fornasini
Univ. Trento

$$\mu(k) = \mu_0(k) \left\{ 1 + \sum \chi_2(k) + \sum \chi_3(k) + \sum \chi_4(k) + \dots \right\}$$

Full Multiple
Scattering

Intermediate
Multiple Scattering

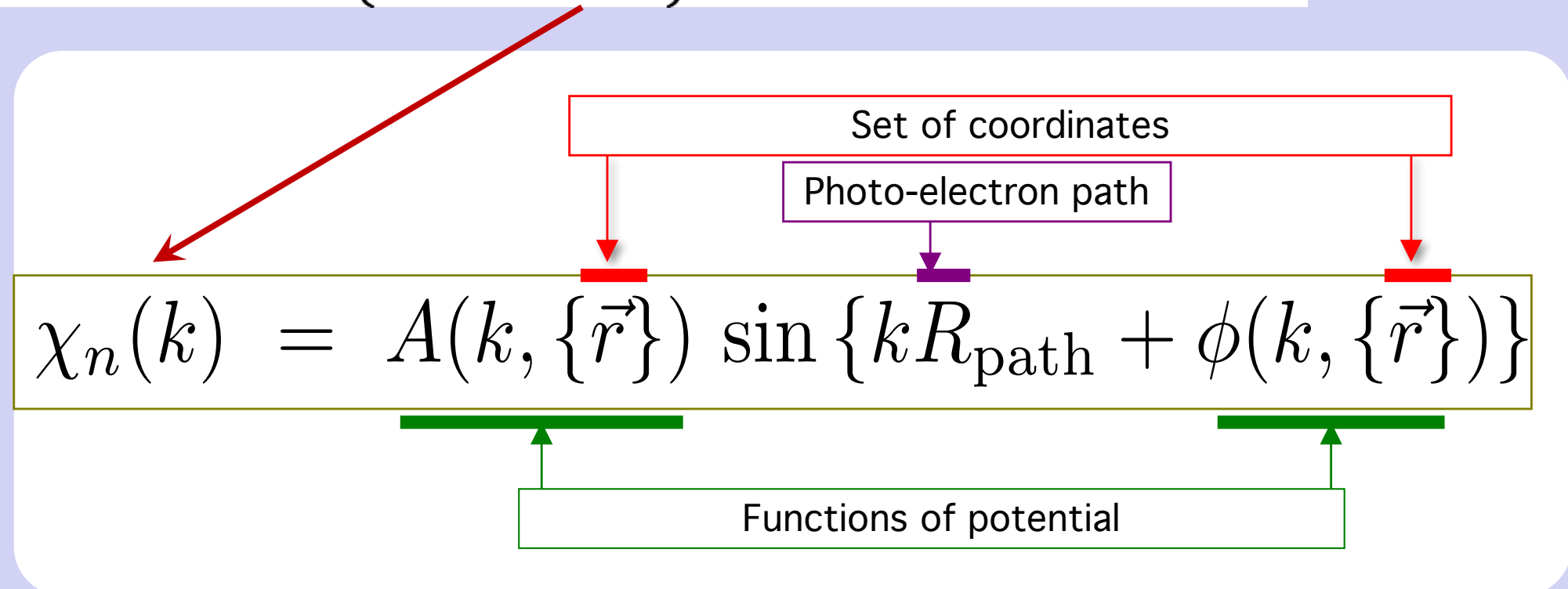
Single Scattering



Photo-electron wave-number k

Multiple scattering contributions

$$\begin{aligned}\mu(k) &= \mu_0(k) \left\{ 1 + \sum \chi_2(k) + \sum \chi_3(k) + \sum \chi_4(k) + \dots \right\} \\ &= \mu_0(k) \left\{ 1 + \sum \chi_n(k) \right\}\end{aligned}$$



Neglecting
thermal disorder !

Intrinsic losses

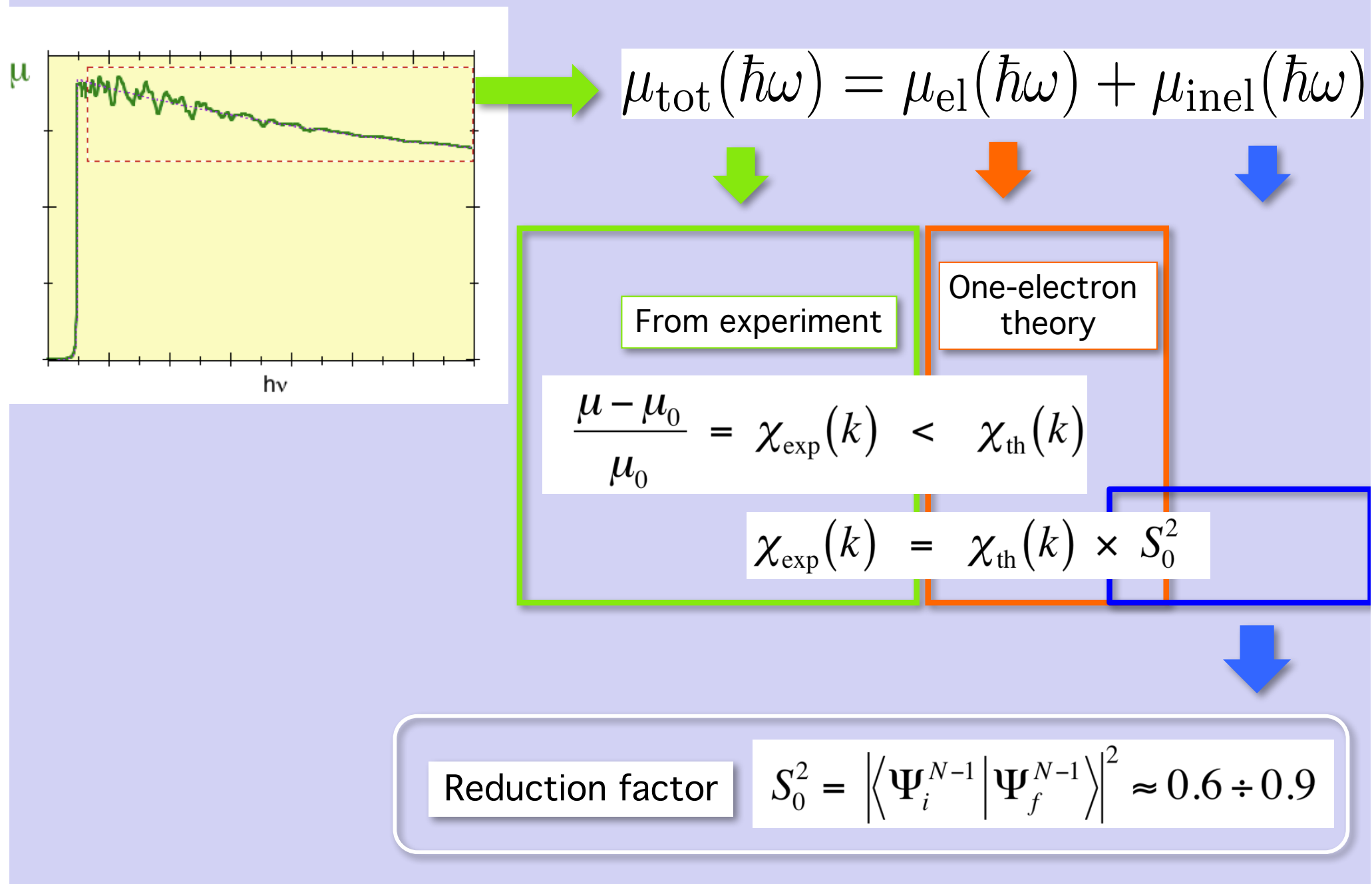


Photo-electron mean-free-path

Core-hole lifetime $\tau_h \rightarrow \lambda_h$

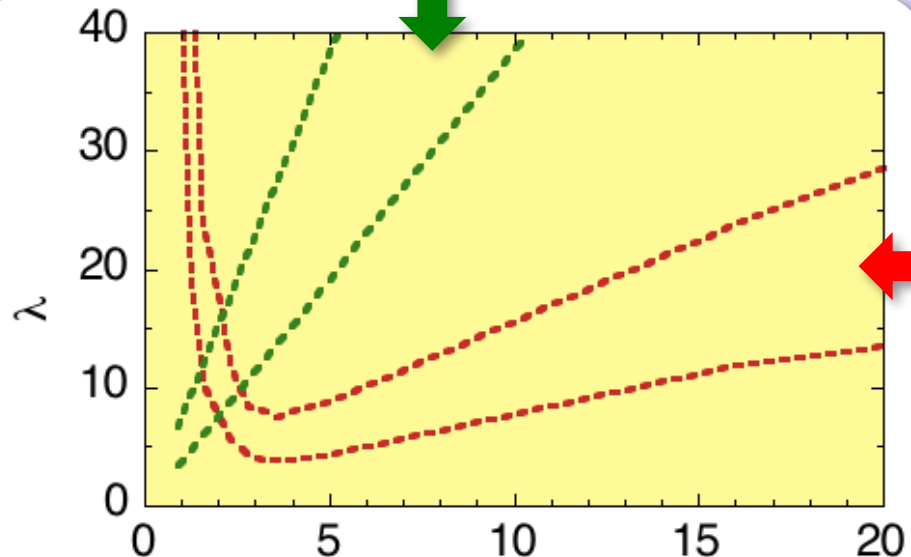
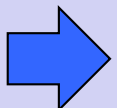


Photo-electron lifetime
 $\tau_e \Leftrightarrow \lambda_e$

TOTAL

$$\frac{1}{\lambda} = \frac{1}{\lambda_h} + \frac{1}{\lambda_e}$$



Reduction factor

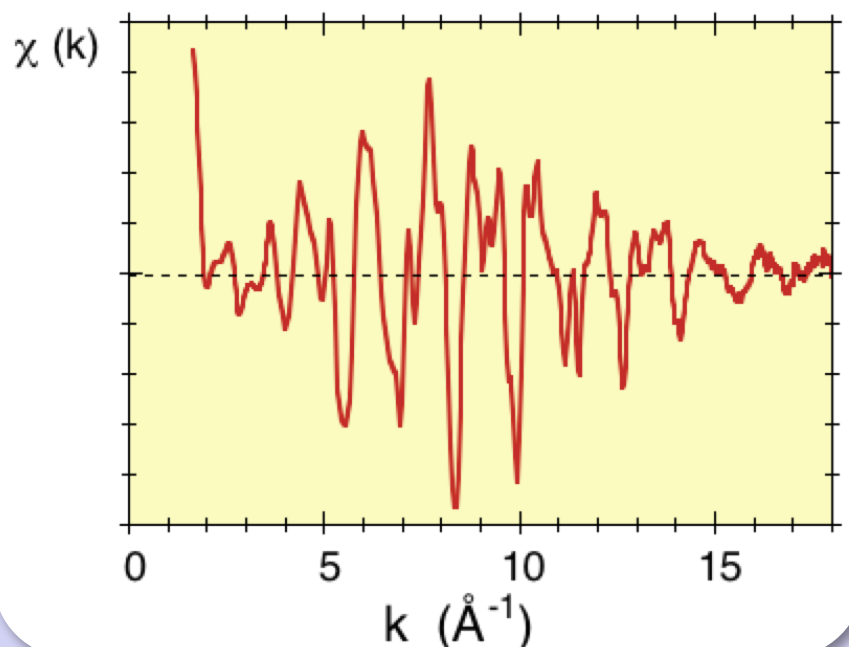
$$\exp\left[-\frac{2R}{\lambda(k)}\right]$$

EXAFS and inelastic effects

Intrinsic
inelastic effects

Photo-electron
mean-free-path

$$\chi(k) = \frac{S_0^2}{k} \sum_{shell} N_s \operatorname{Im} \left[f_s(k, \pi) e^{2i\delta_l} \frac{e^{-2R_s/\lambda(k)}}{R_s^2} \exp(2ikR_s) \right]$$



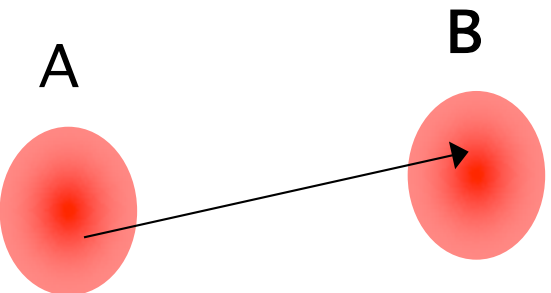
Atoms frozen
at equilibrium positions !



Thermal disorder effects ?

Vibrational disorder

Paolo
Fornasini
Univ. Trento



Period of atomic vibrations

$$\tau_{\text{vib}} \approx 10^{-12} \text{ s}$$

Photoelectron time of flight

$$\tau_{\text{EXAFS}} \approx 10^{-15} \text{ s}$$

One photoelectron



Instantaneous distance

EXAFS spectrum

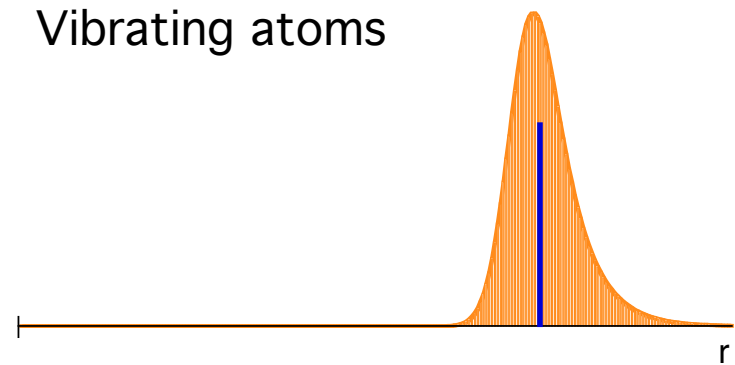


Distribution of distances

Fixed atoms



Vibrating atoms



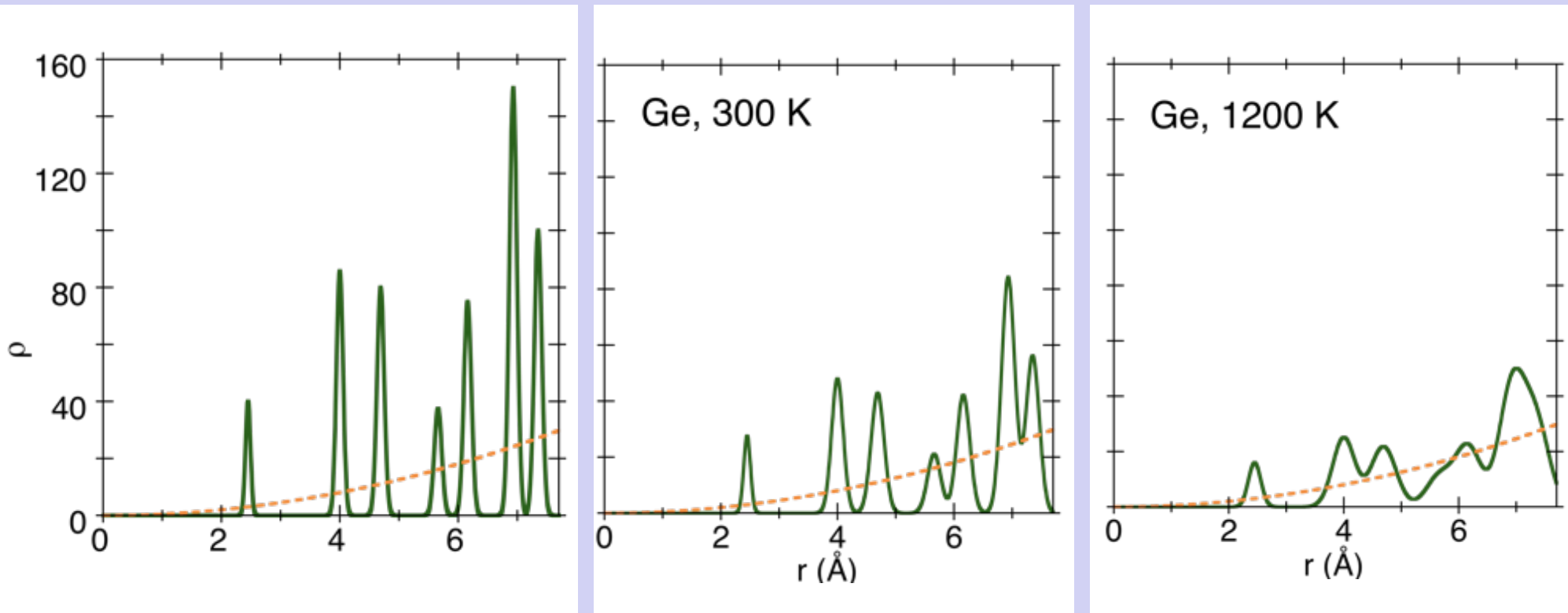
Distance



Distribution of distances

Vibrational disorder in crystals

Simulated radial distributions for c-Ge

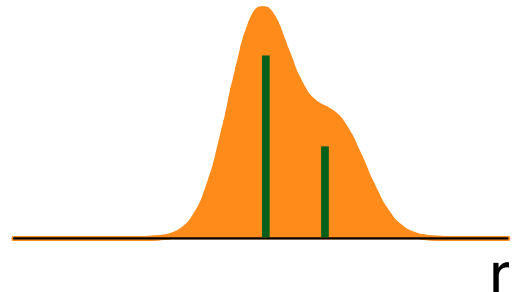
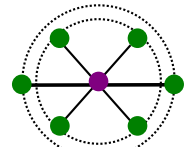


Separability of coordination shells ?

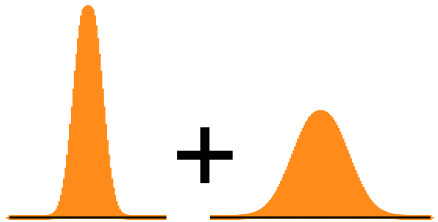
Structural disorder

Paolo
Fornasini
Univ. Trento

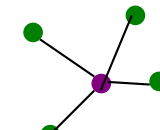
Distorted shells in crystals



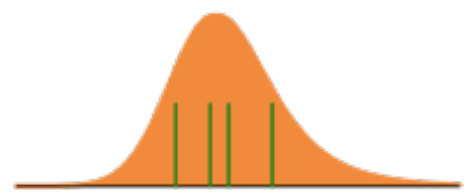
Sites disorder in crystals



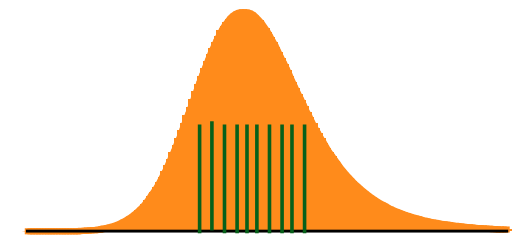
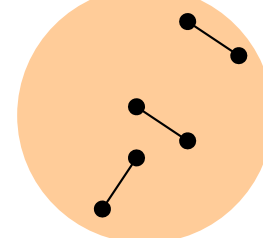
Non-crystalline systems



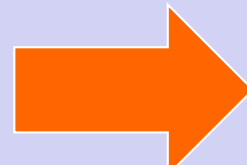
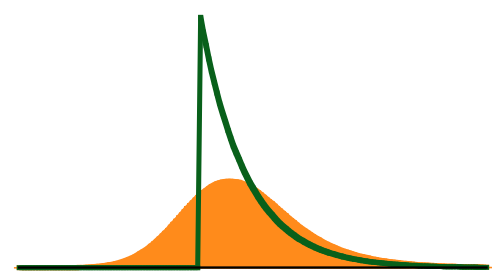
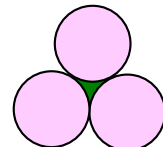
e.g.: a-Ge



Nano-structures



Free-volume models

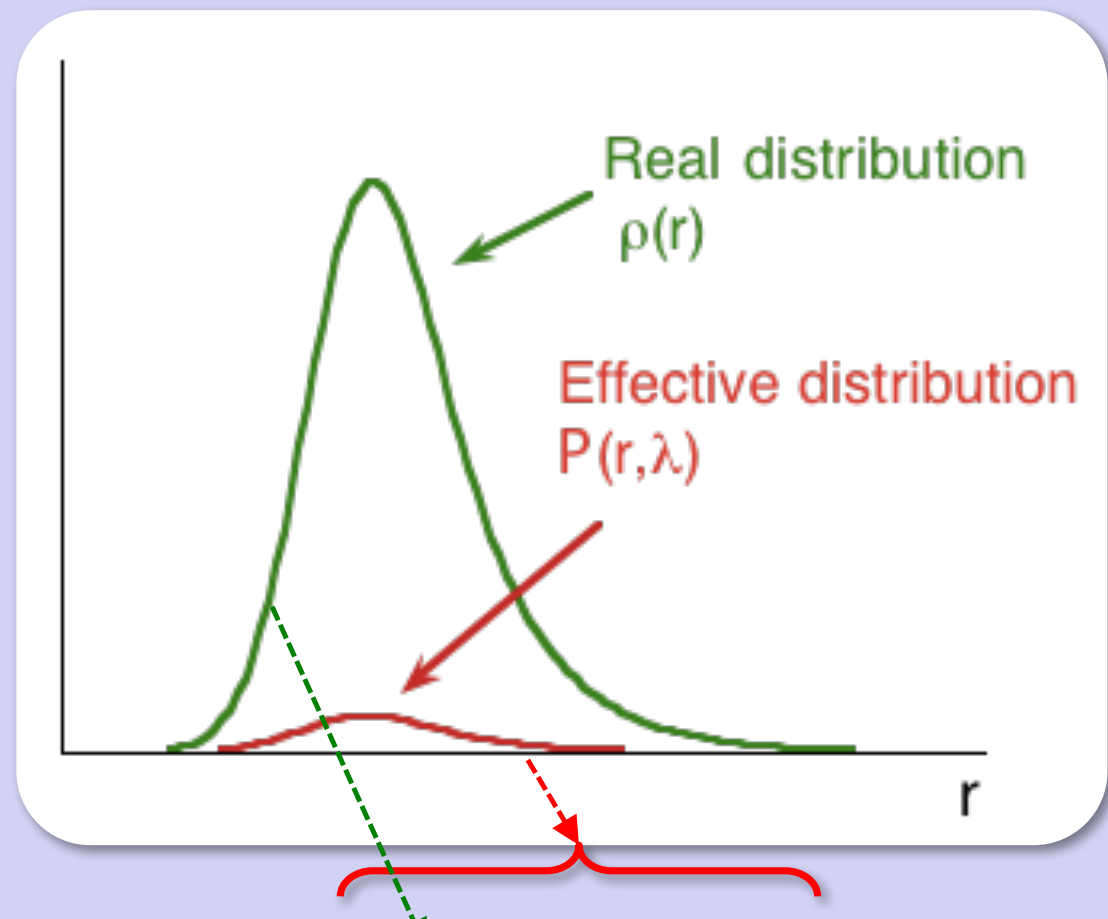


Enlarged
distributions
of distances

Distributions of distances

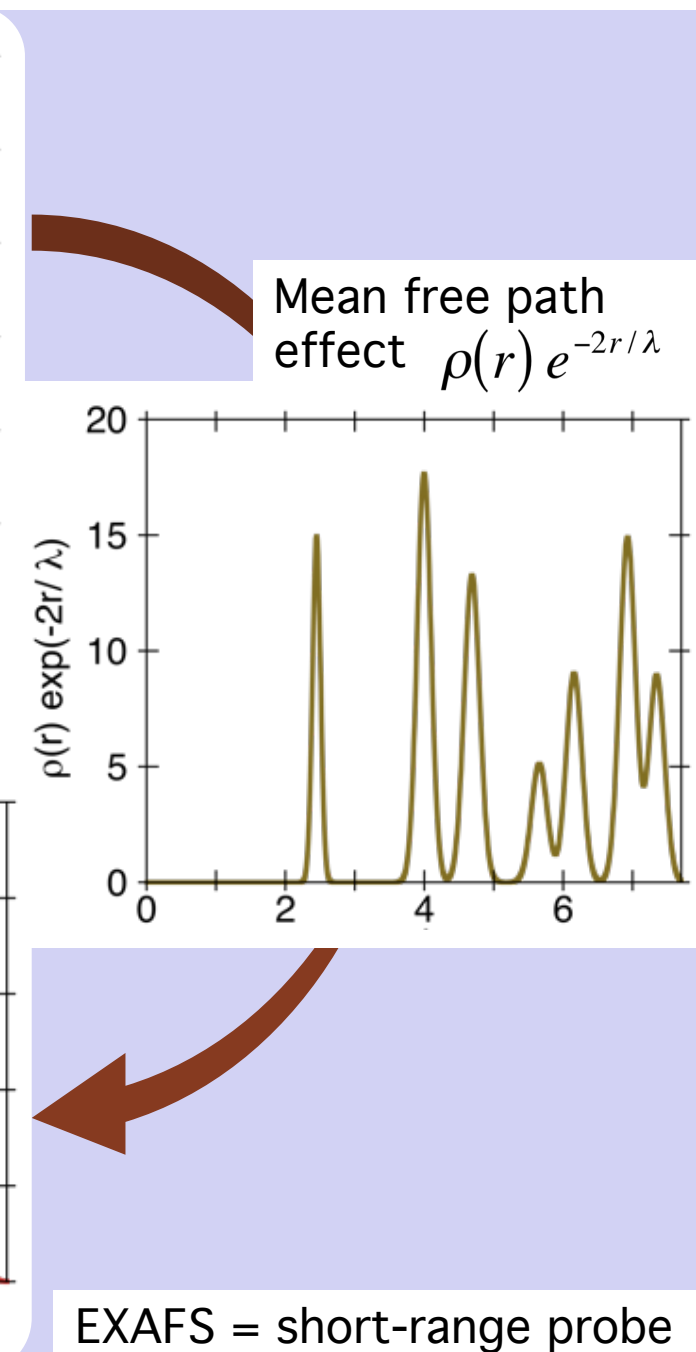
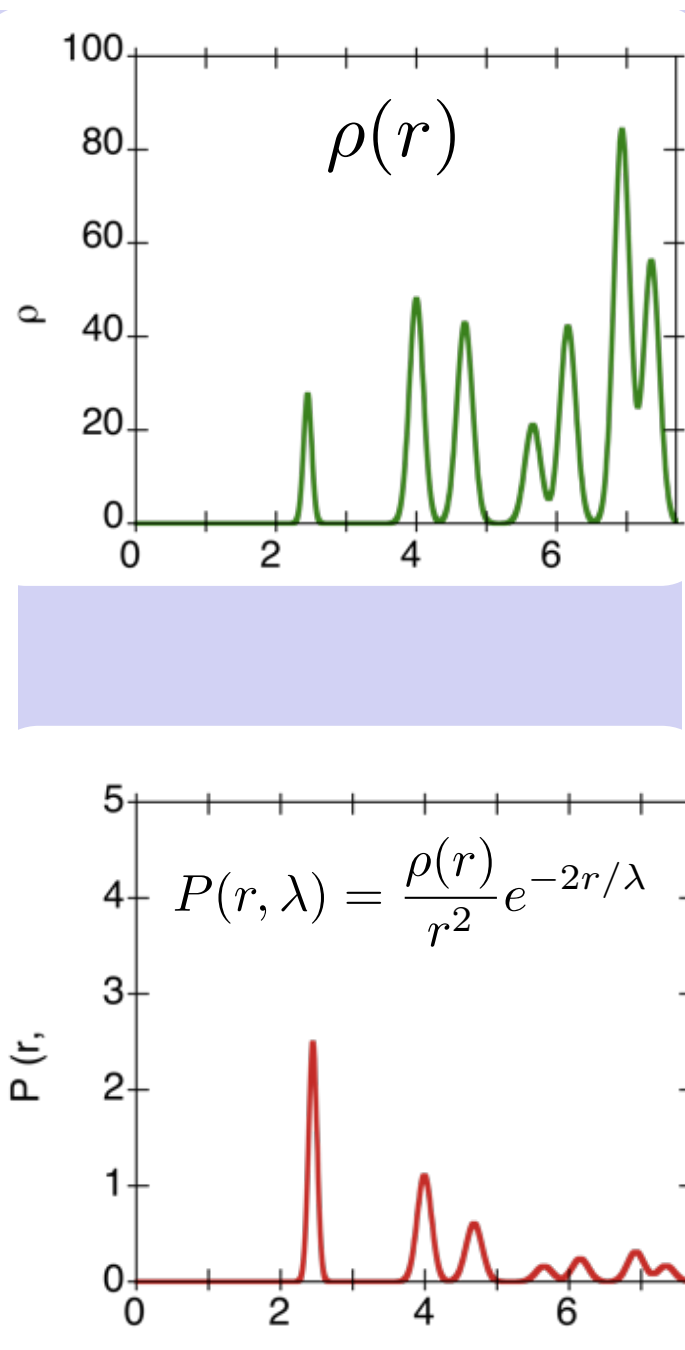
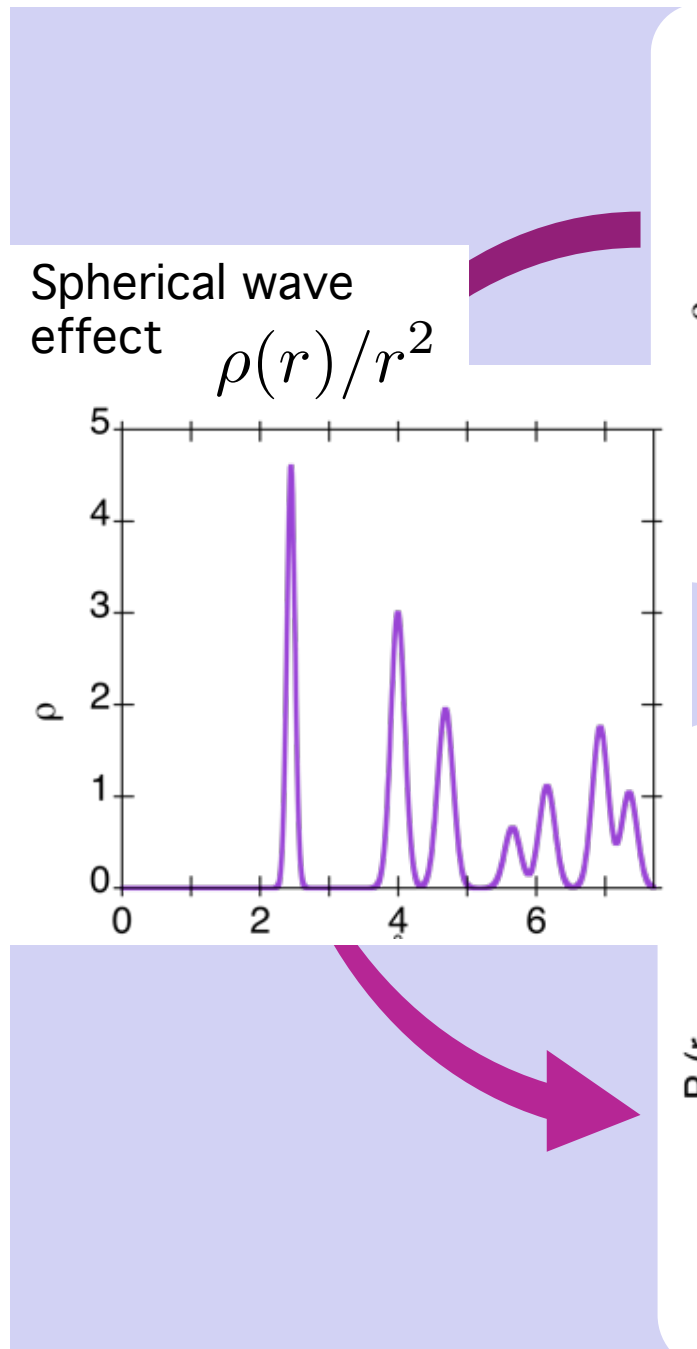
Thermal + structural disorder

⇒ distribution of distances



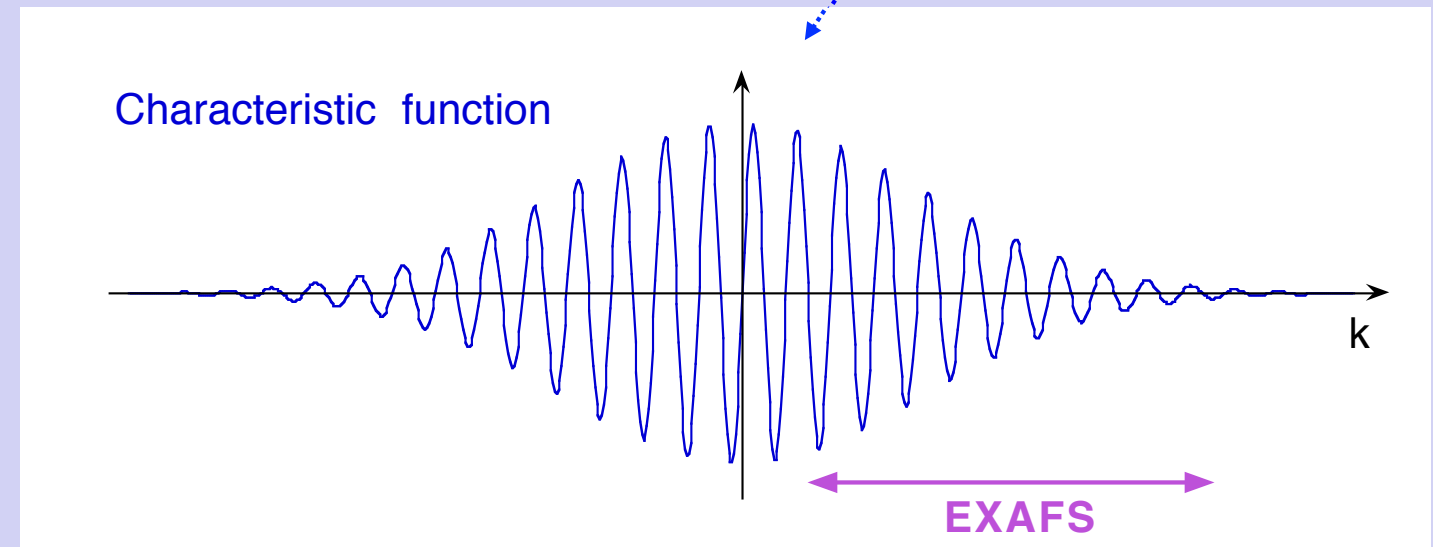
$$\chi(k) = \frac{S_0^2}{k} \sum_{\text{shells}} N_s \operatorname{Im} \left[f_s(k, \pi) e^{2i\delta_1} \int_0^\infty \rho_s(r) \frac{e^{-2r_s/\lambda(k)}}{r_s^2} e^{2ikr_s} dr \right]$$

Real and effective distributions



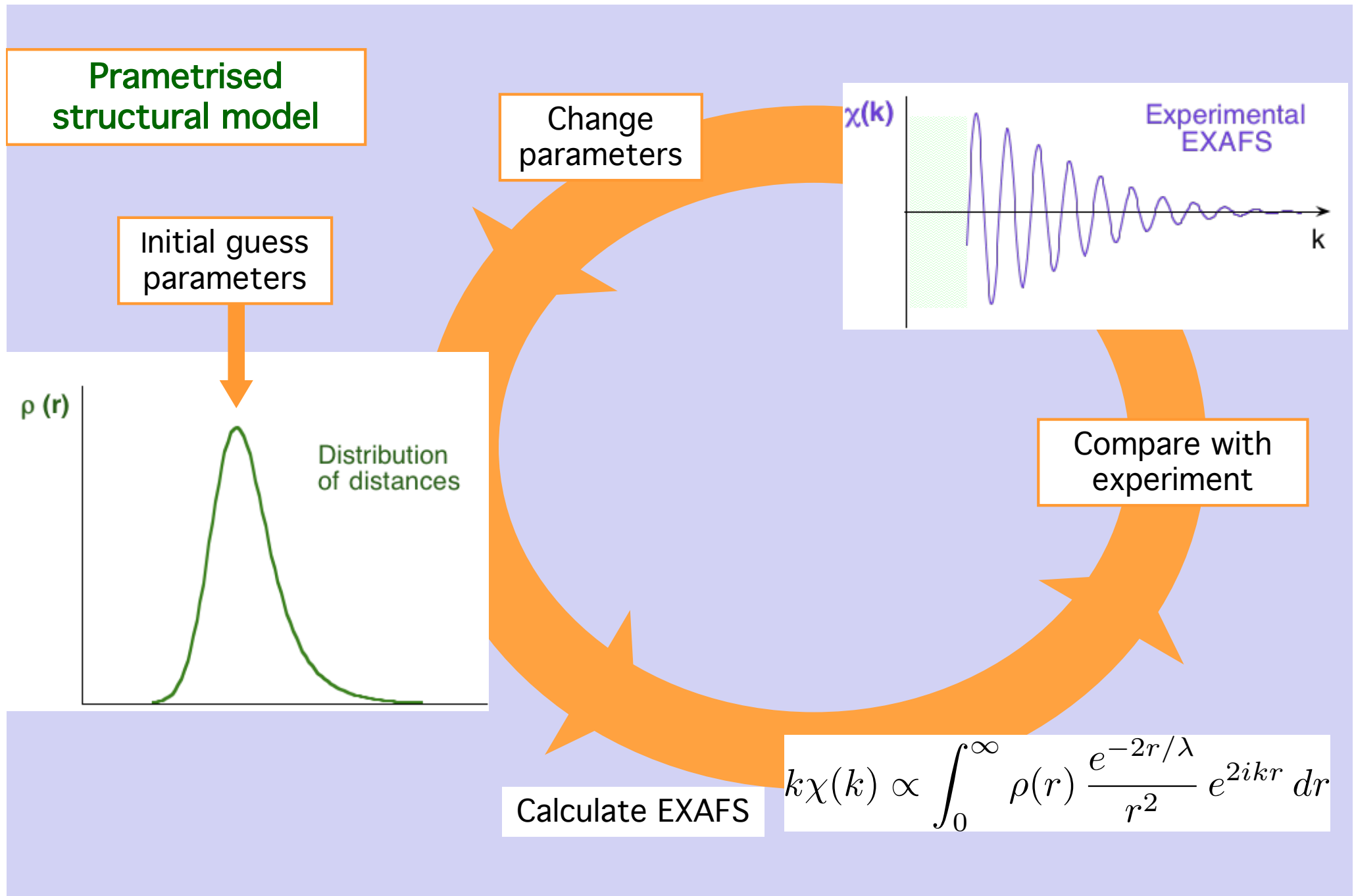
The inversion problem

$$\chi(k) = \frac{S_0^2}{k} \sum_{shell} N_s \operatorname{Im} \left[f_s(k, \pi) e^{2i\delta_l} \int_0^\infty \rho_s(r) \frac{e^{-2r_s/\lambda(k)}}{r_s^2} e^{2ikr_s} dr \right]$$

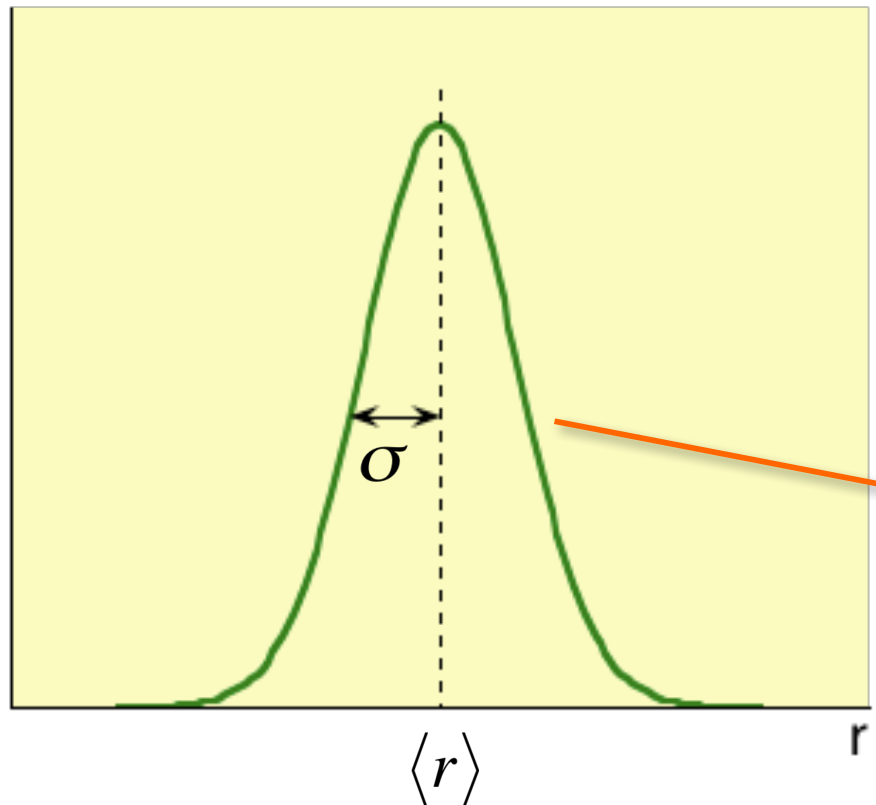


$\chi(k) \Rightarrow \rho(r)$?

Structural models and fitting procedure



The simplest model: gaussian approximation



$$P(r, \lambda) = \frac{1}{\sigma \sqrt{2\pi}} \exp \left[\frac{(r - \langle r \rangle)^2}{2\sigma^2} \right]$$

$$C_2 = \sigma^2 = \langle (r - \langle r \rangle)^2 \rangle$$

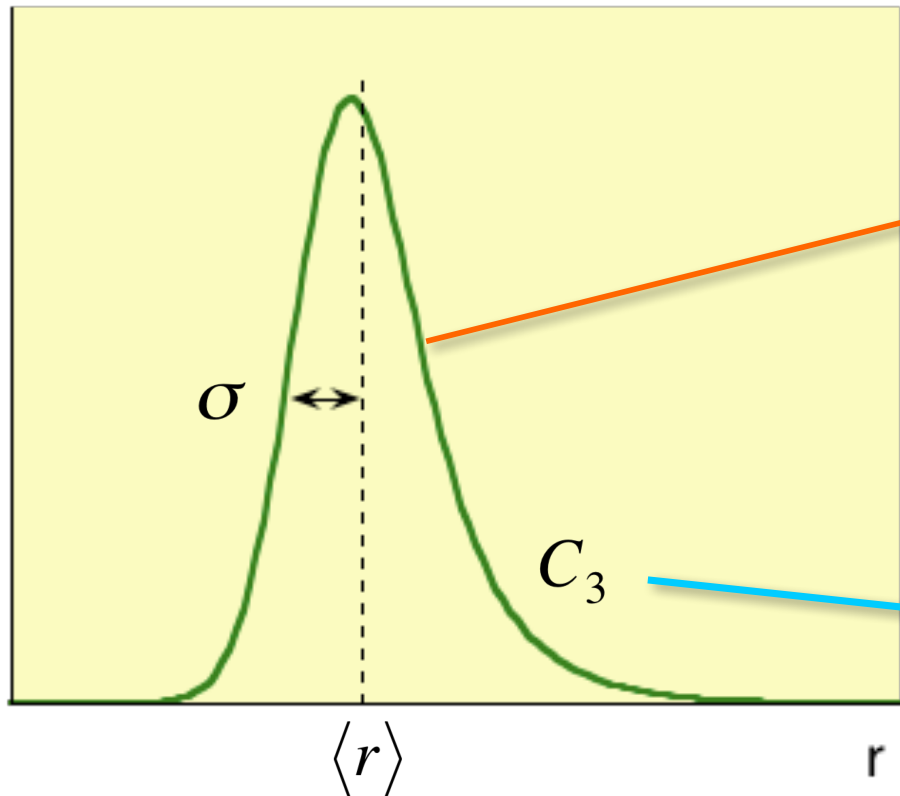
Distribution width
(EXAFS Debye-Waller factor)

$$C_1 = \langle r \rangle_{\text{eff}} = \langle r \rangle_{\text{real}} - \frac{2\sigma^2}{\langle r \rangle} \left(1 - \frac{\langle r \rangle}{\lambda} \right)$$

Average distance

Including weak asymmetry

Asymmetric distribution



$$C_2 = \sigma^2 = \langle (r - \langle r \rangle)^2 \rangle$$

$$C_3 = \langle (r - \langle r \rangle)^3 \rangle$$

Third cumulant
Asymmetry parameter

$$C_1 = \langle r \rangle_{\text{eff}} = \langle r \rangle_{\text{real}} - \frac{2\sigma^2}{\langle r \rangle} \left(1 - \frac{\langle r \rangle}{\lambda} \right)$$

Better for first shell

EXAFS including asymmetry (one shell)



- Theory (interaction potentials + scattering theory)
- Experiment (reference samples)

Inelastic terms

Back-scattering amplitude

Total phase-shift

$$k \chi(k) = \frac{S_0^2 e^{-2C_1/\lambda}}{C_1^2} |f(k, \pi)| N \exp[-2k^2\sigma^2] \sin\left[2kC_1 - \frac{4}{3}k^3C_3 + \phi(k)\right]$$

Coordination number

N

Debye-Waller

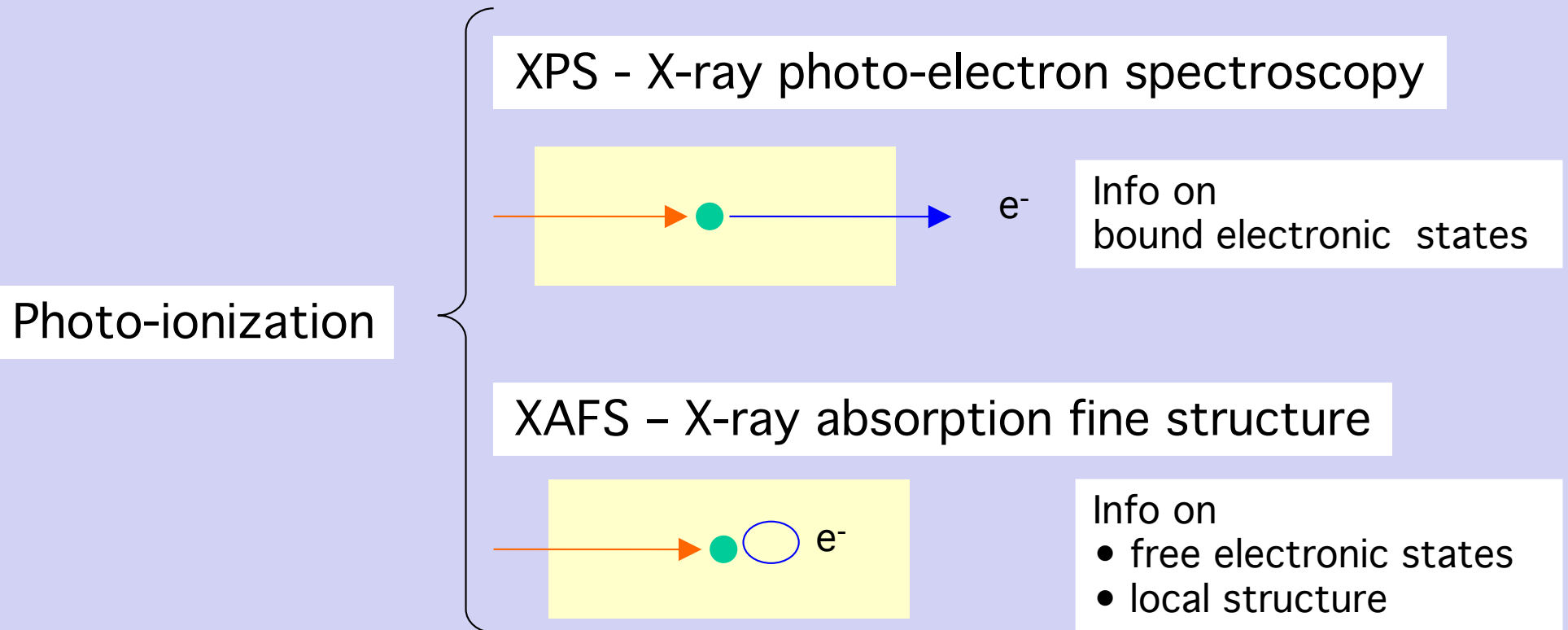
σ^2

Average distance and asymmetry

C_1

C_3

XAFS and other techniques

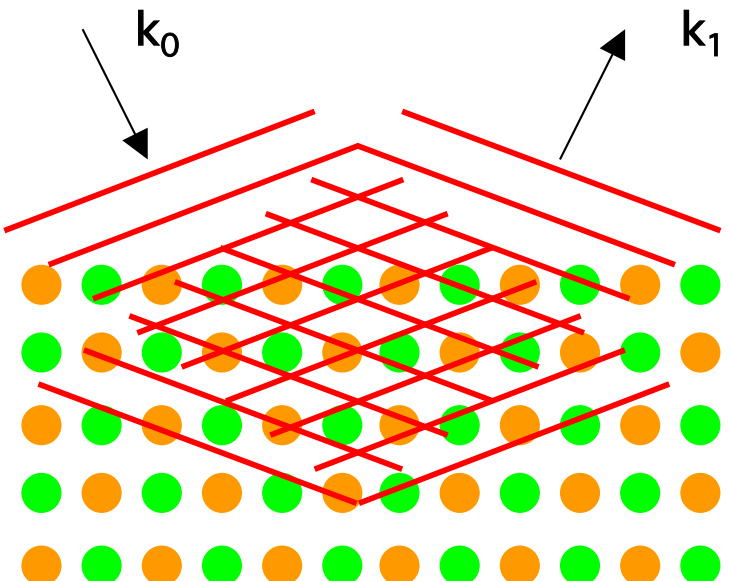


XAFS = structural probe – Comparison with diffraction ?

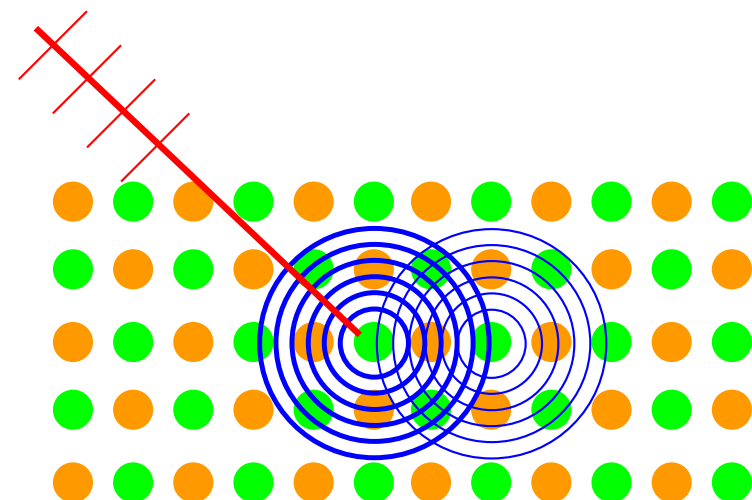
Bragg scattering .vs. EXAFS

Paolo
Fornasini
Univ. Trento

Bragg scattering



EXAFS



X-ray or neutron plane waves

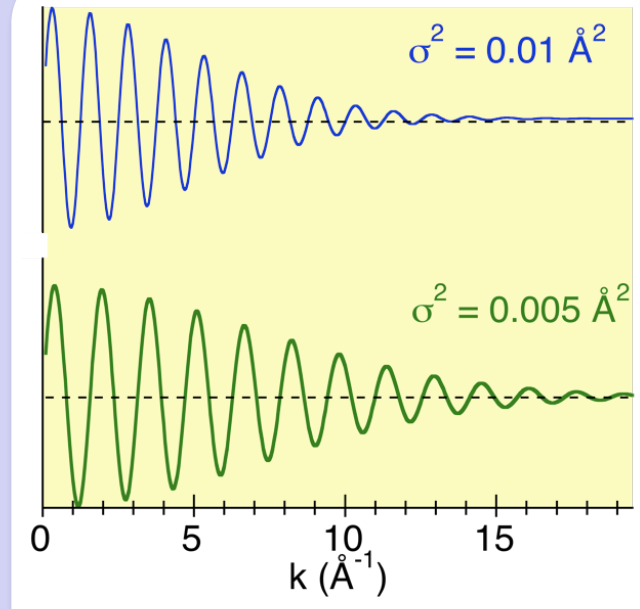
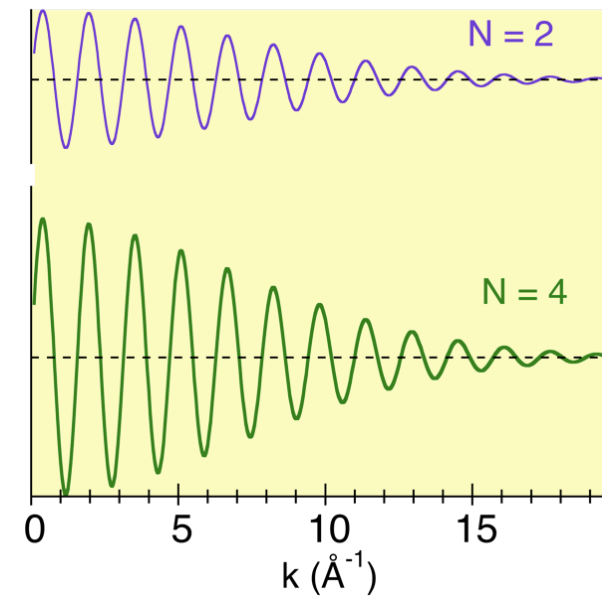
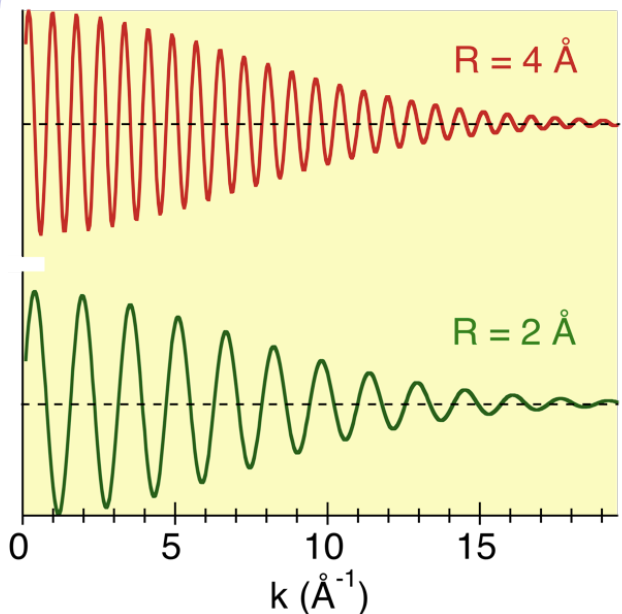
Structural probe

photo-electron spherical wave

- long-range sensitivity
- atomic positions
- atomic thermal factors

- short-range sensitivity
- inter-atomic distances
- relative displacements

EXAFS: a structural probe



Inter-atomic
distance

Coordination
number

Disorder

- Selectivity of atomic species
- Insensitivity to long-range order

Main EXAFS applications

Paolo
Fornasini
Univ. Trento

Non-crystalline
materials

mono-atomic

many-atomic

Active sites
embedded
in a matrix

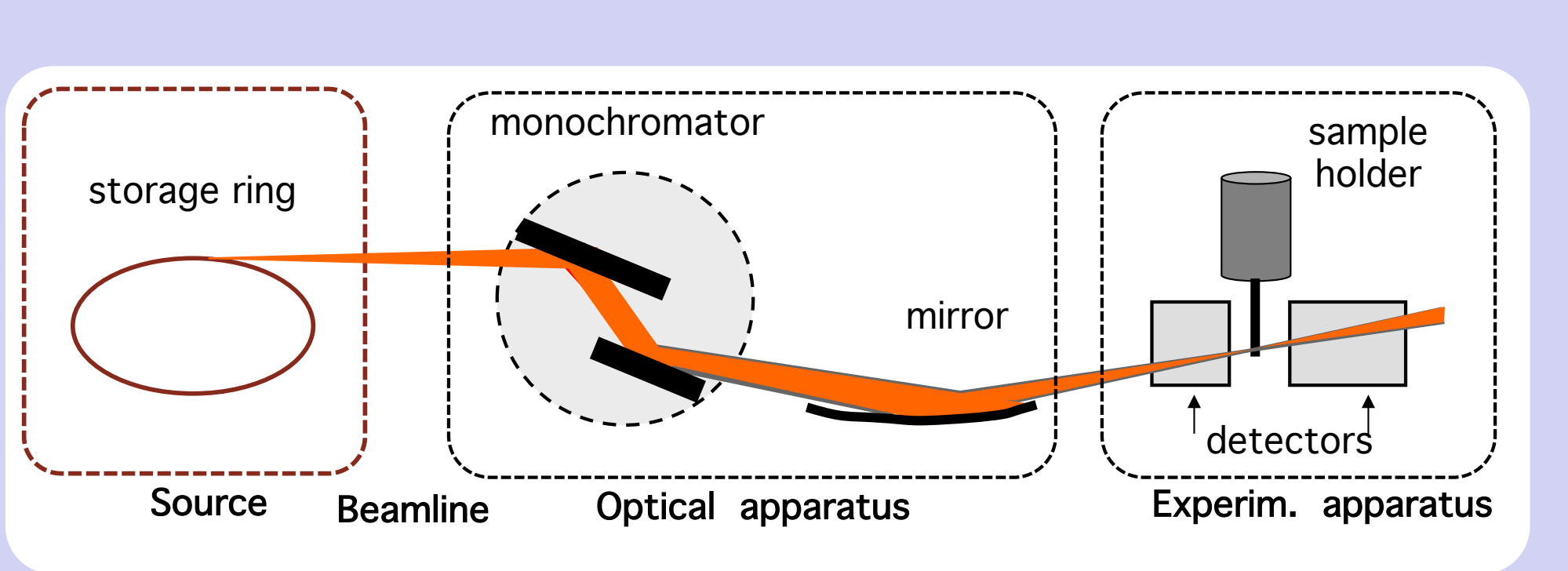
- Inorganic heterogeneous catalysts
- Metallo-proteins
- Impurities in semiconductors
- Luminescent atoms

Local properties
different from
average properties

- Crystalline ternary random alloys
- Lattice dynamics studies
- Negative thermal expansion

EXAFS experiments

XAFS: experimental layout



Sample conditioning:

cryostat
oven
reactor
manipulators

Detection:

transmission
fluorescence
electron yield
.....

Alternative layouts:

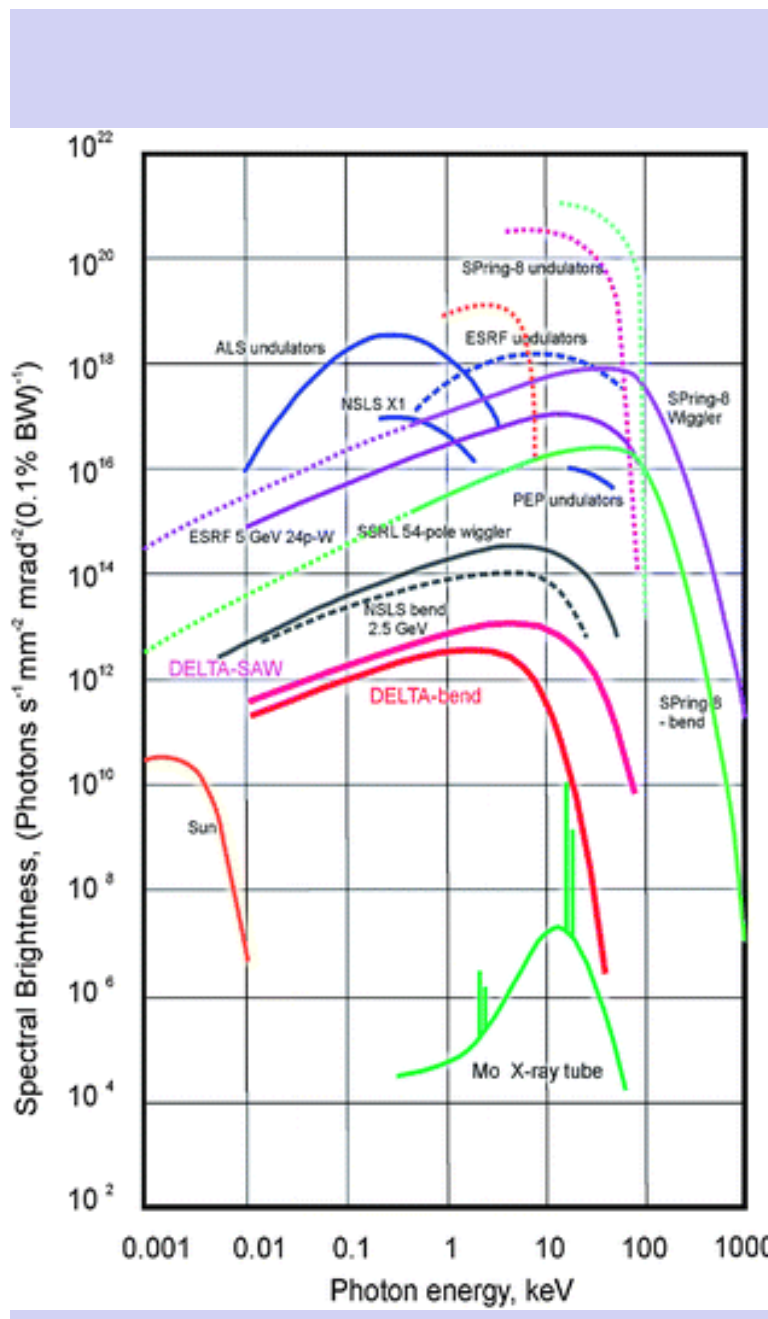
- dispersive EXAFS
- refl-EXAFS
-

XAFS: experimental

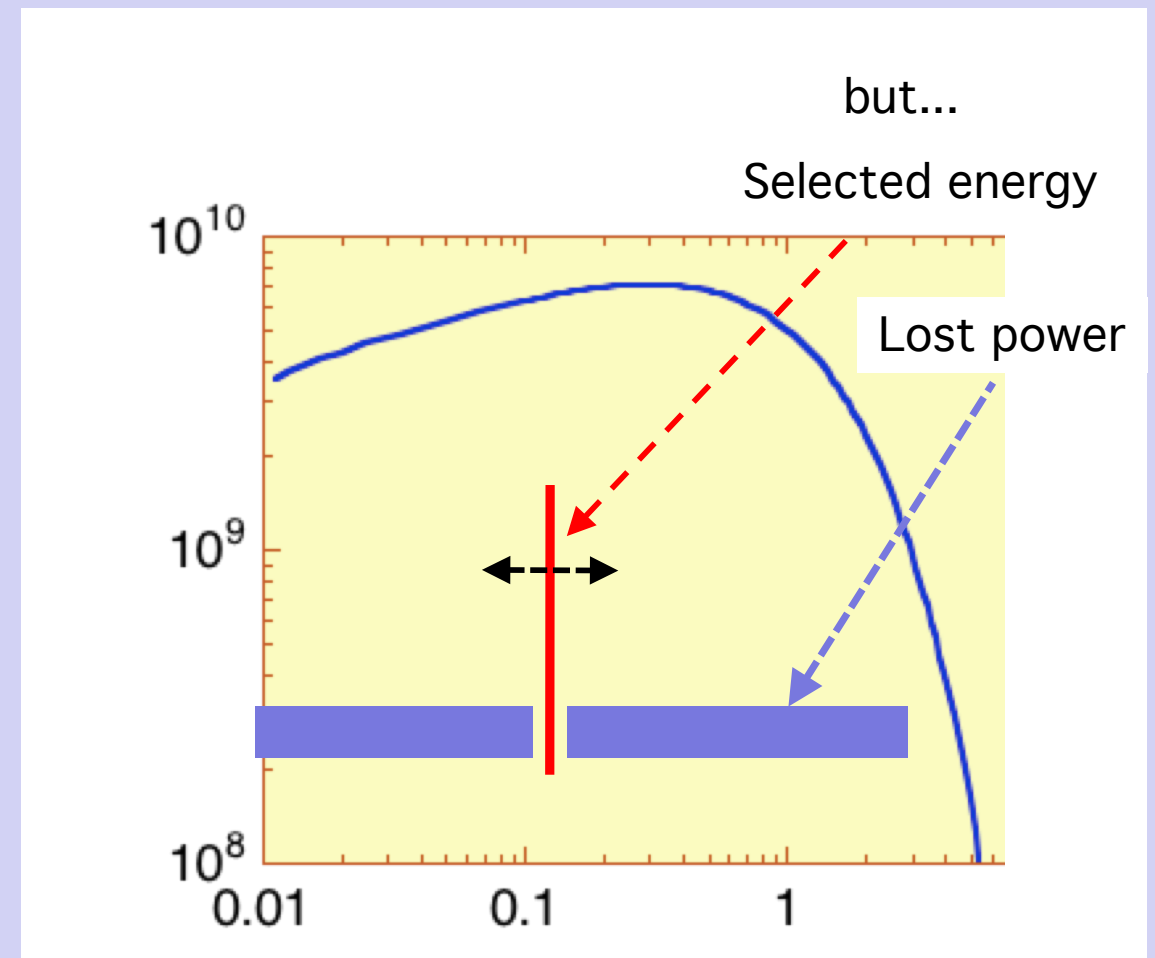
♠ Sources

Wigglers and bending magnets

Paolo
Fornasini
Univ. Trento



Intense and continuum spectrum – OK for EXAFS



Energy of n-th harmonic (one electron)

$$E_n(\theta) = \frac{2hc\gamma^2 n / \lambda_u}{1 + K^2/2 + \gamma^2\theta^2}.$$

To obtain a continuous spectrum:

1. Angle-integrated flux
2. Large horizontal e-beam size
(high-beta sections)
3. Modify K by modifying the gap
 - 3a – Vertical shift of magnet arrays
 - 3b - Tapered undulators

Collimated intense beams, useful for:

- small samples (e.g. pressure measurements)
- fast measurements

XAFS: experimental

- ♠ Monochromators and mirrors

X-ray crystal monochromators

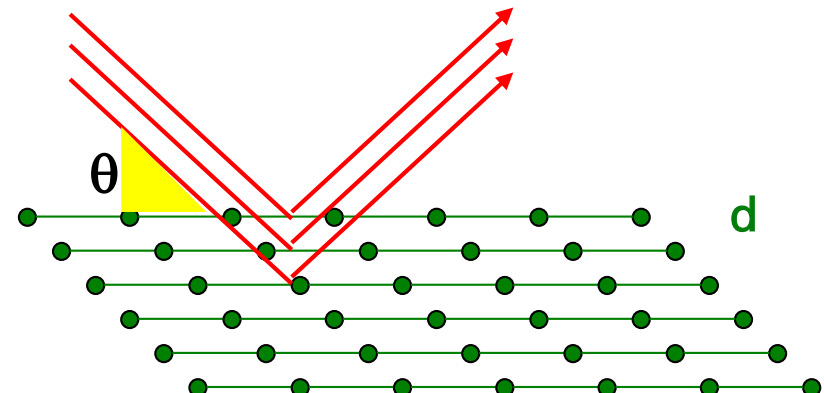
Paolo
Fornasini
Univ. Trento

Bragg law

$$2d_{hkl} \sin\theta = n\lambda$$

Angle \Leftrightarrow wavelength

$$2d_{hkl}[\text{\AA}] \sin\theta = \frac{n \cdot 12.4}{E[\text{keV}]}$$



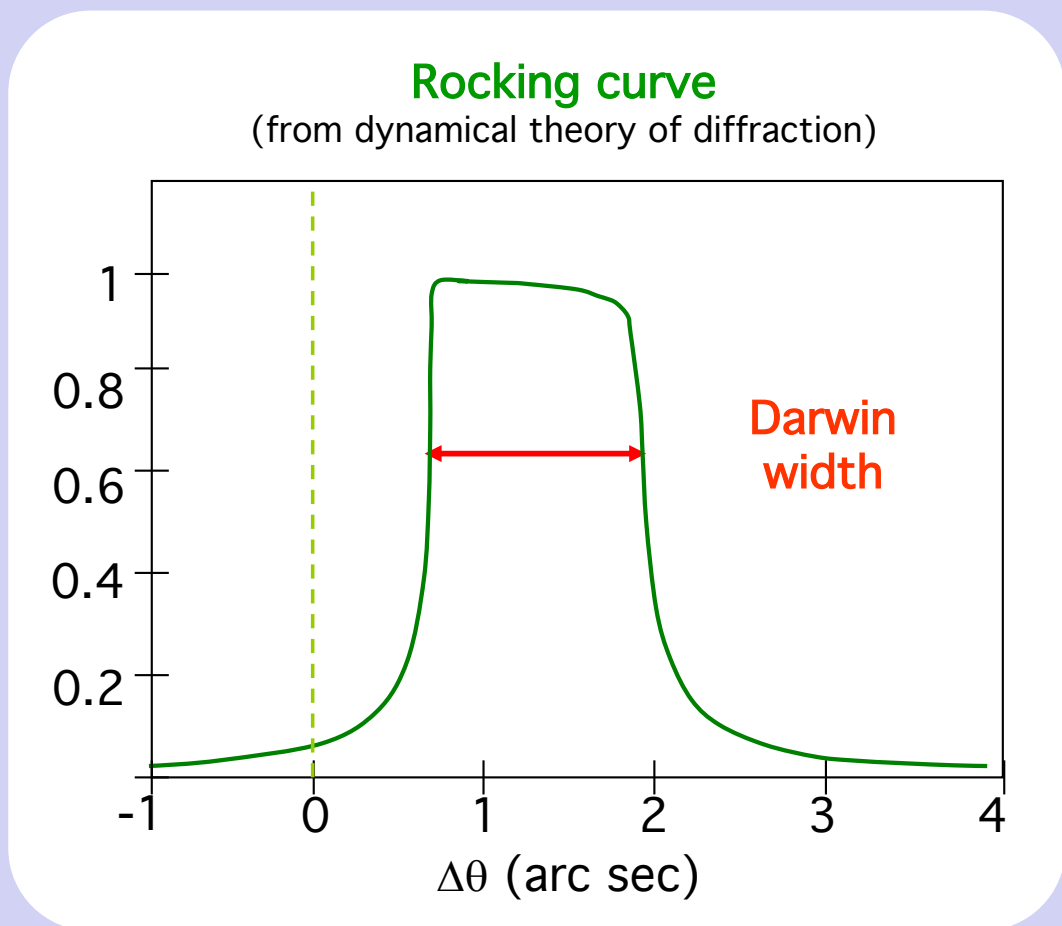
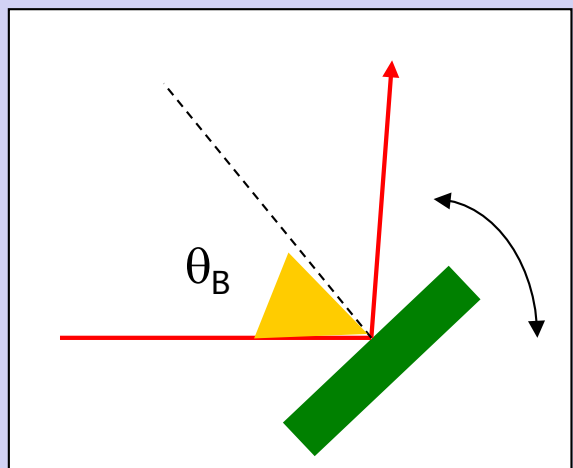
2d

	2d
Si (111)	6.2708
Si (220)	3.84
Si (311)	3.28
Si (331)	2.5
Si (511)	2.08
Ge (111)	6.5328
Ge (220)	4.0004



- Forbidden 'reflections'
- Harmonics
- Spurious reflections

Crystal reflectivity



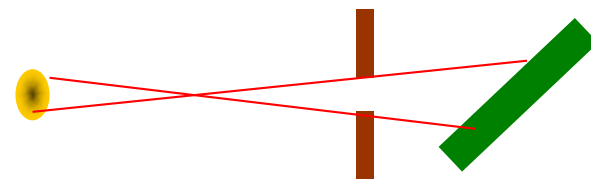
Higher order reflections have narrower rocking curves.

Energy resolution

Darwin width
(Intrinsic resolution)

+

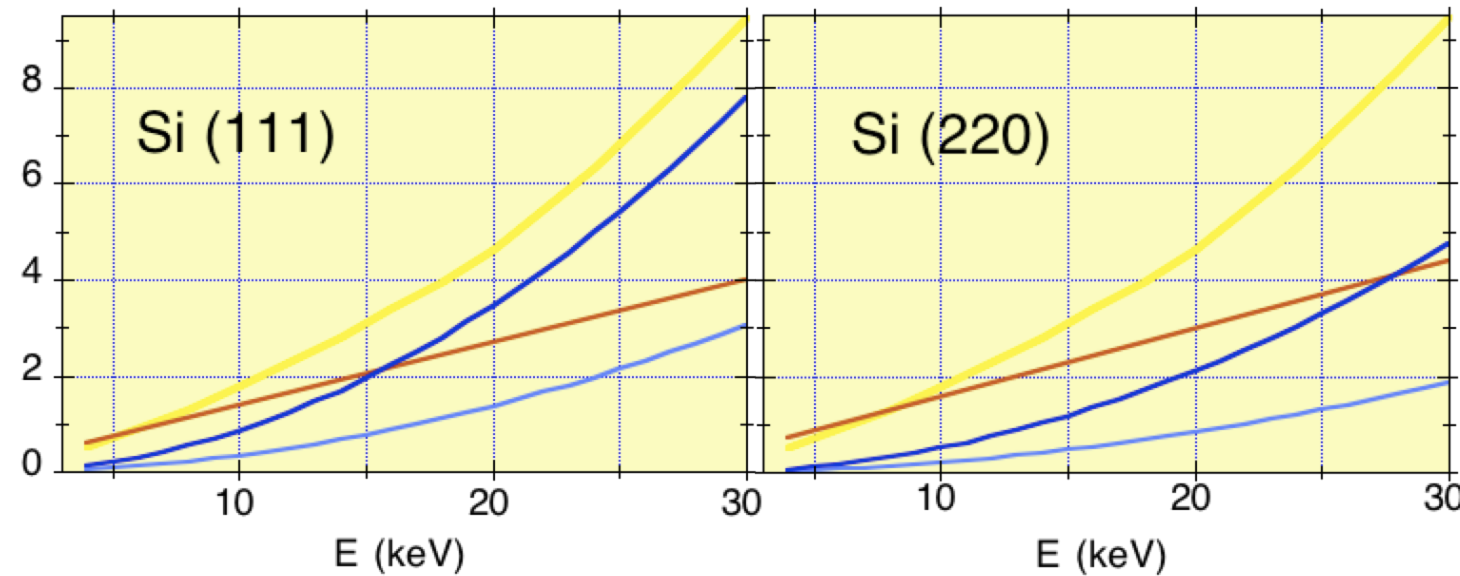
Beam divergence



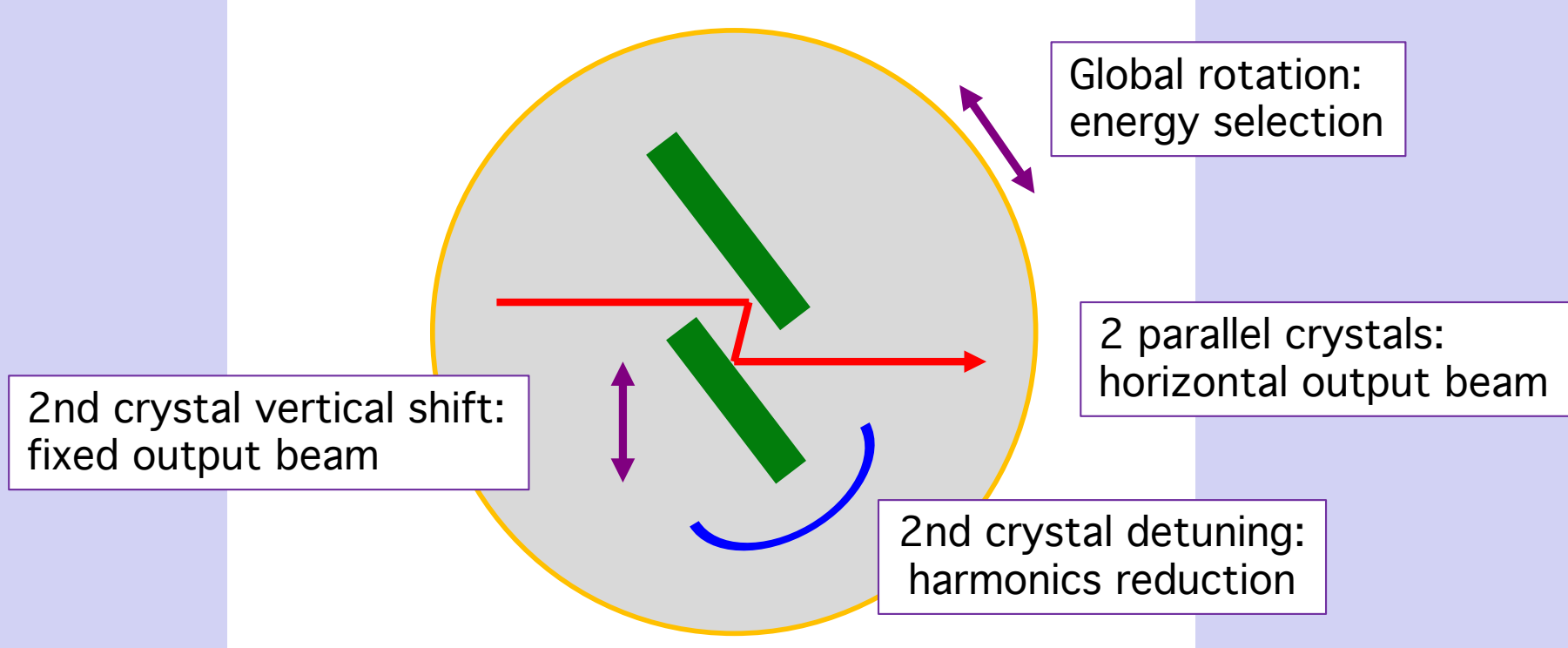
=

Total angle $\Delta\Theta$

$$\frac{\Delta E}{E} = \frac{\Delta\lambda}{\lambda} = \Delta\Theta \cotg\theta_B$$

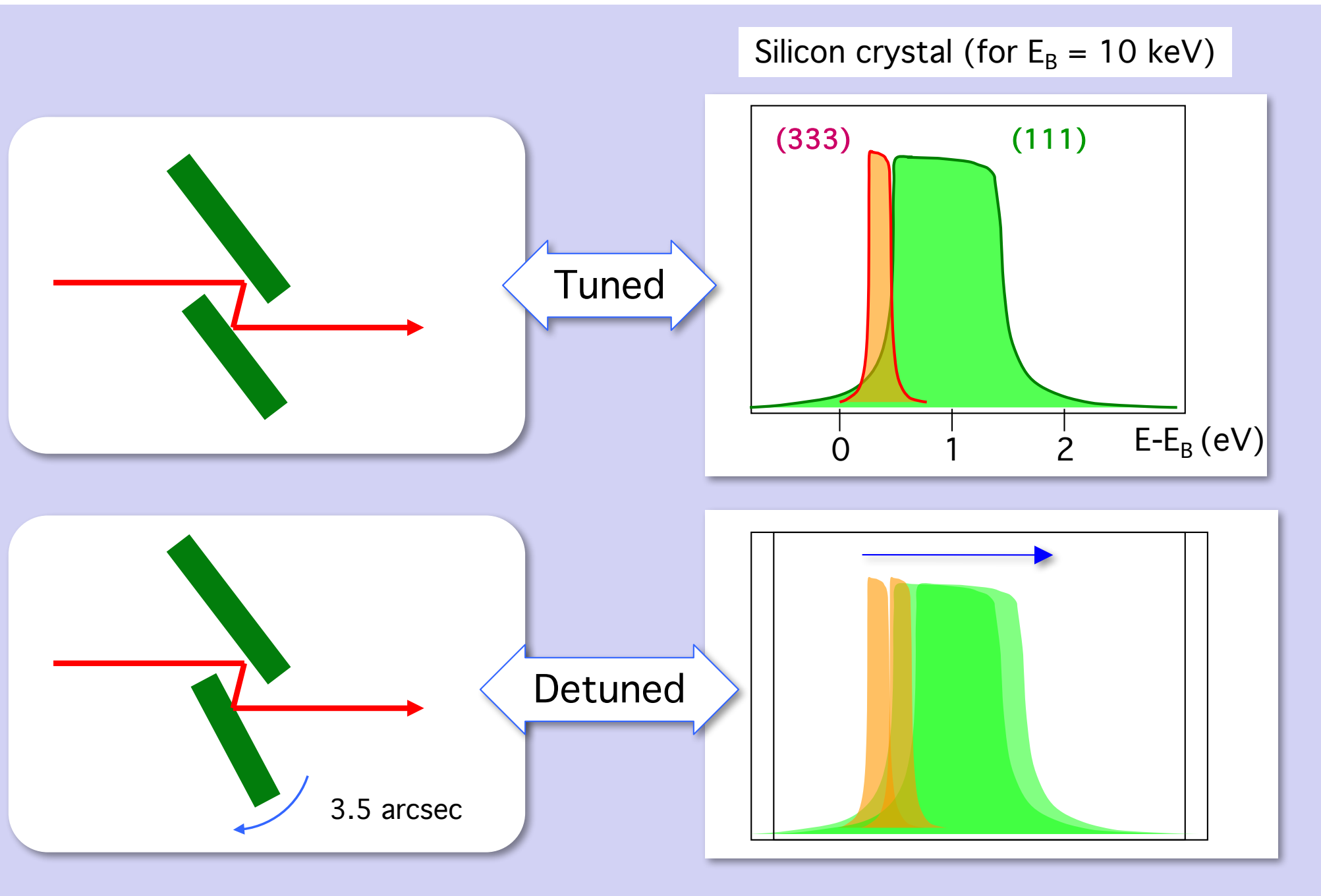


Two-independent-crystals monochromators



But: ☺ Mechanical complexity
☹ possible instabilities

Independent crystals detuning



X-ray mirrors – harmonics rejection

Negligible reflectivity from metal surfaces → no traditional mirrors

Complex refractive index

$$n = 1 - \delta - i\beta$$

$$\delta \simeq 10^{-6} - 10^{-5}$$

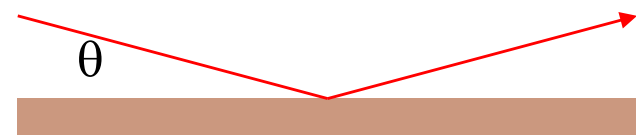
$$n_{\text{real}} < 1$$

Total external reflection for $\theta < \theta_c$

$$\theta_c = \sqrt{2\delta} \simeq \lambda\sqrt{\rho}$$

$$\downarrow$$

$$\theta_c \simeq 10^{-3} \text{ rad}$$



$$\rightarrow \theta_c \propto \lambda$$

$$\downarrow$$

$$\theta_c(\lambda/n) < \theta < \theta_c(\lambda)$$



harmonics rejection

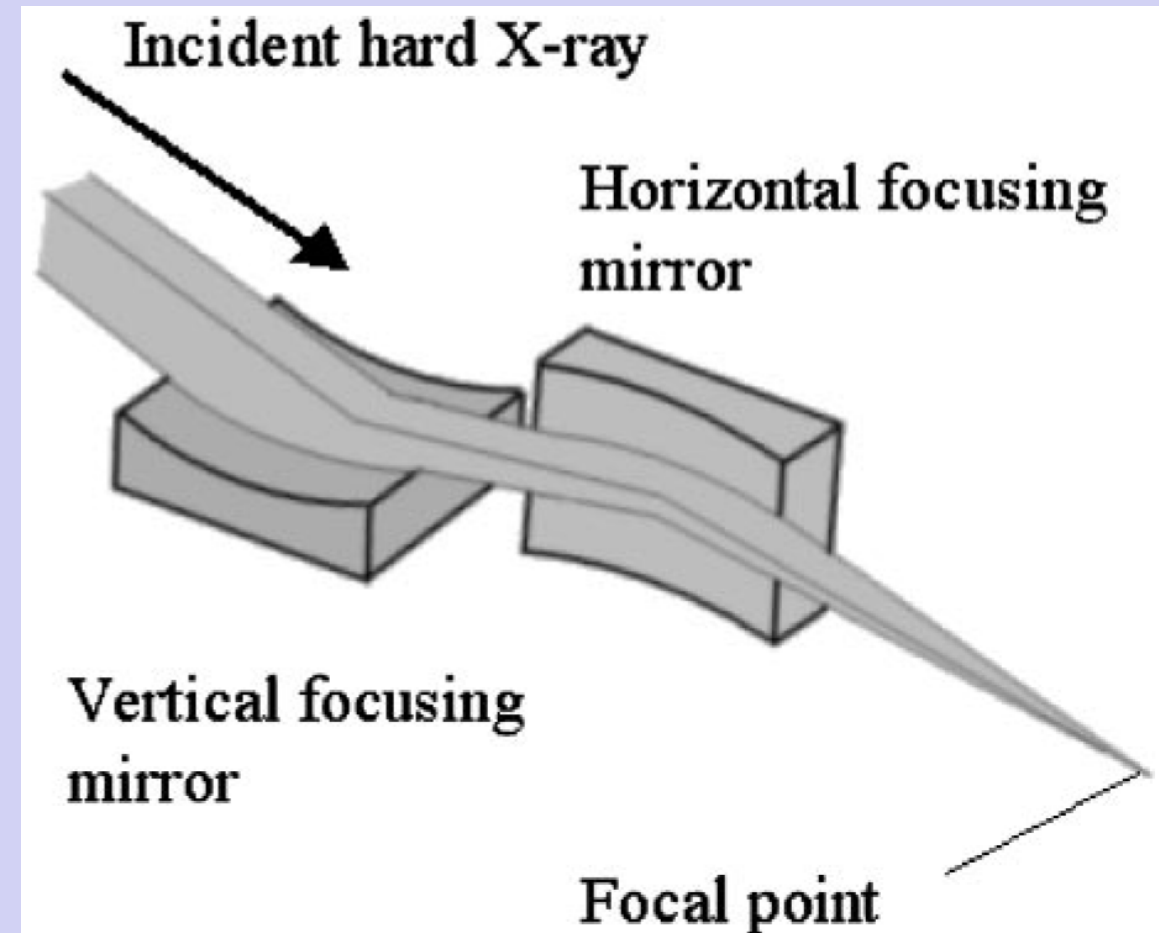
X-ray mirrors – beam focalisation

Paolo
Fornasini
Univ. Trento

Surface bending



Beam collimation
and
focalisation



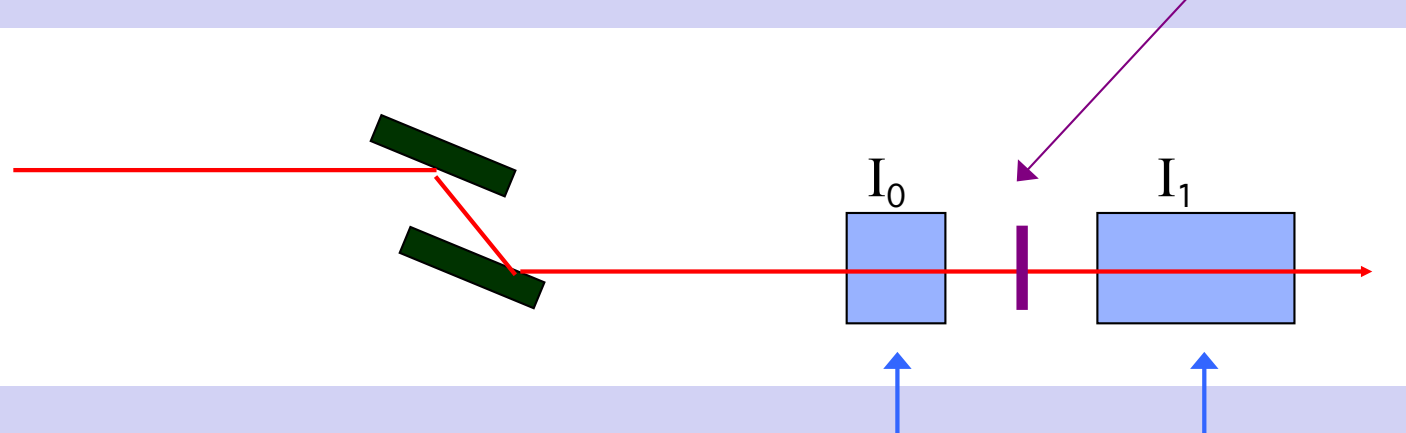
XAFS: experimental

♠ Detection schemes

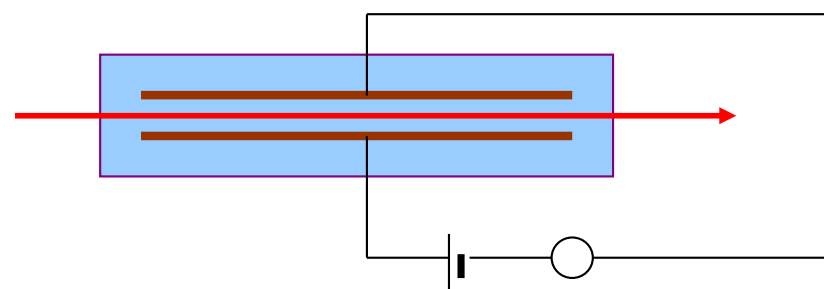
XAFS: direct transmission measurements

Sample:

- Powders or thin films
- Thickness $\approx 10 \mu\text{m}$
- No holes or inhomogeneities



Detectors: ionisation chambers



$$E \approx 100 \text{ V/cm}$$

$$I \approx 10^{-10} \div 10^{-8} \text{ A}$$

Direct transmission measurements



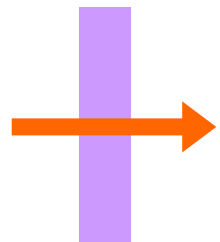
Bulk information
(not from surface)
from:

Thin samples

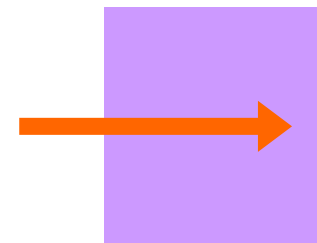
Non-diluted samples

Homogeneous samples

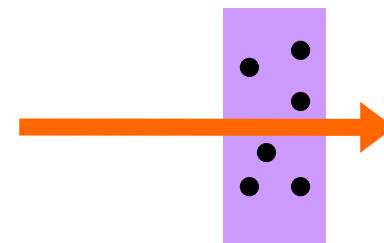
High accuracy attainable



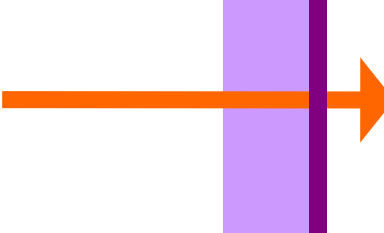
Thick samples



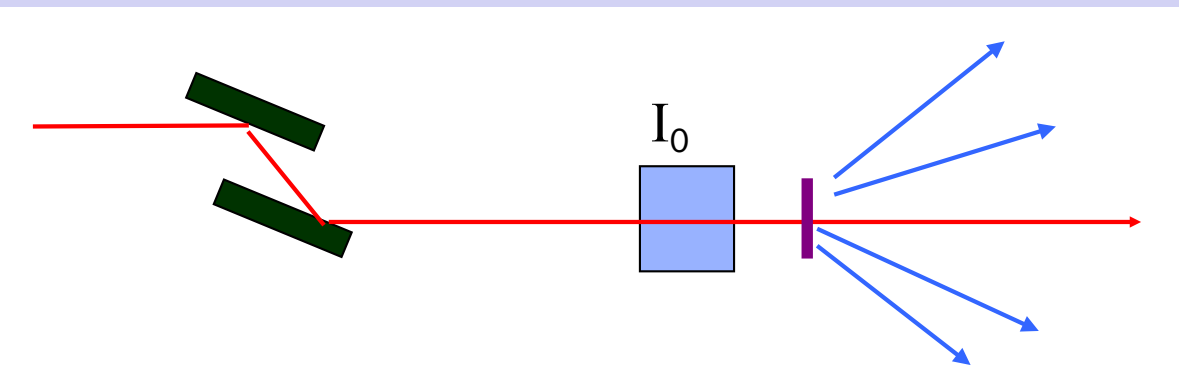
Diluted samples



Surface
information



Indirect detection methods



Detection
of decay products

- X-ray fluorescence

FLY = FLuorescence Yield

- Electrons

{

- AEY = Auger Electron Yield
- PEY = Partial Eletron Yield
- TEY = Total Electron Yield

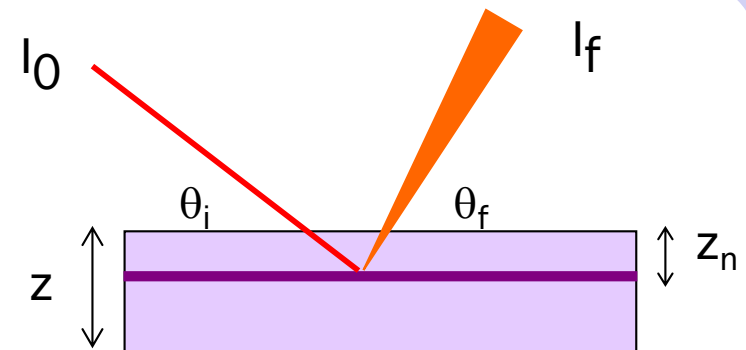
- Optical luminescence

XEOL-PLY =

X-ray Ecxitied Optical Luminescence
Photo Luminescence Yield

XAFS: fluorescence detection (FLY)

a = absorbing species



Fluorescence from a thin layer

$$I_f(z_n) dz = I_0(\omega) \exp\left[-\frac{\mu_{\text{tot}}(\omega)z_n}{\sin\theta_i}\right] \eta_f u_a(\omega) \frac{dz}{\sin\theta_i} \exp\left[-\frac{\mu_{\text{tot}}(\omega_f)z_n}{\sin\theta_f}\right] \frac{\Omega}{2\pi}$$

Absorption Fluorescence Absorption

Total fluorescence: Sample of thickness z and $\theta_i = \theta_f = 45^\circ$

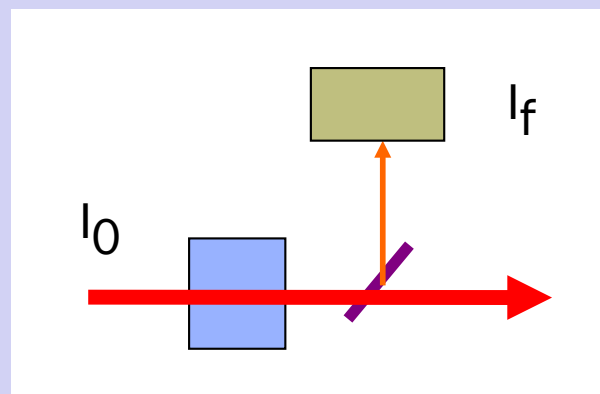
$$I_f = I_0(\omega) \eta_f \frac{\Omega}{4\pi} \frac{\mu_a(\omega)}{\mu_{\text{tot}}(\omega) + \mu_{\text{tot}}(\omega_f)} \{1 - \exp(-A)\}$$

$A = -\sqrt{2} z [\mu_{\text{tot}}(\omega) + \mu_{\text{tot}}(\omega_f)]$

Fluorescence: thin samples

$$I_f = I_0(\omega) \eta_f \frac{\Omega}{4\pi} \frac{\mu_a(\omega)}{\mu_{\text{tot}}(\omega) + \mu_{\text{tot}}(\omega_f)} \{1 - \exp(-A)\}$$

$$A = -\sqrt{2} z [\mu_s(\omega) + \mu_s(\omega_f)]$$



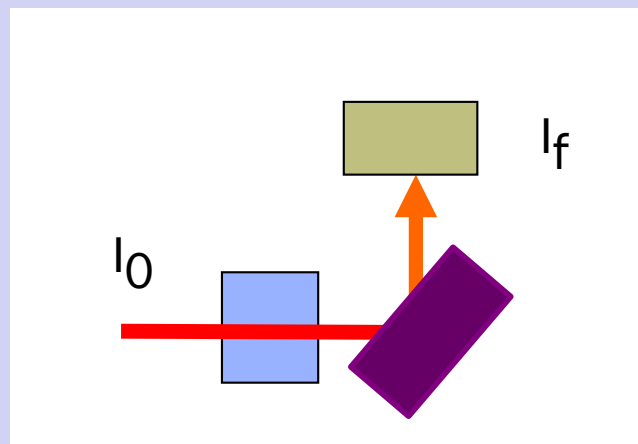
Small fraction of I_0 absorbed

$$1 - \exp(-A) \approx 1 - 1 - A = -A$$

$$I_f \propto \mu_a(\omega)$$

Fluorescence: thick samples

$$I_f = I_0(\omega) \eta_f \frac{\Omega}{4\pi} \frac{\mu_a(\omega)}{\mu_{\text{tot}}(\omega) + \mu_{\text{tot}}(\omega_f)} \{1 - \exp(-A)\}$$



All I_0 is absorbed

$$A = -\sqrt{2} z [\mu_s(\omega) + \mu_s(\omega_f)]$$

$$1 - \exp(-A) \approx 1$$

$$I_f = I_0(\omega) \eta_f \frac{\Omega}{4\pi} \frac{\mu_a(\omega)}{\mu_{\text{tot}}(\omega) + \mu_{\text{tot}}(\omega_f)}$$

"a" concentrated

$$\mu_a(\omega) \approx \mu_{\text{tot}}(\omega)$$

no XAFS

$$\mu_{\text{tot}}(\omega) \gg \mu_{\text{tot}}(\omega_f)$$

NO

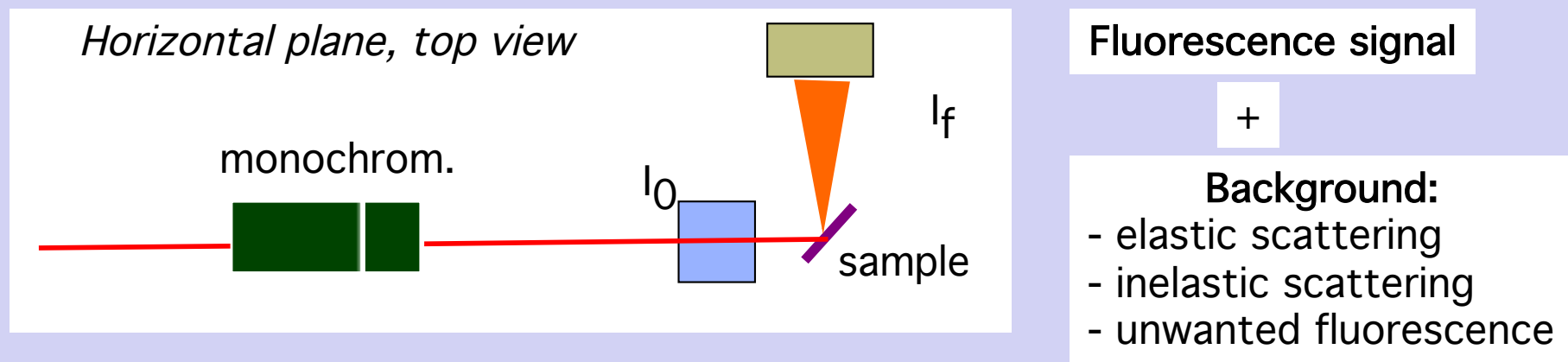
"a" diluted (<1%)

$$\mu_a(\omega) \ll \mu_{\text{tot}}(\omega)$$

$$I_f \propto \mu_a(\omega)$$

OK

Fluorescence detection



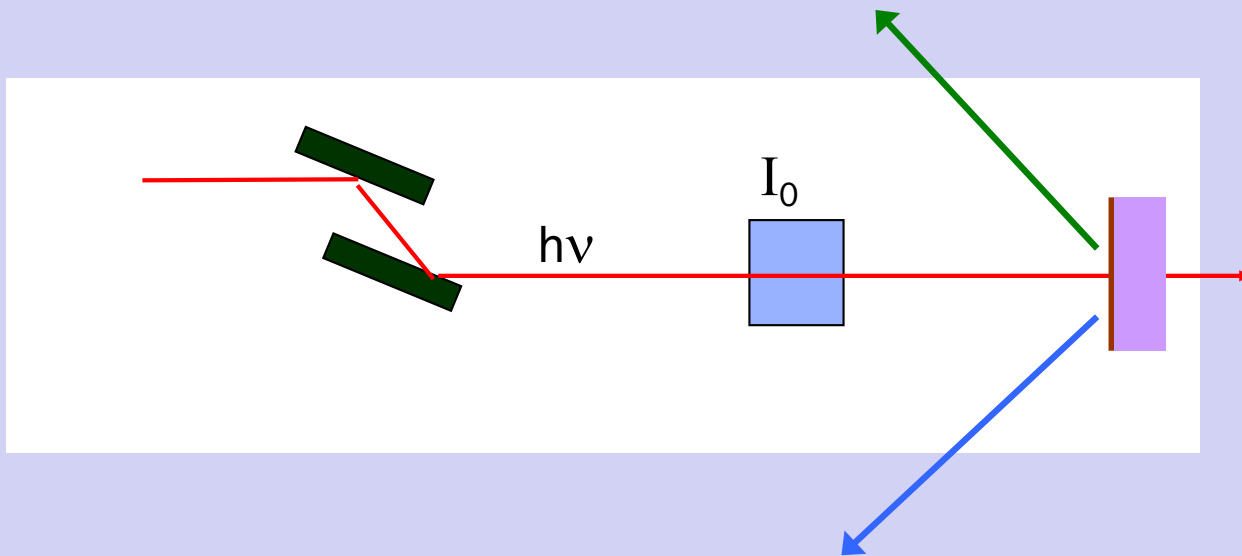
To reduce background :

- A) Detection at 90° minimises scattering (less effective for large solid angles)
- B) Detection schemes
 - 1. Filter + slits systems
 - 2. Multi-element solid state detectors (energy dispersive)
 - 3. Crystal analysers

XAFS: electron detection (a)

Photo-electrons:

- Energy varies with $h\nu$
 - Intensity $\propto \mu x$
- ⇒ XAFS signal



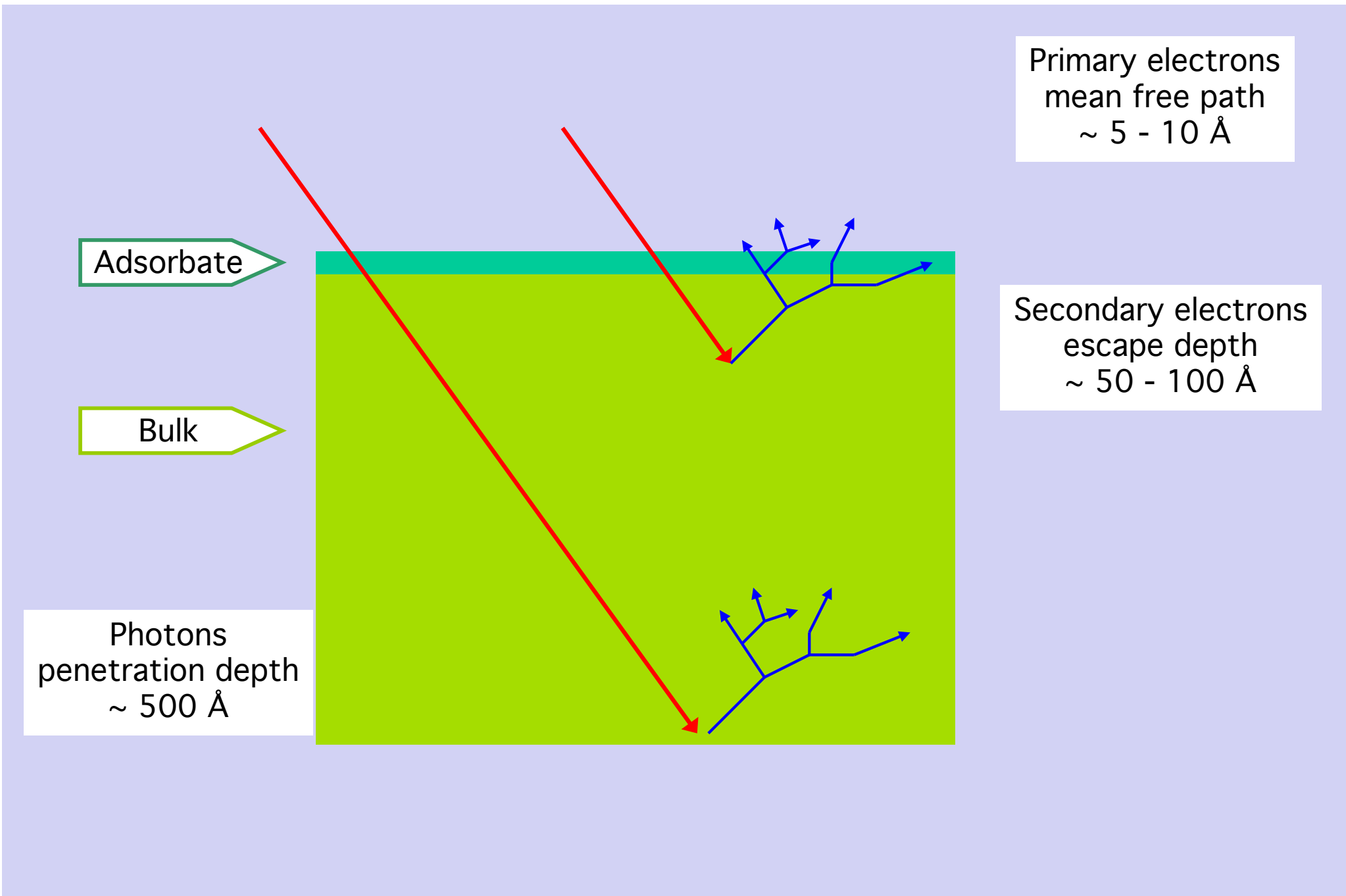
Auger electrons:

- Fixed energy ⇒ atomic selectivity
 - Intensity $\propto \mu x$
- ⇒ XAFS signal

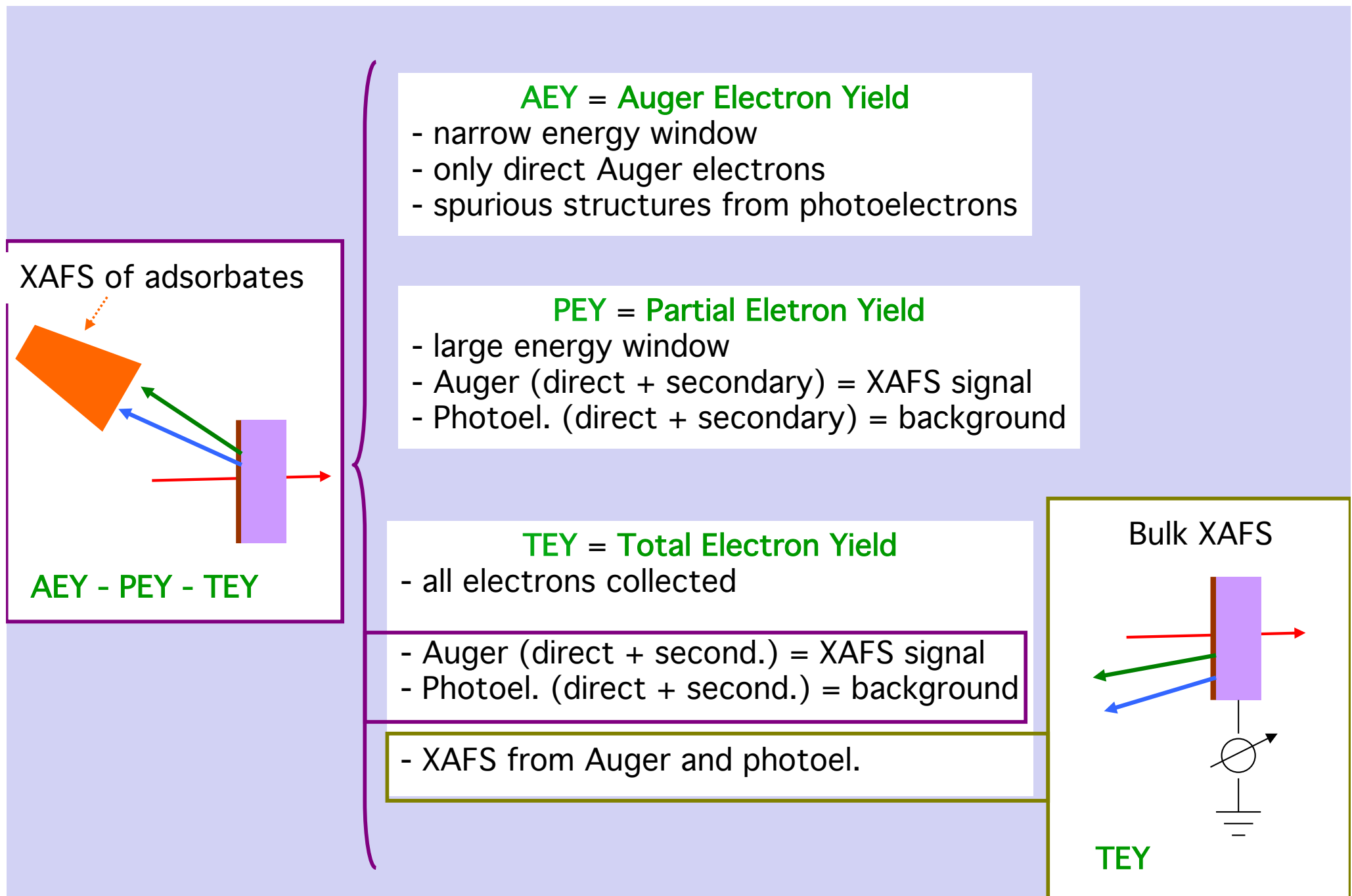
Electron mean free path:

- adsorbates
- thin layers

Indirect processes and escape depth



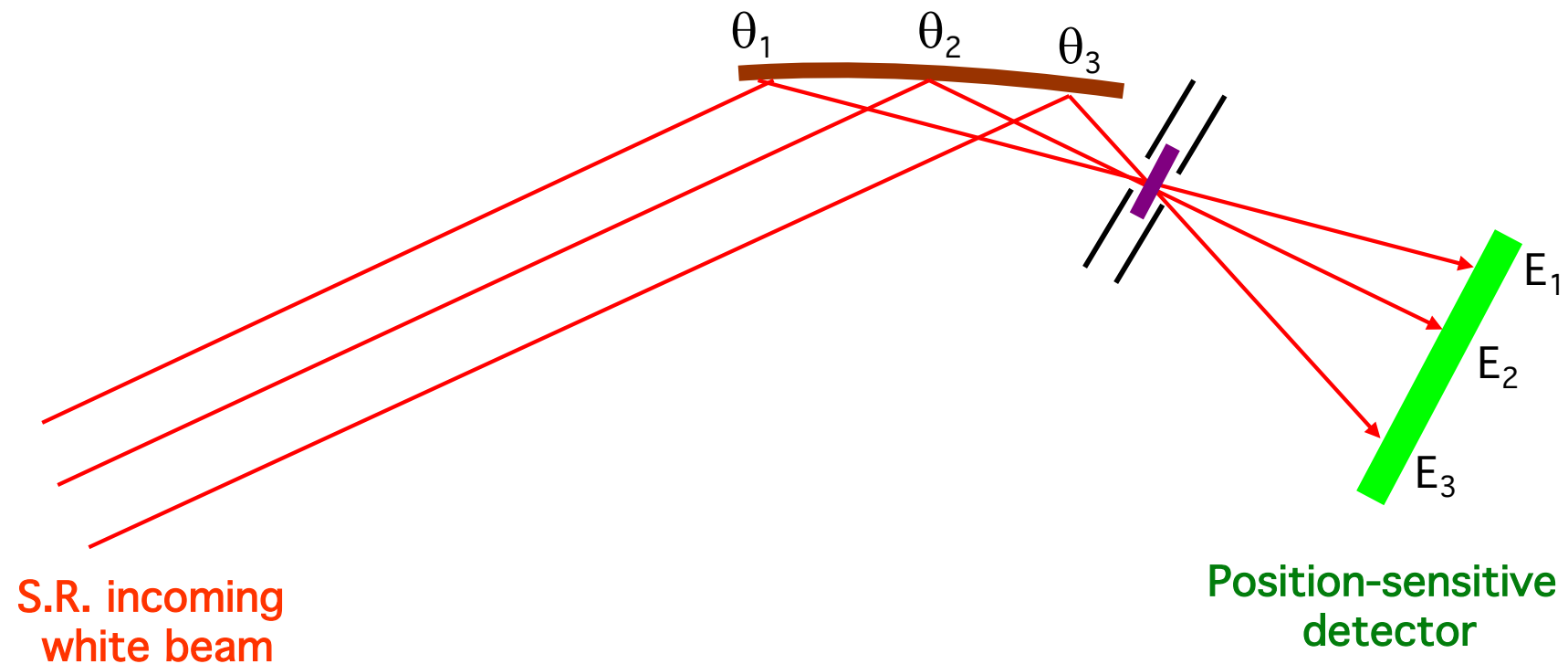
XAFS: electron detection (b)



Dispersive XAFS (a)

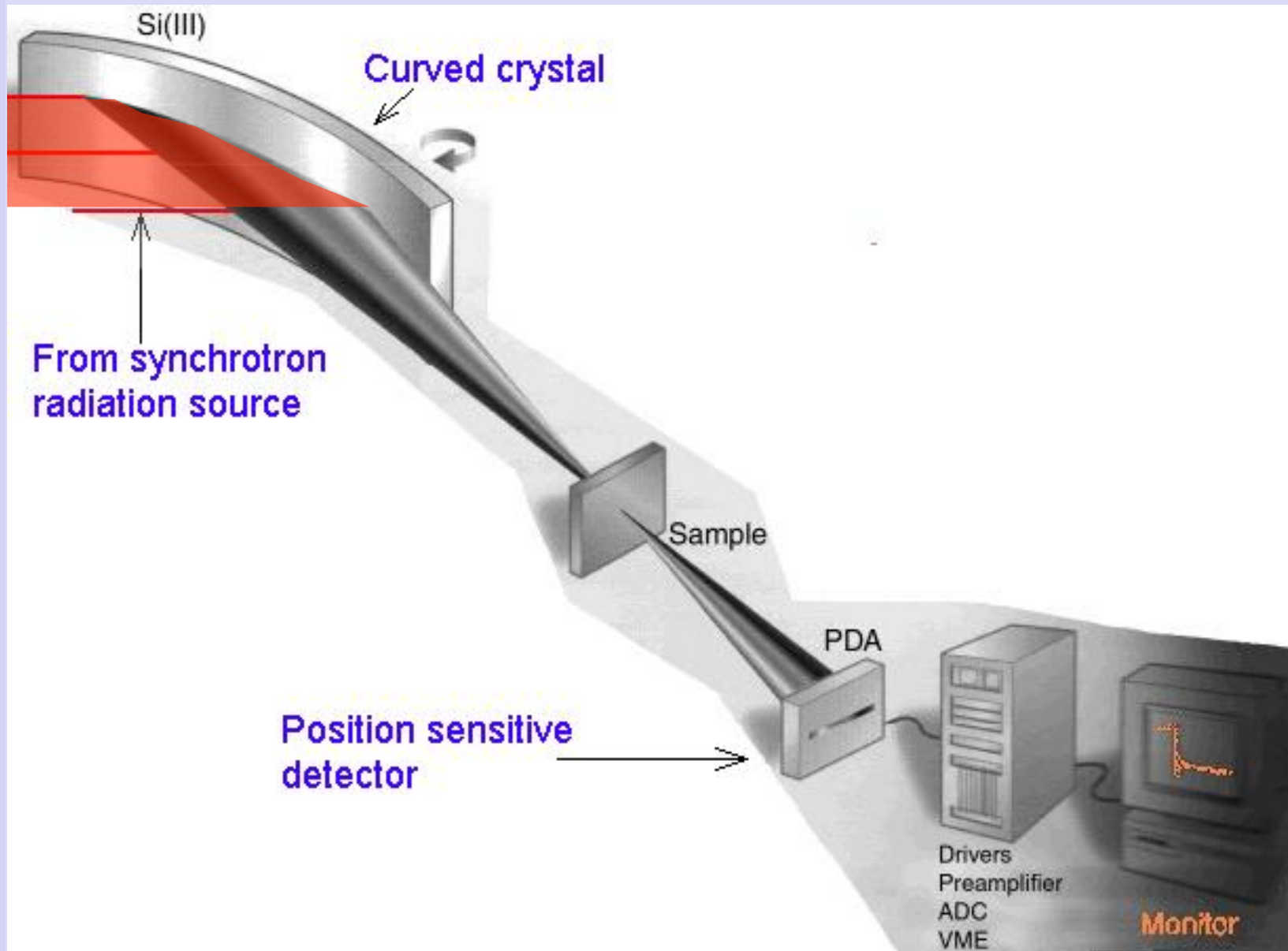
$$2d \sin\theta = \lambda$$

Curved crystal poly-chromator



Dispersive XAFS (b)

Paolo
Fornasini
Univ. Trento



Dispersive XAFS (b)

- 😊 No mechanical movements (no dead times)
- 😊 Simultaneous acquisition of all data points
- 😊 Acquisition time determined by acceptable statistics

OK for time-resolved measurements

- 😢 Critical in terms of temporal and spatial beam stability and sample presentation
- 😢 Only transmission mode
- 😢 X-ray beam not perfectly focussed through the sample
- 😢 No reference measurements during acquisition

NO accurate quantitative results

EXAFS: data analysis, examples

List of available software:

<http://www.esrf.eu/Instrumentation/software/data-analysis/Links/xafs>

FEFF project (University of Washington, USA):

<http://leonardo.phys.washington.edu/feff/>

IFEFFIT (University of Chicago, USA) + Athena, Artemis, Demeter

[http://cars9.uchicago.edu/ifeffit/.](http://cars9.uchicago.edu/ifeffit/)

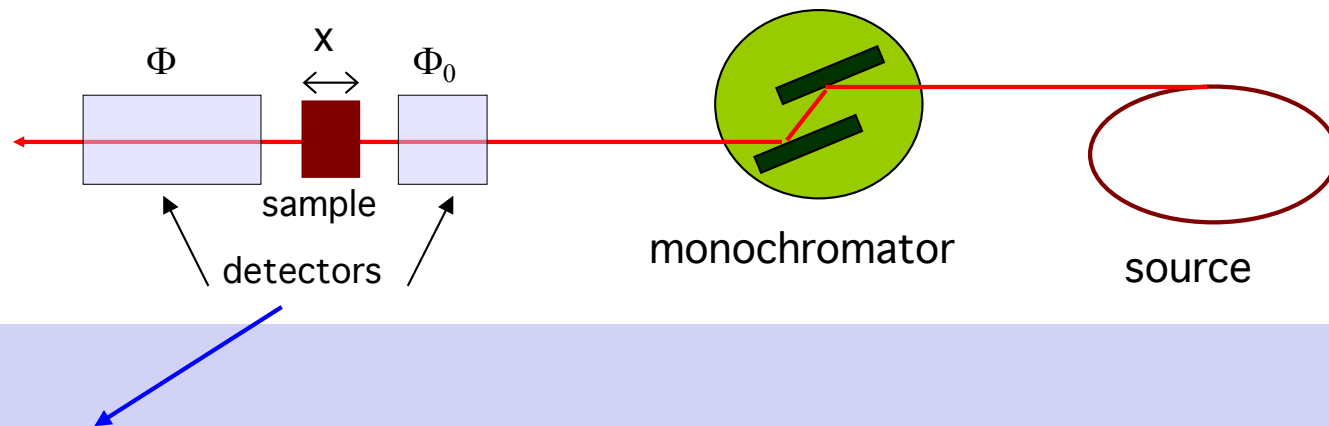
GNXAS project (University of Camerino, Italy):

http://gnxas.unicam.it/XASLABwww/pag_gnxas.html

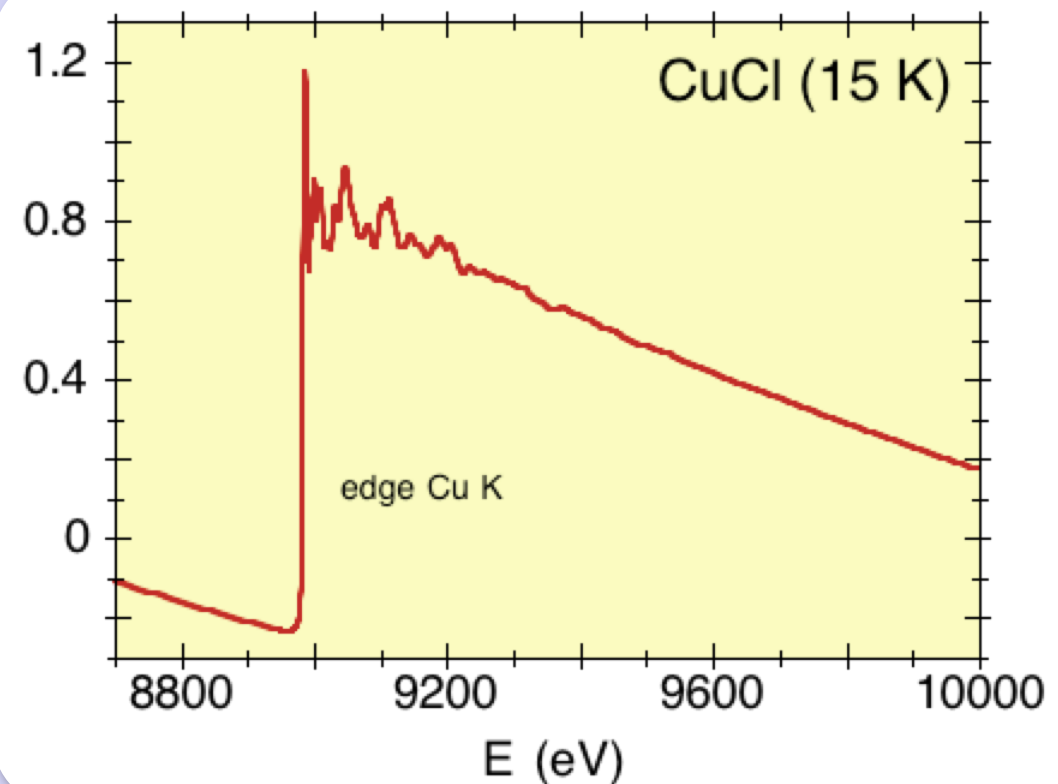
EXAFS data analysis

- ♠ Extraction of EXAFS signal

Total absorption coefficient

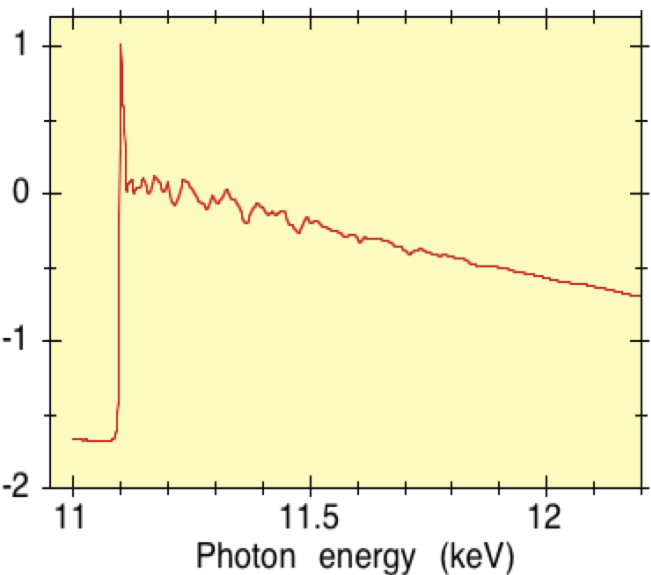


$$\ln \frac{I_0}{I} = \ln \frac{\Phi_0}{\Phi} + C' = \mu_{\text{tot}} x + C'$$

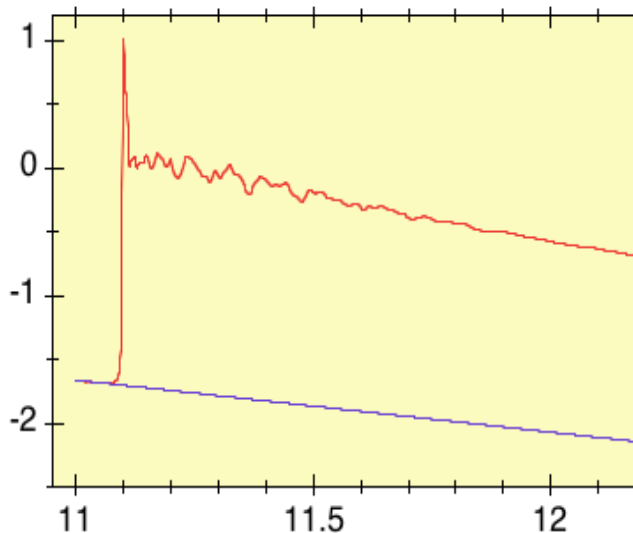


Edge absorption coefficient

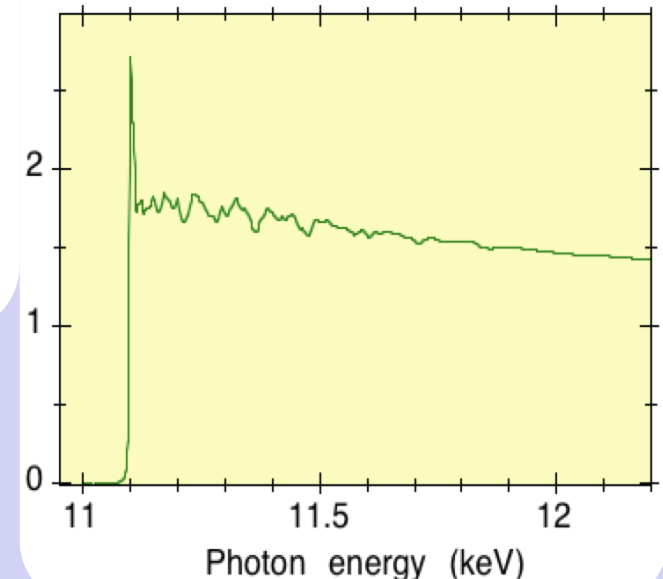
Experimental signal



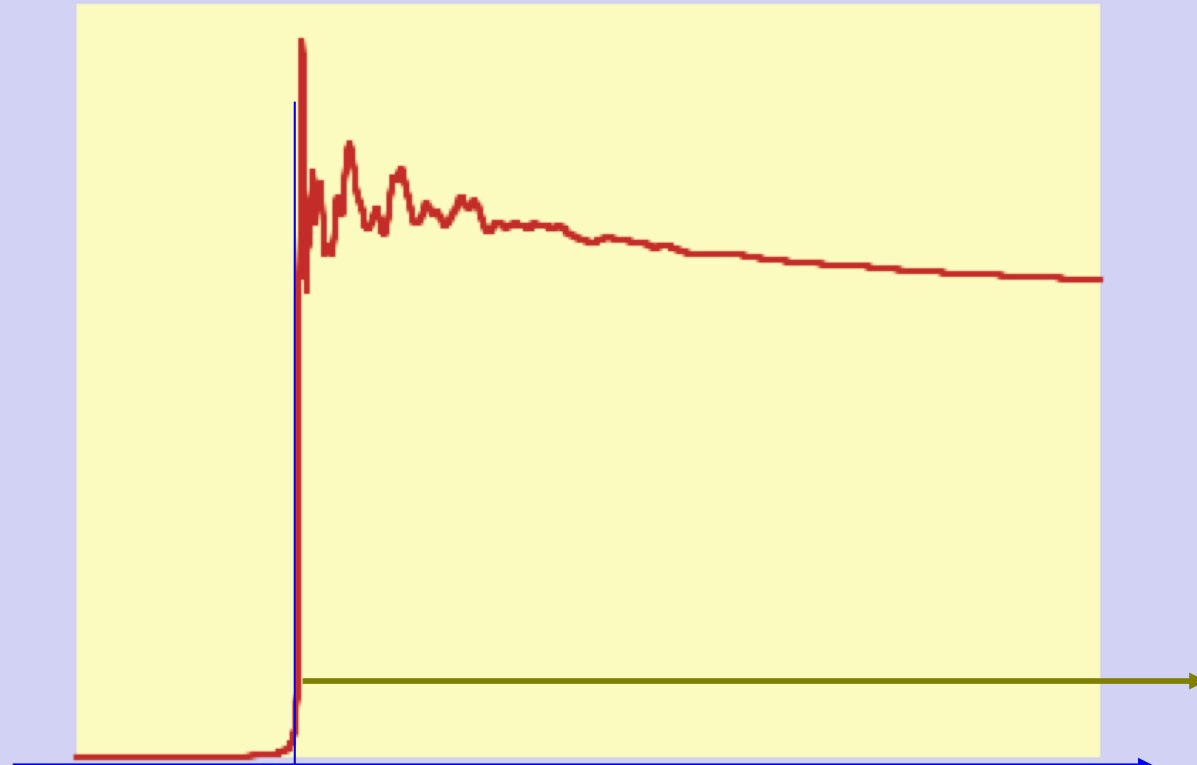
Extrapolation of pre-edge behaviour



Edge absorption coefficient



Photoelectron wavenumber

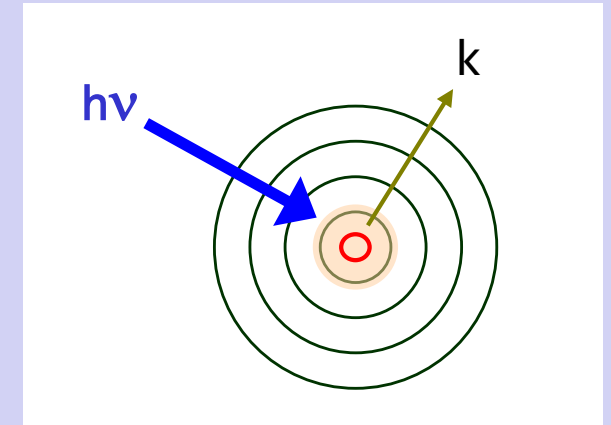


Edge
energy

?

$E = h\nu$, photon energy

Experimental
convention



Photoelectron
wavenumber

$$k = \sqrt{\frac{2m}{\hbar^2} (h\nu - E_s)}$$

$E_s = 1\text{st maximum of 1st derivative}$

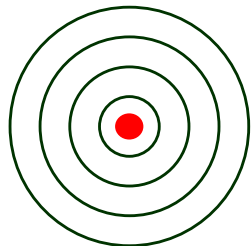
Atomic absorption coefficient

EXAFS function

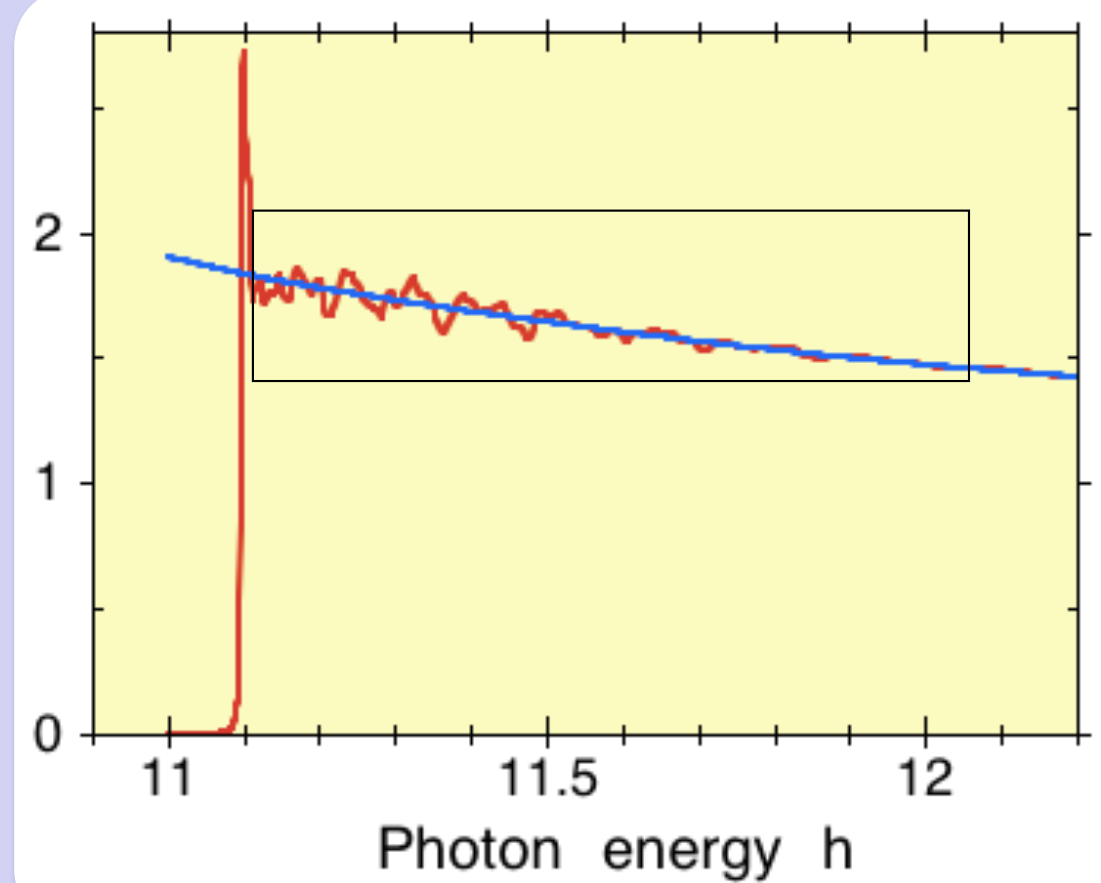
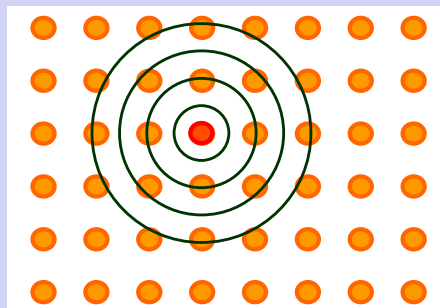
$$\chi(k) = \frac{\mu - \mu_0}{\mu_0}$$

μ_0 ?

Isolated atom



Embedded atom

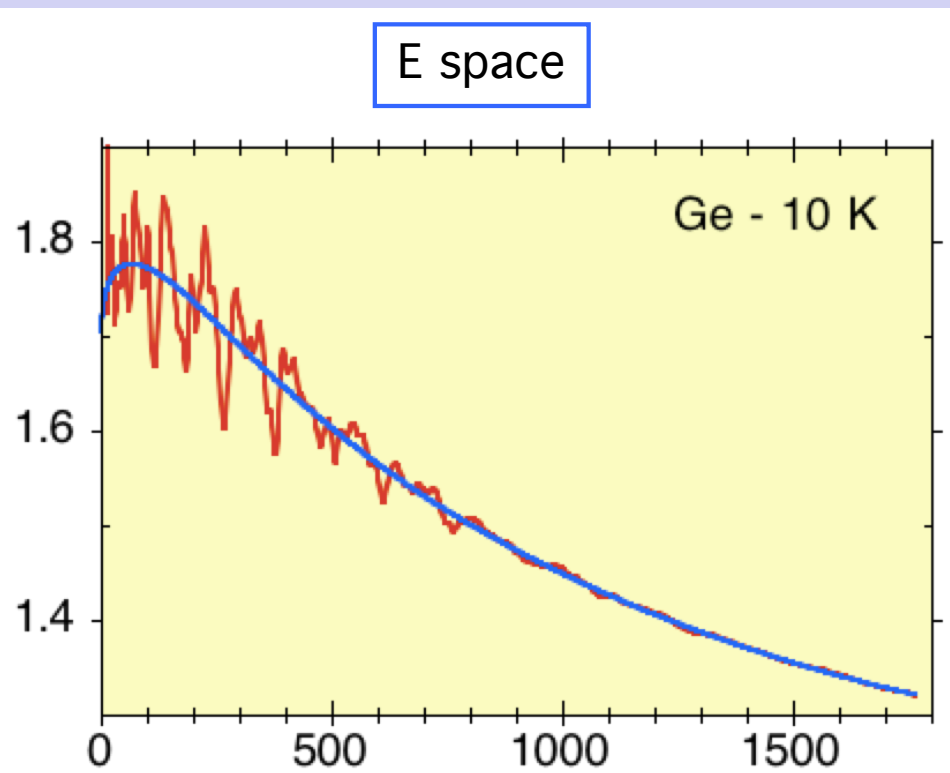


Best-fitting polynomial spline

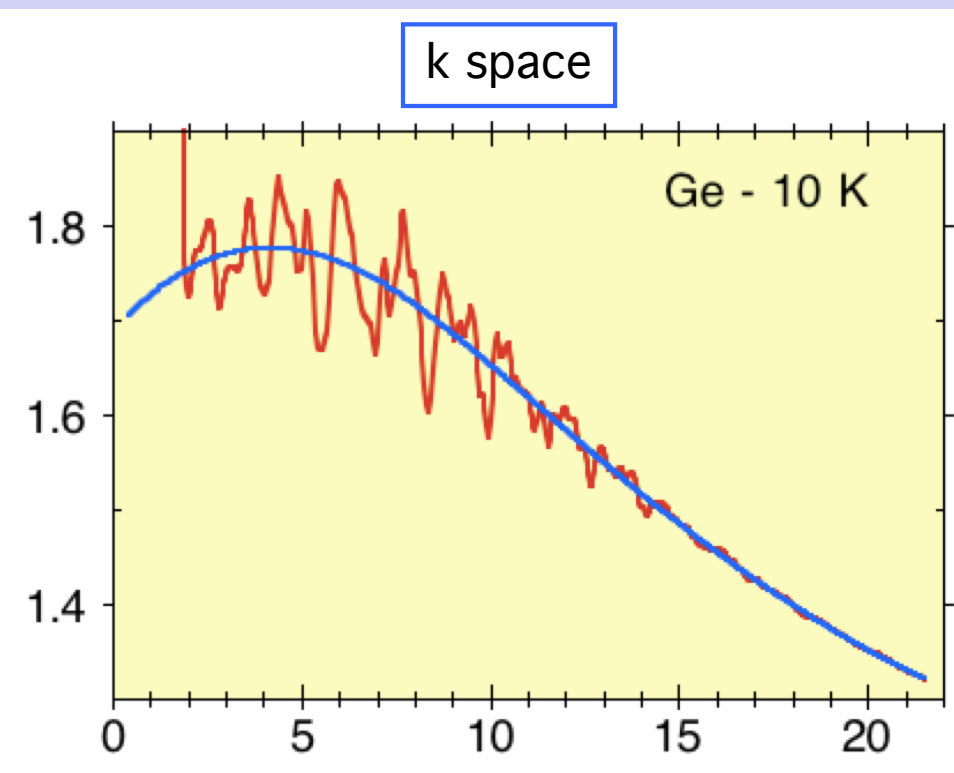
$$\chi(k) = \frac{\mu - \mu_0}{\mu_0}$$

Polynomial spline - best fit

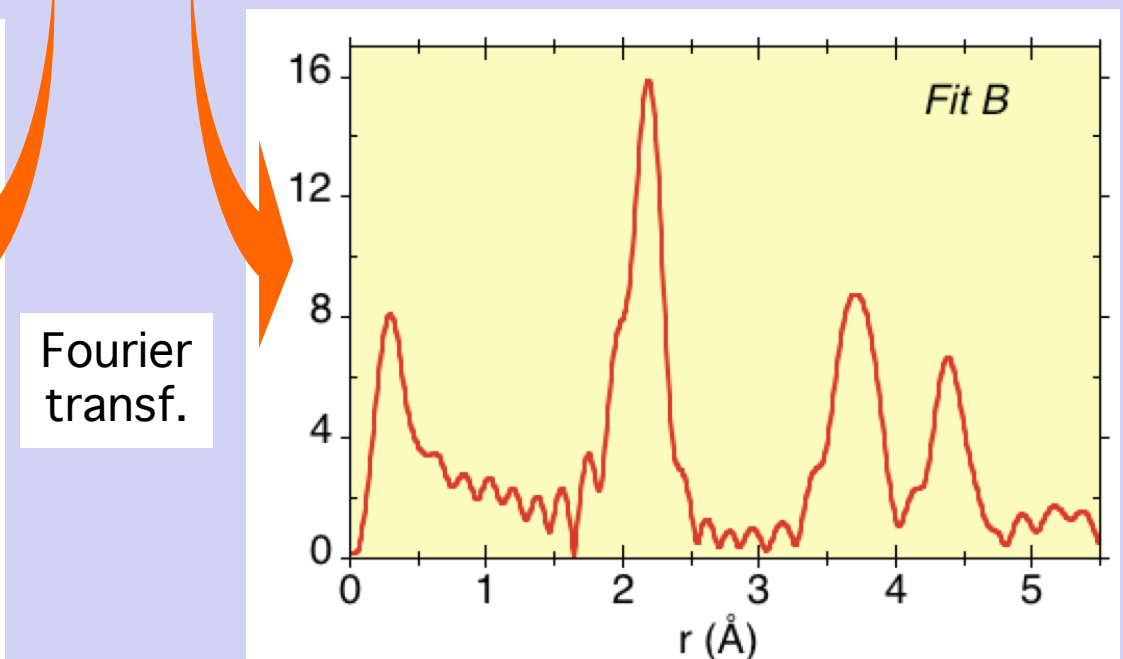
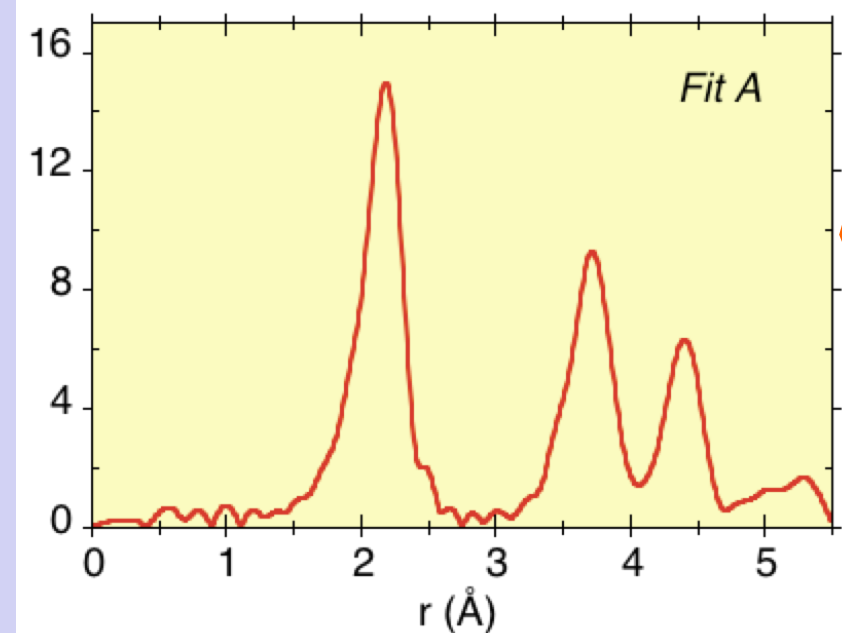
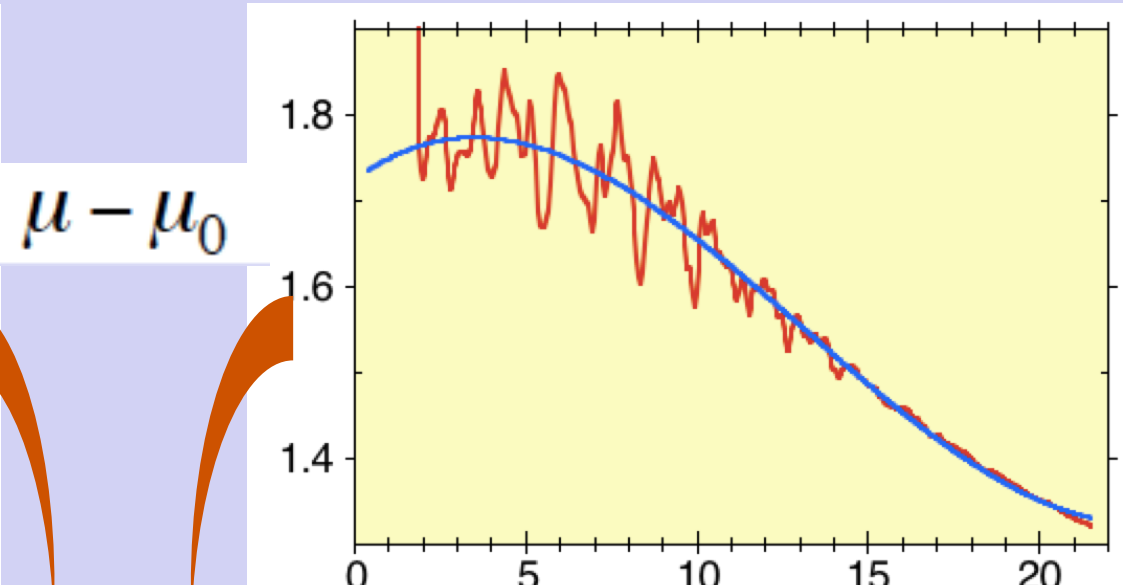
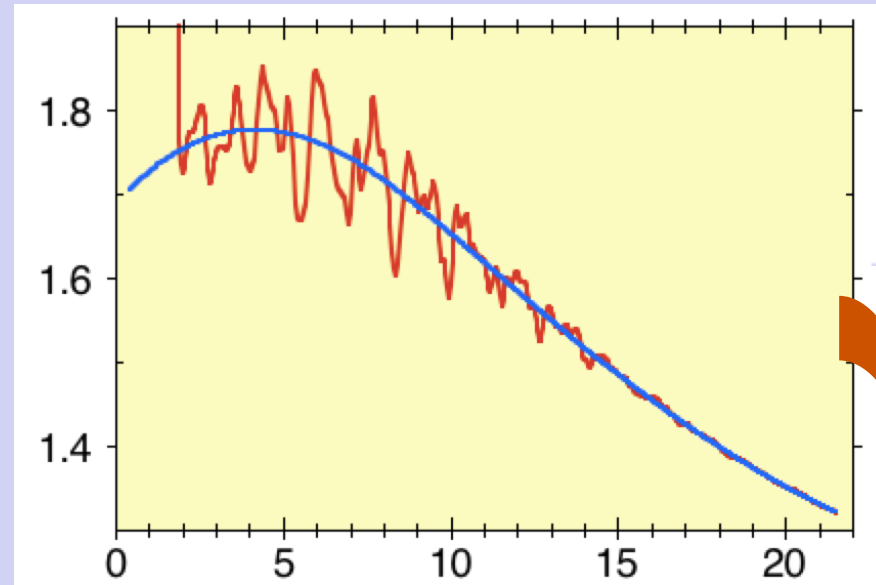
E space



k space



Fit optimization



$\mu - \mu_0$

Fourier
transf.

Fit B

Quantitative analysis of EXAFS

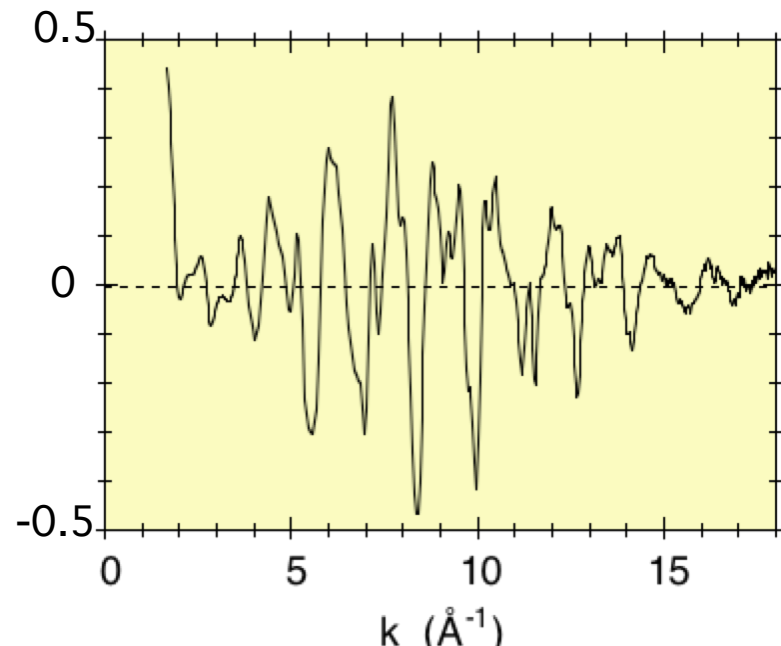
$$\chi(k) = \sum_i A_i(k) \sin \Phi_i(k)$$

Sum over: {

- S.S. paths (coord. shells)
- M.S. paths

Input for each path:

- backscattering amplitude
- phaseshifts
- inelastic terms

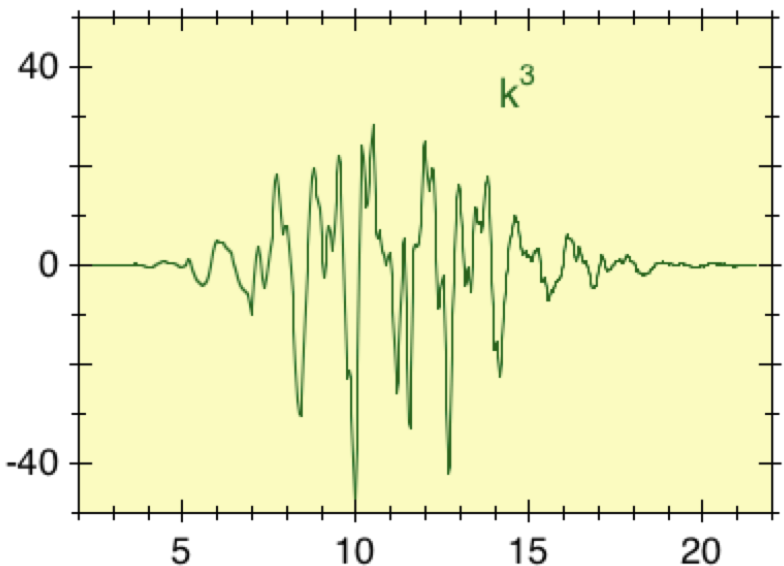


Different analysis procedures

EXAFS data analysis

♠ Fourier transform

Data analysis - Fourier Transform $k \rightarrow r$



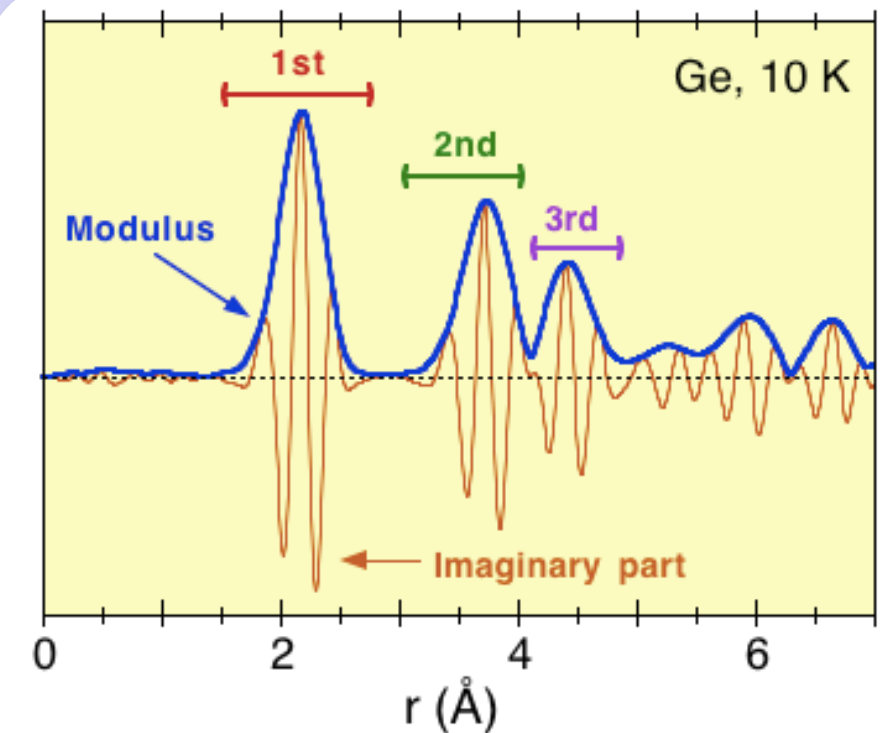
$$F(r) = \int_{k_{min}}^{k_{max}} \chi(k) k^n W(k) e^{2ikr} dk$$

weight window

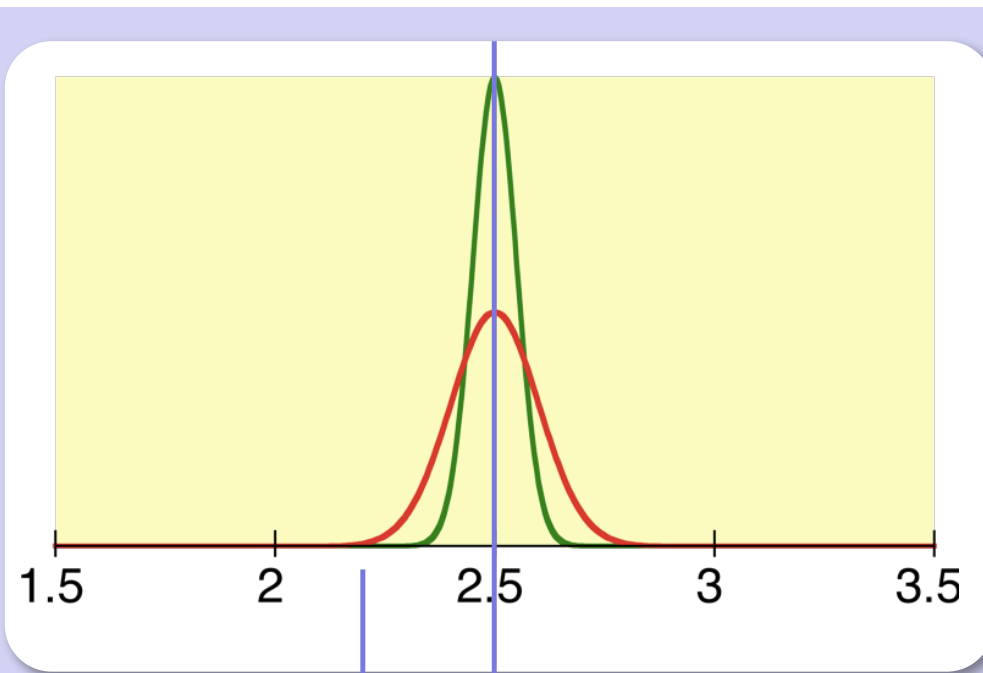
Peak's position and shape influenced by:



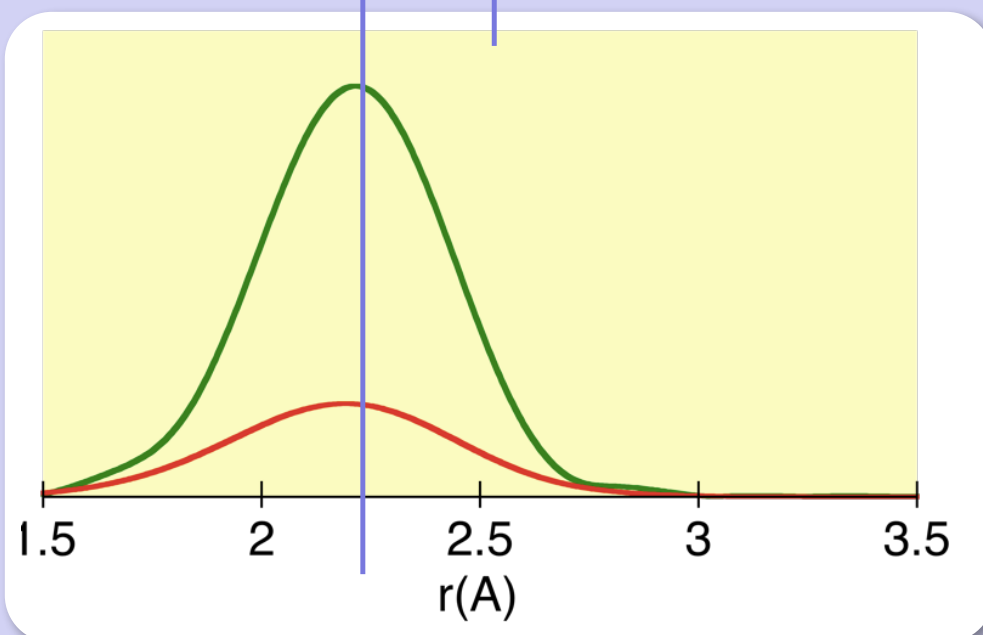
- total phaseshifts
- disorder
- Fourier transform window



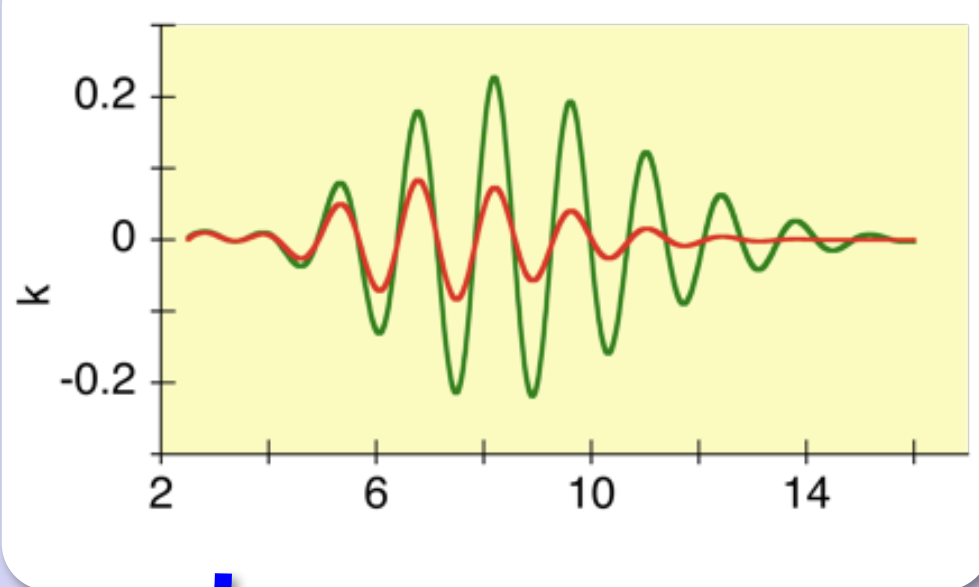
Fourier Transform and distribution



EXAFS simulation
(Ge phases and amplit.)

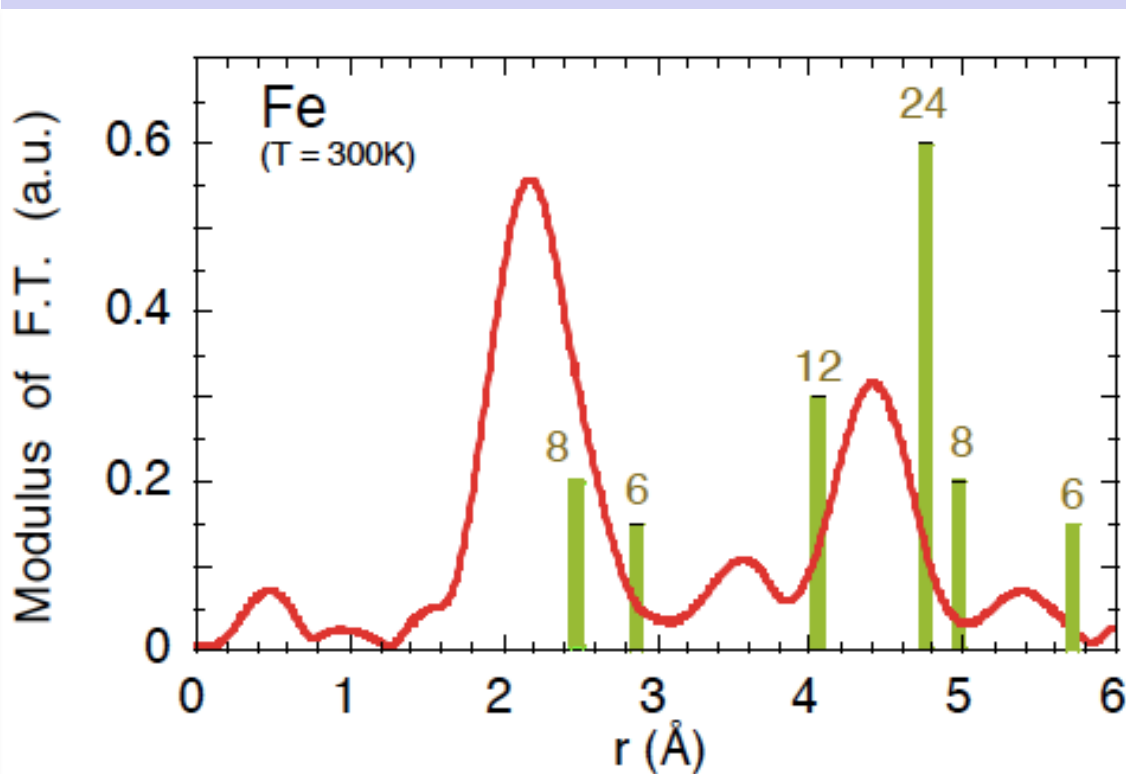
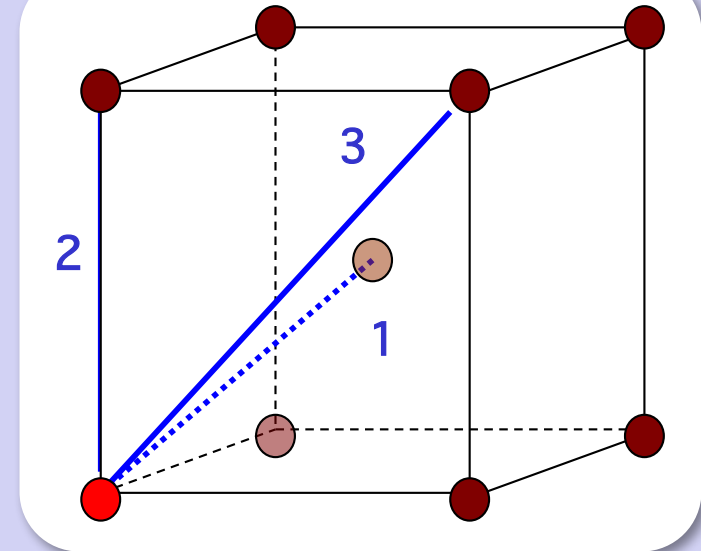


F.T.: $k=2.5-16$
 K^3 , square w.



bcc structure (26-Fe)

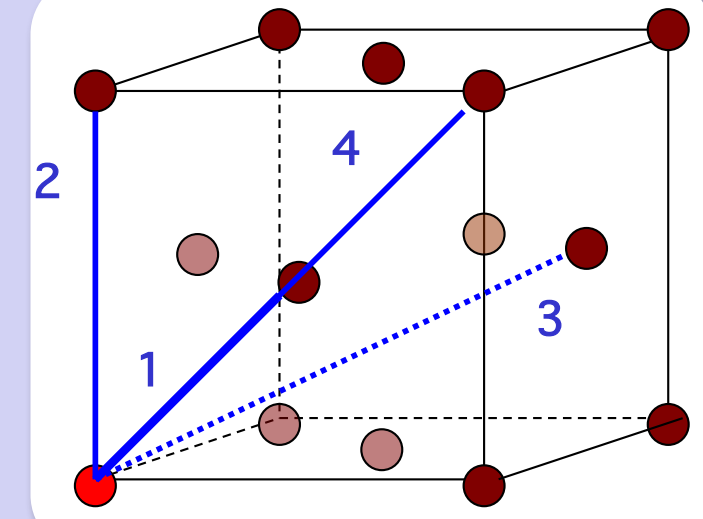
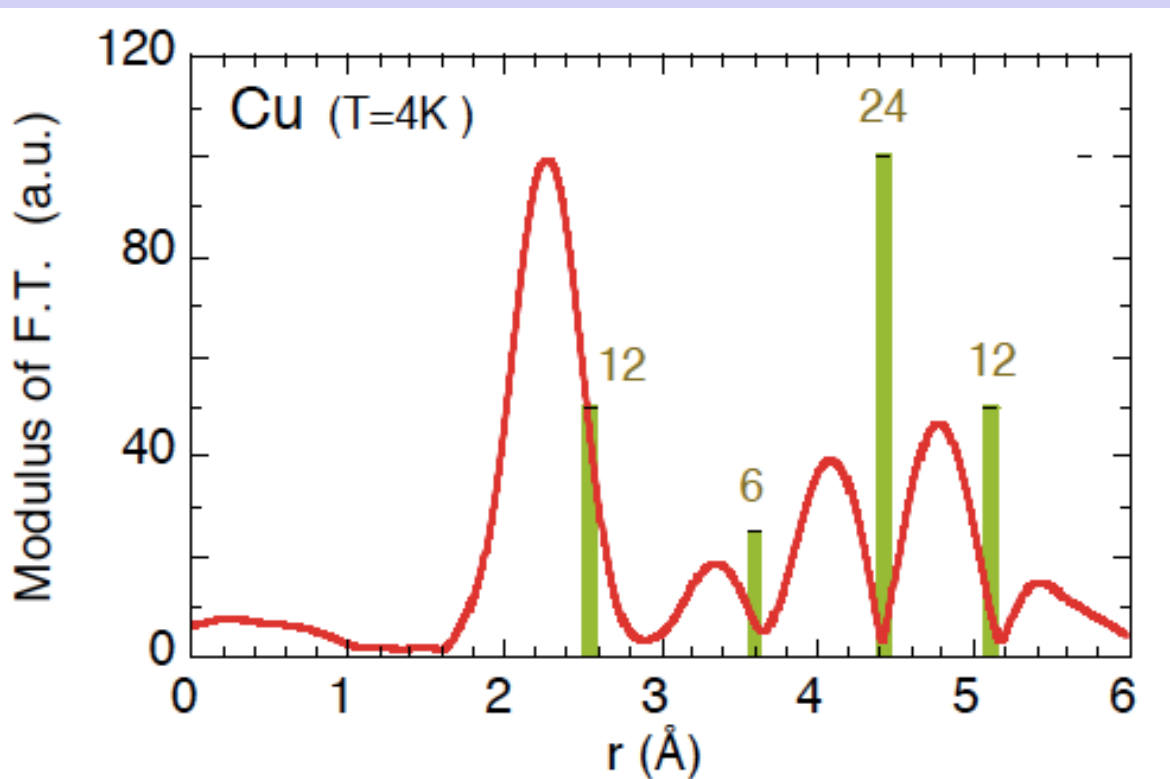
i	N _i	R _i (Å)
1	8	2.48
2	6	2.86
3	12	4.05
4	24	4.75
5	8	4.96
6	6	5.73



- Peak shift
- Superposition of shells

fcc structure (29-Cu)

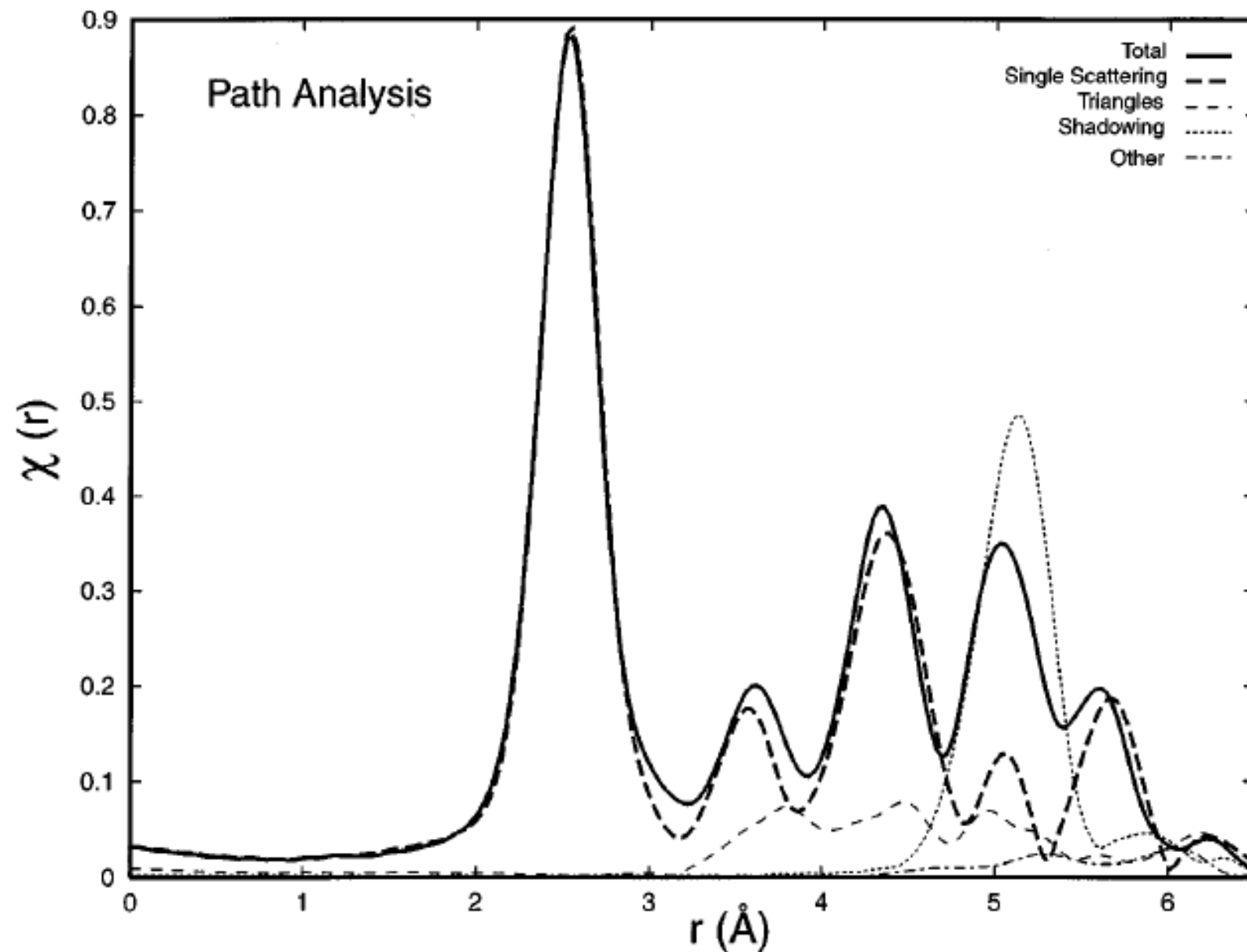
i	N _i	R _i (Å)
1	12	2.55
2	6	3.61
3	24	4.42
4	12	5.10
5	24	5.70
6	8	6.25



- Peak shift
 - Focussing effect
-
- A diagram showing three red circles representing atoms in the first coordination shell (labeled 1, 2, and 4). A horizontal dotted line passes through the centers of these three atoms. A red circle representing the origin is positioned on this line. The distance between the origin and each of the three atoms is indicated by a vertical dashed line.

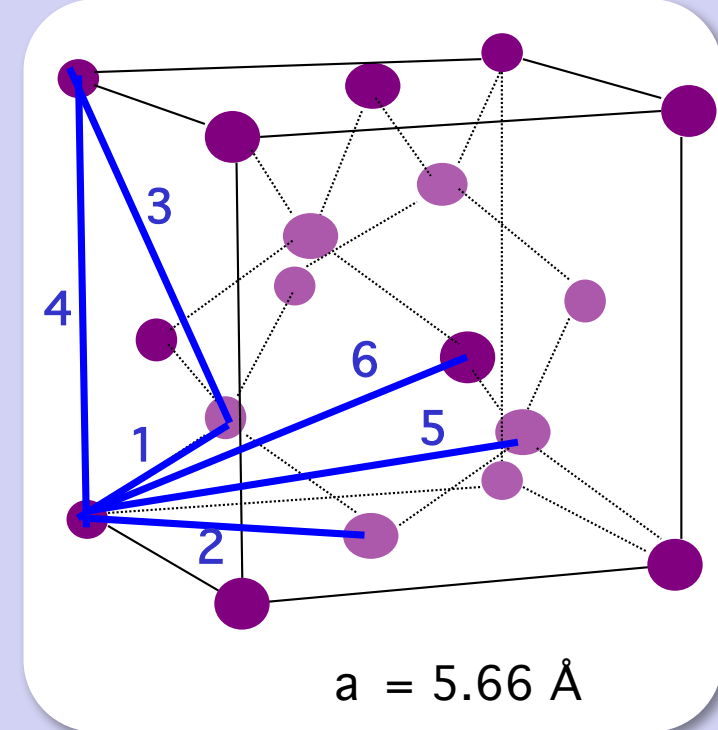
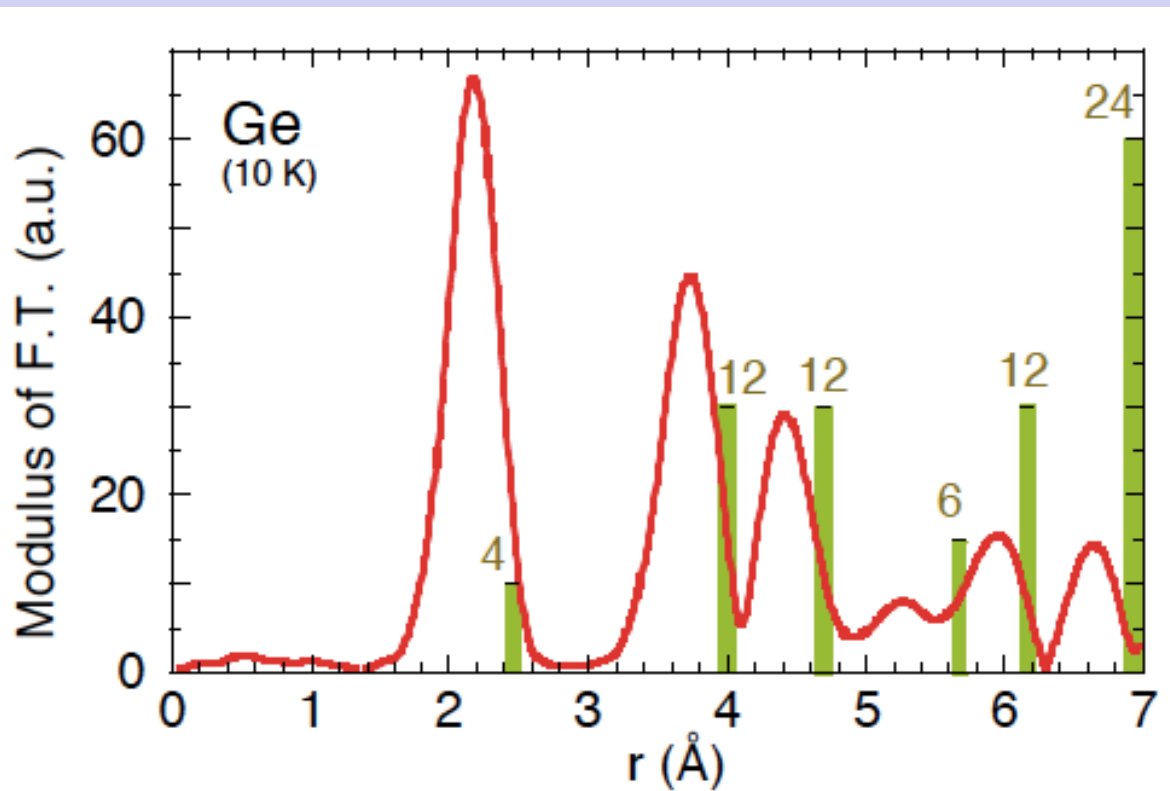
29 - Copper: fcc structure – Multiple Scattering

Paolo
Fornasini
Univ. Trento

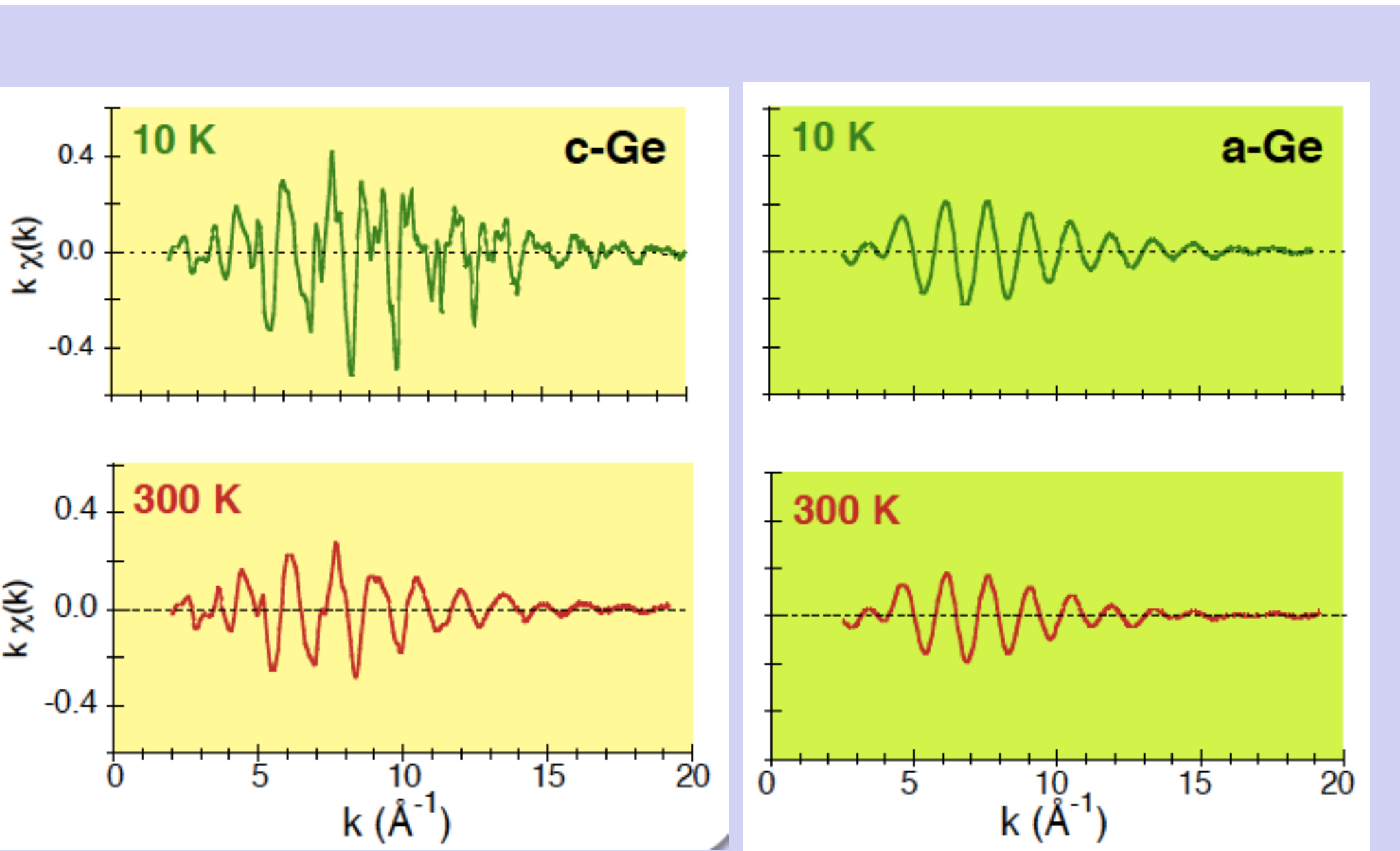


Diamond structure (32-Ge)

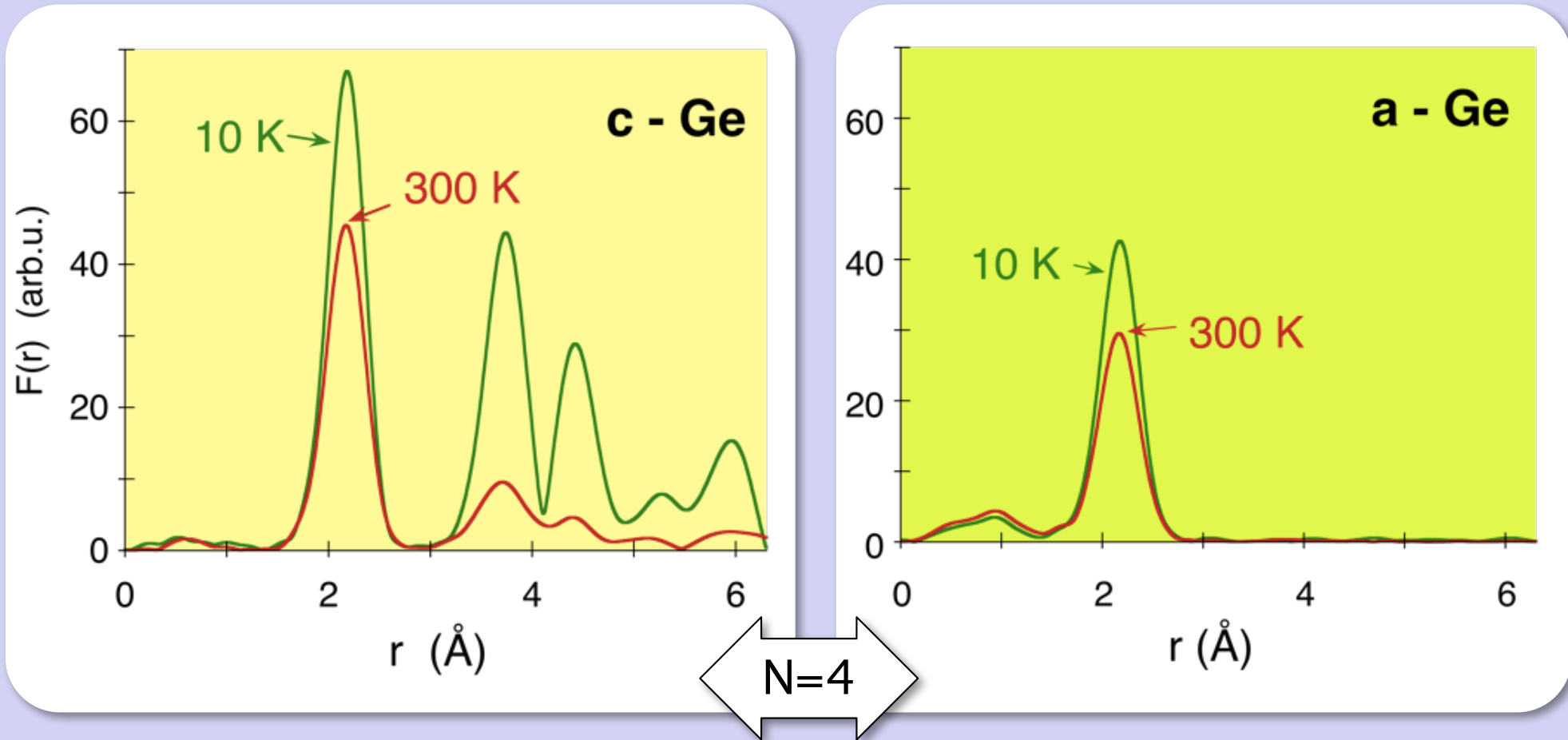
i	N _i	R _i (Å)
1	4	$a(\sqrt{3})/4$
2	12	$a/\sqrt{2}$
3	12	$a(\sqrt{11})/4$
4	6	a
5	12	$a(\sqrt{19})/4$
6	24	$a(\sqrt{6})/2$



Crystalline and amorphous Ge – EXAFS signals



Crystalline and amorphous Ge: F.T.



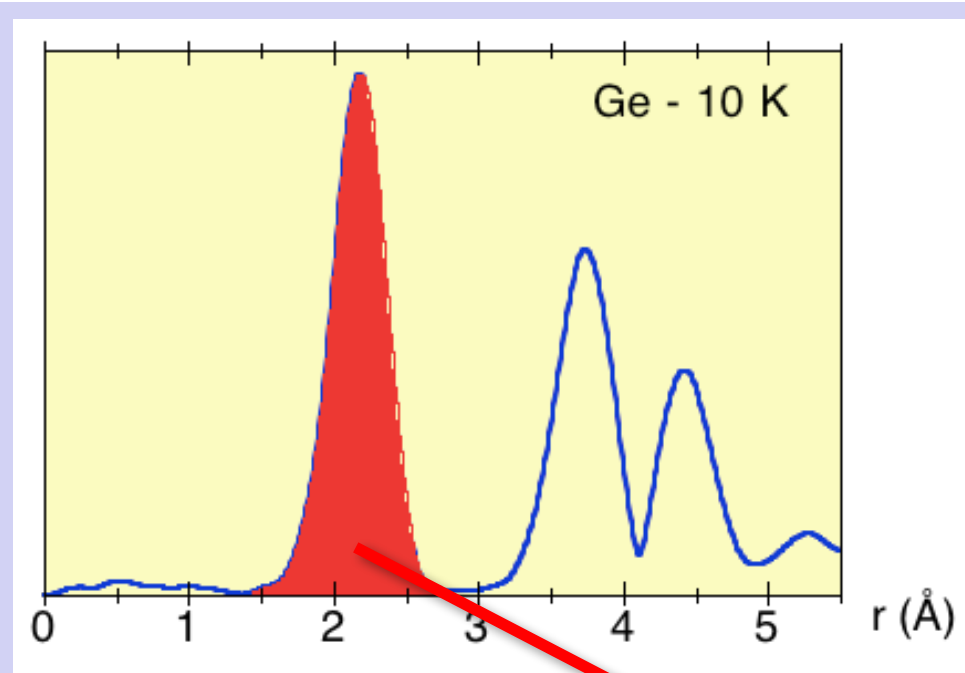
- Structural disorder
- stronger for outer shells

- Only 1st shell
- Thermal disorder
- Structural disorder

EXAFS data analysis

- ♠ First shell analysis

1st-shell Fourier back-transform

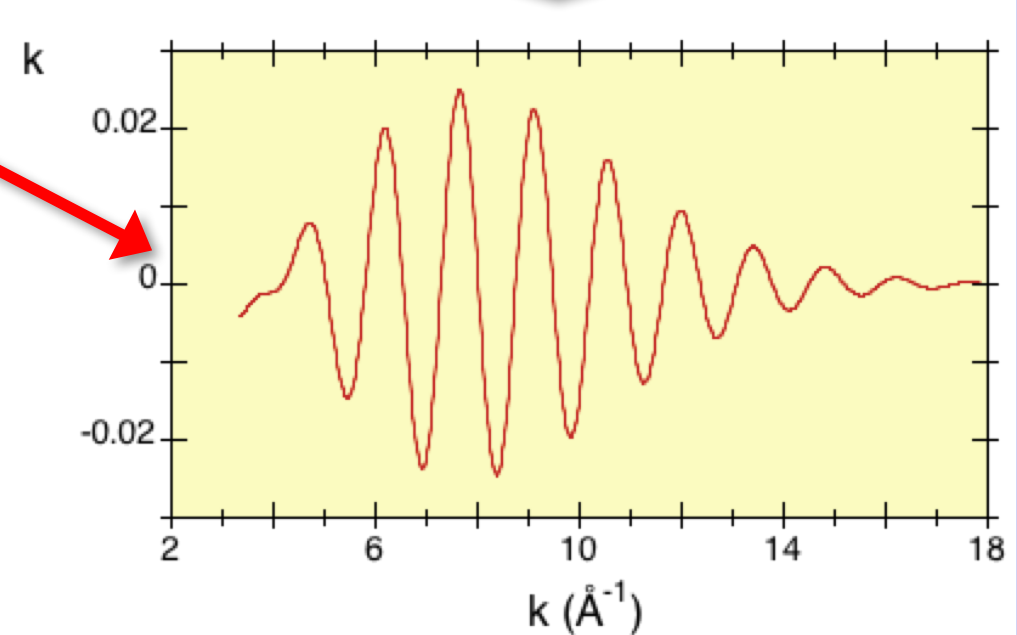


$$\chi'(k) = (2/\pi) \int_{r_{\min}}^{r_{\max}} F(r) W'(r) e^{-2ikr} dr$$

First-shell
contribution

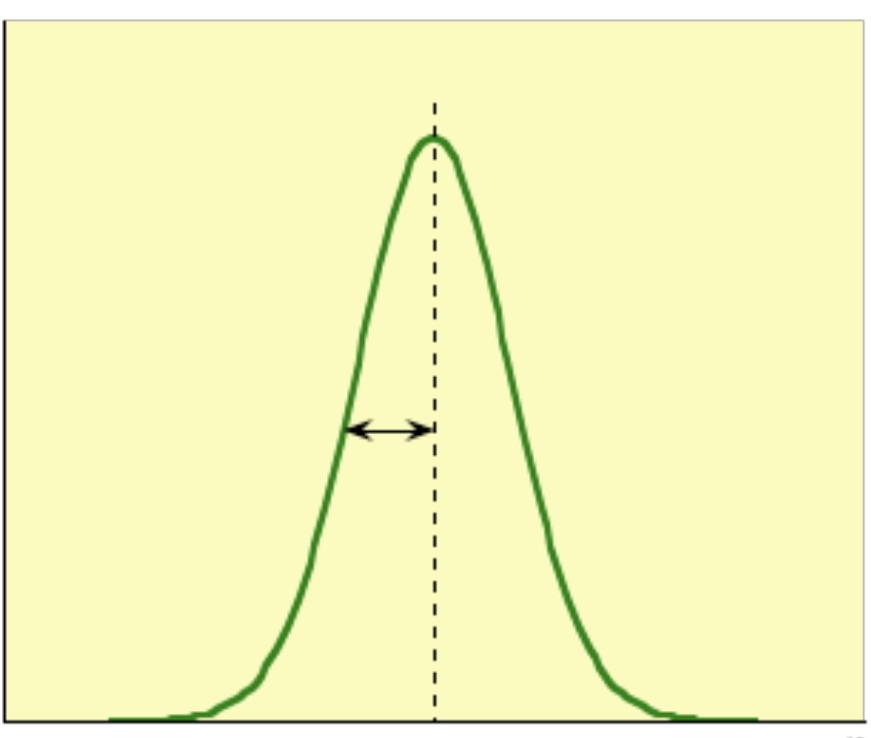


- No peak superposition
- No Multiple Scattering
- F.T. artefacts

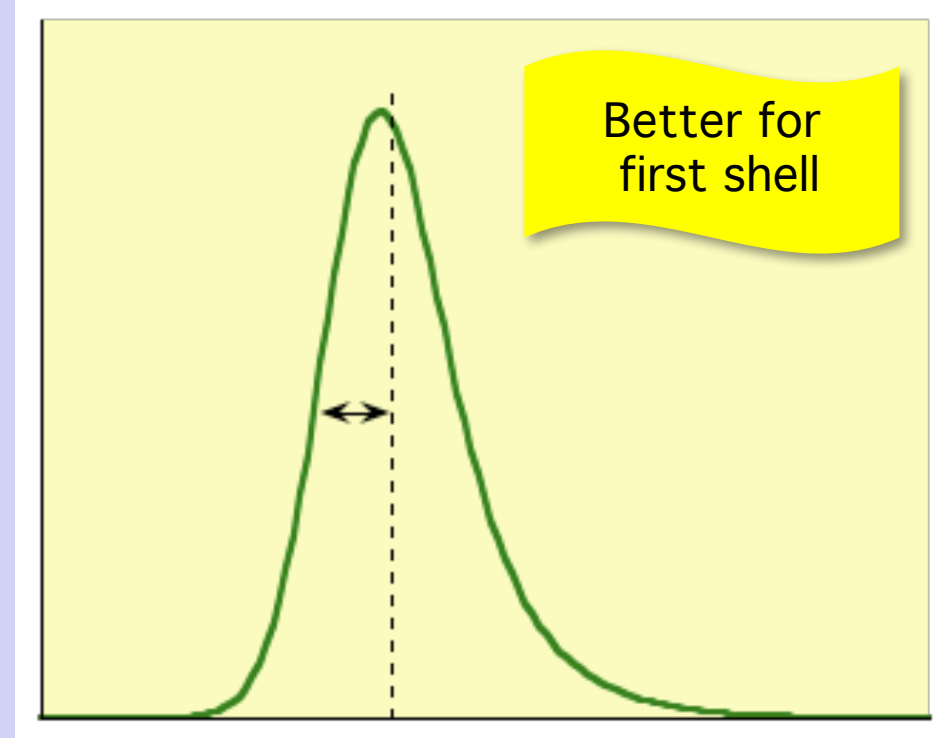


1st-shell distribution of distances

Gaussian approximation



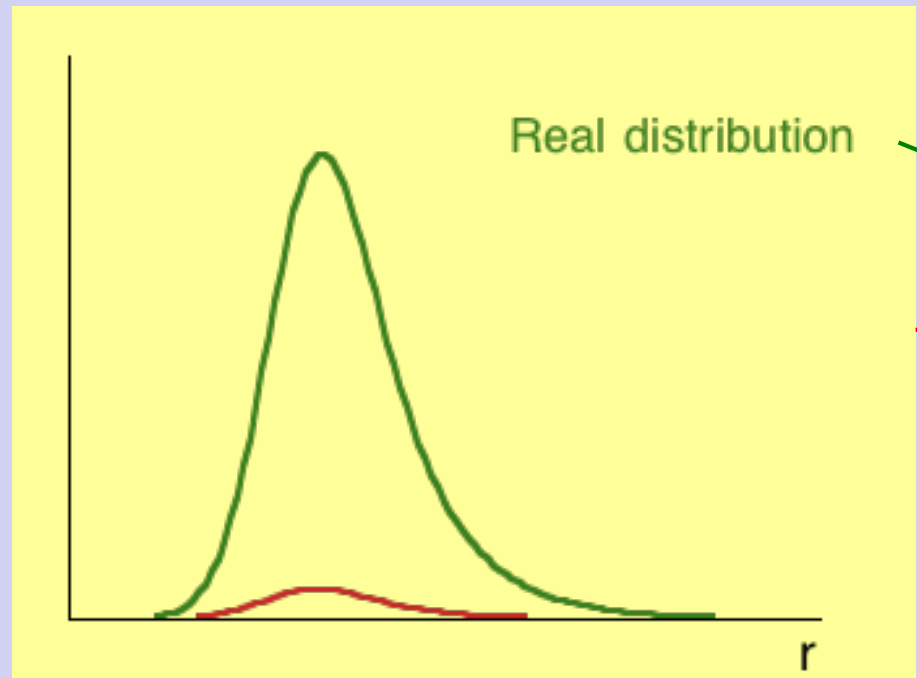
Asymmetric distribution



$$\sigma^2 = \langle (r - \langle r \rangle)^2 \rangle$$

$$C_3 = \langle (r - \langle r \rangle)^3 \rangle$$

Real and effective distributions



$$\rho_s(r) \frac{e^{-2r_s/\lambda(k)}}{r_s^2}$$

$$\langle r \rangle_{\text{eff}} = \langle r \rangle_{\text{real}} - \frac{2\sigma^2}{\langle r \rangle} \left(1 - \frac{\langle r \rangle}{\lambda} \right)$$

$$C_1$$

$$\langle r \rangle$$

EXAFS for first shell, including asymmetry

Approx.: Single Scattering
Plane waves

- Theory (interaction potentials + scattering theory)
- Experiment (reference samples)

Inelastic
terms

Back-scattering
amplitude

Total
phase-shift

$$k \chi(k) = \frac{S_0^2 e^{-2C_1/\lambda}}{C_1^2} |f(k, \pi)| N \exp[-2k^2\sigma^2] \sin\left[2kC_1 - \frac{4}{3}k^3C_3 + \phi(k)\right]$$

Coordination number

N

σ^2

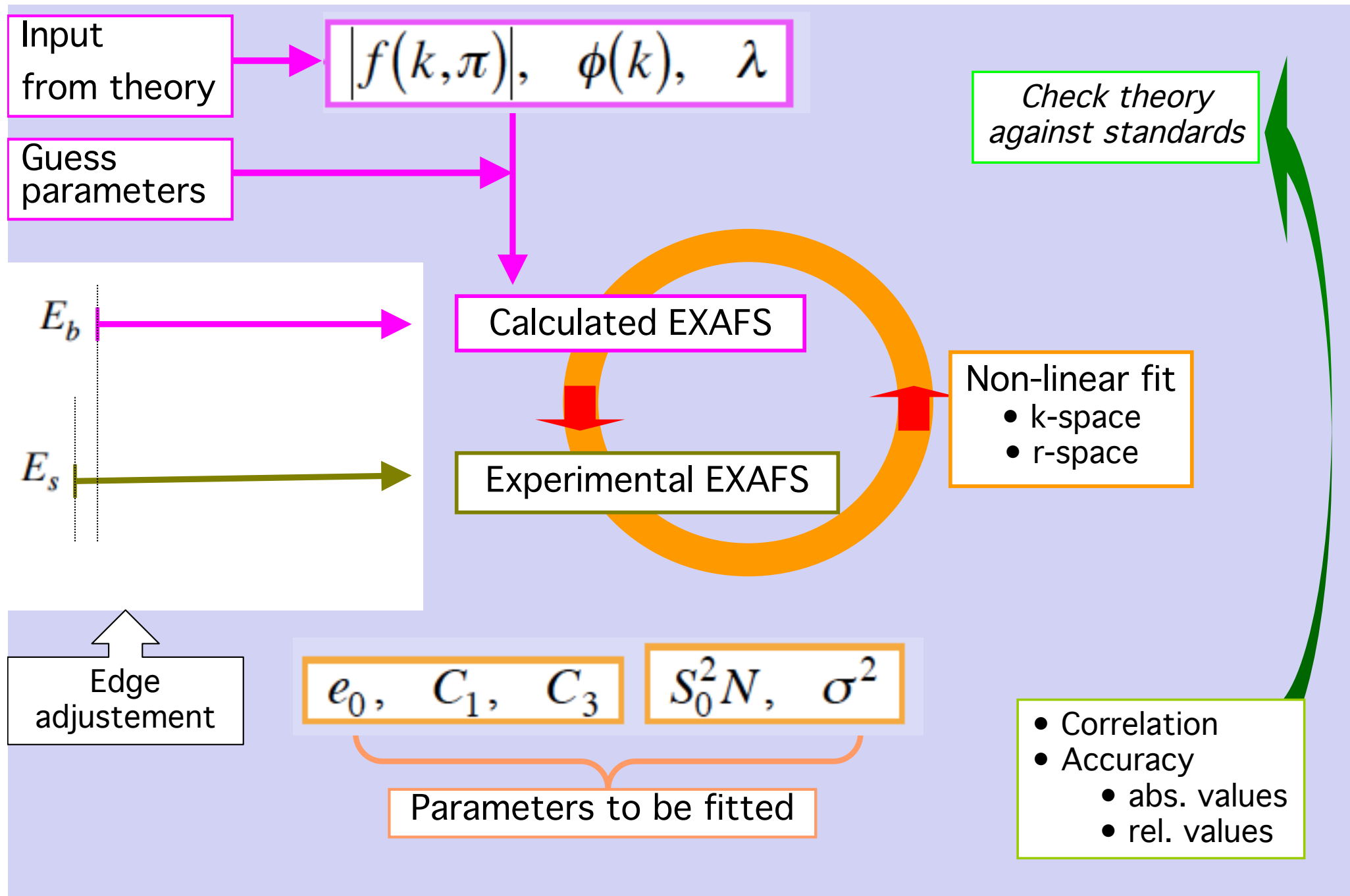
Debye-Waller

Average distance and asymmetry

C_1

C_3

Non-linear fitting method

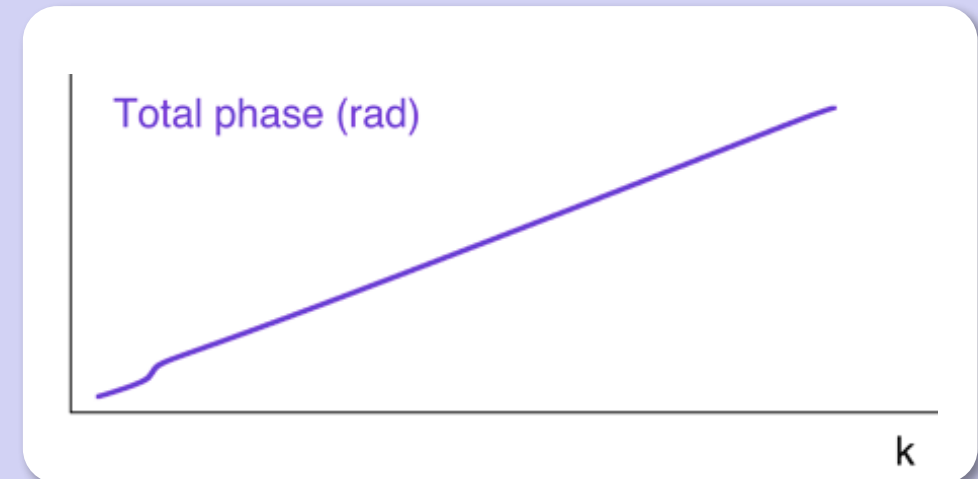
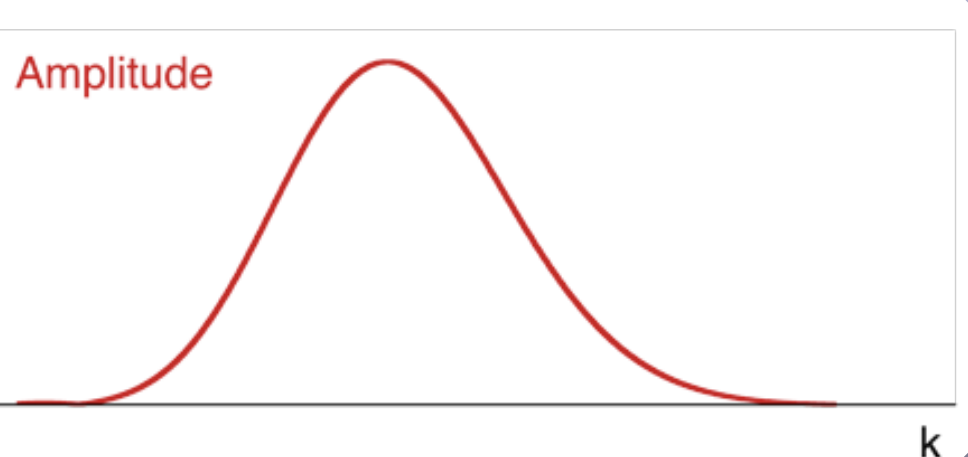


EXAFS data analysis

- ♠ 1st shell phase and amplitude analysis

Separate evaluation of phase and amplitude

From complex Fourier transform and back-transform



$$A(k) = \frac{S_0^2 e^{-2C_1/\lambda}}{C_1^2} |f(k, \pi)| N \exp\left[-2k^2 C_2 + \frac{2}{4} k^4 C_4 + \dots\right]$$



$$\Phi(k) = 2kC_1 - \frac{4}{3}k^3C_3 + \dots + \phi(k)$$



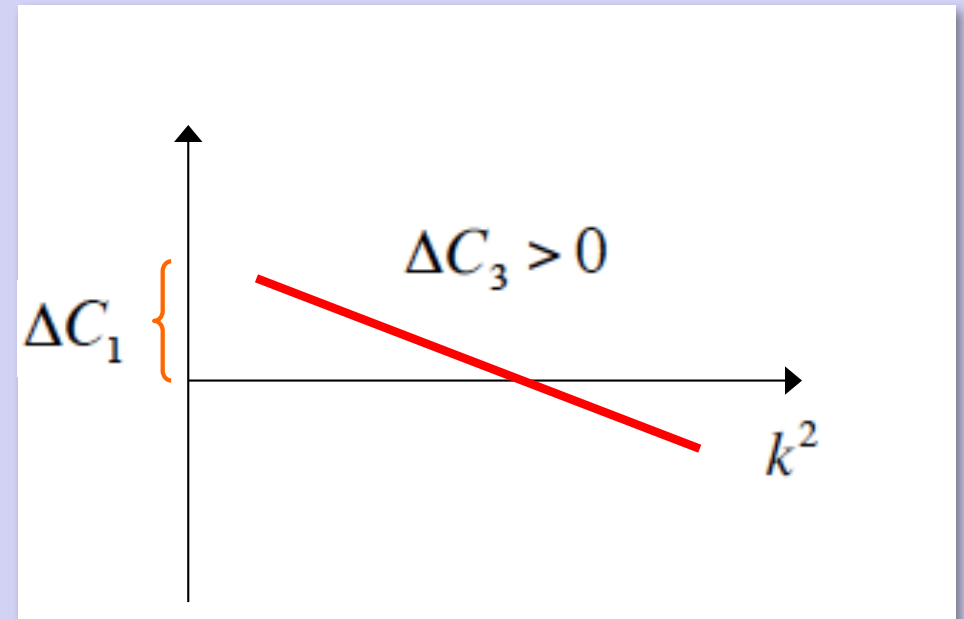
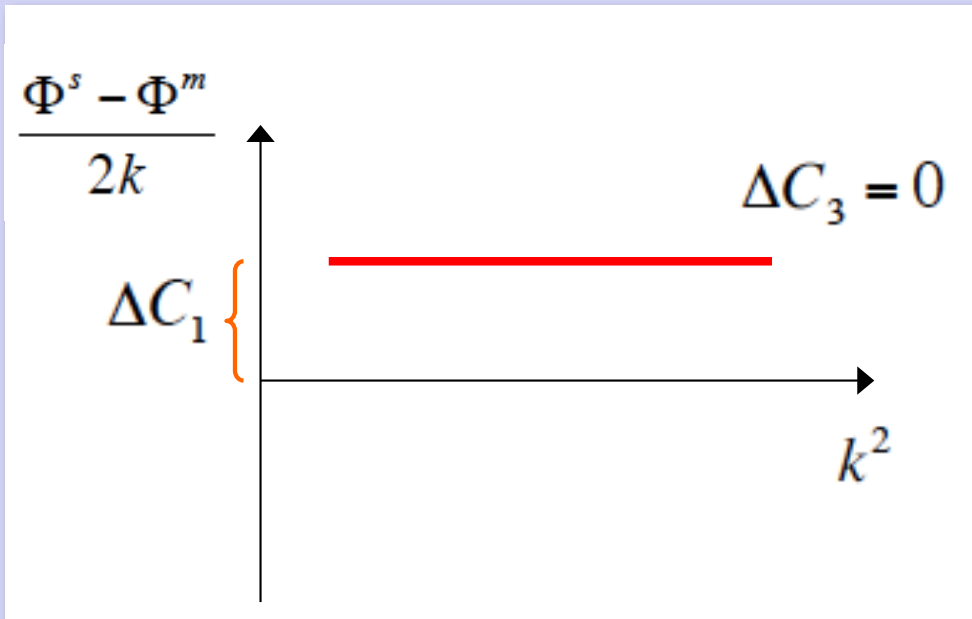
“Ratio method” - phases

If suitable model compound available ...

s = sample
 m = model

$$\Phi^s - \Phi^m = 2k(C_1^s - C_1^m) - \frac{4}{3}k^3(C_3^s - C_3^m)$$

$$\frac{\Phi^s - \Phi^m}{2k} = (C_1^s - C_1^m) - \frac{4}{3}k^2(C_3^s - C_3^m)$$



“Ratio method” – amplitudes – 2 cumulant

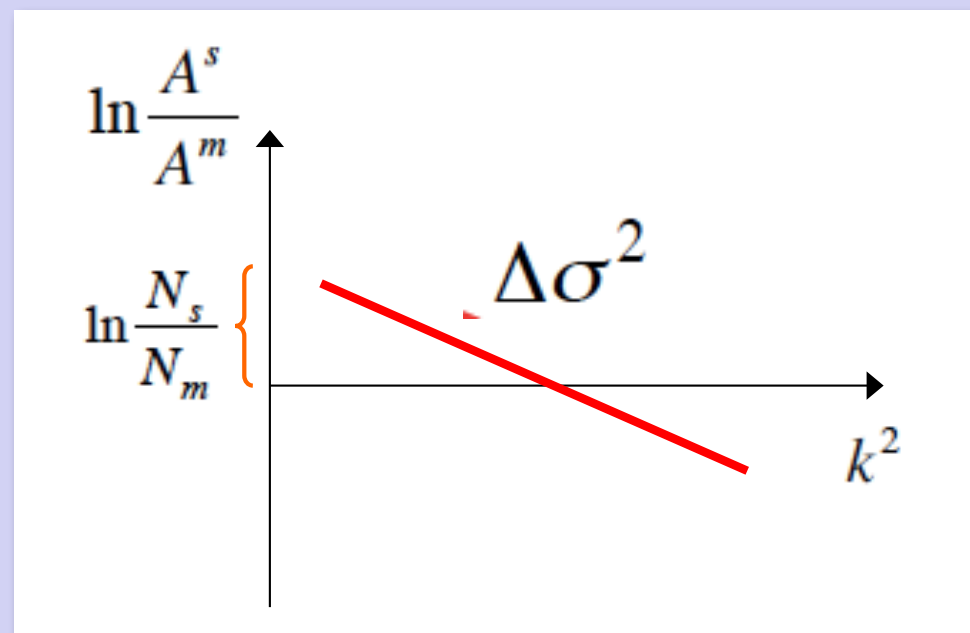
If suitable model compound available ...

s = sample
 m = model

$$\ln \frac{A^s}{A^m} \cong \ln \frac{N^s}{N^m} - 2k^2(\sigma_s^2 - \sigma_m^2)$$

intercept

Slope



“Ratio method” - results

Ratio of coordination numbers

$$\frac{N^s}{N^m}$$

Relative values :

$$\begin{cases} \Delta C_1 \\ \Delta \sigma^2 \\ \Delta C_3 \end{cases}$$

→ Thermal expansion

Width difference

Asymmetry difference

“Ratio method” - OK when ...

- Only Single Scattering
- Only one distance
- Suitable reference model available

$$\chi(k) = A(k) \sin \Phi(k)$$



- First coordination shell, one distance
 - Same sample-model environment
T or p-dep. Studies
Amorphous .vs. crystalline samples



- 1st shell, different sample-model environment
 - Separated outer shells, weak M.S.



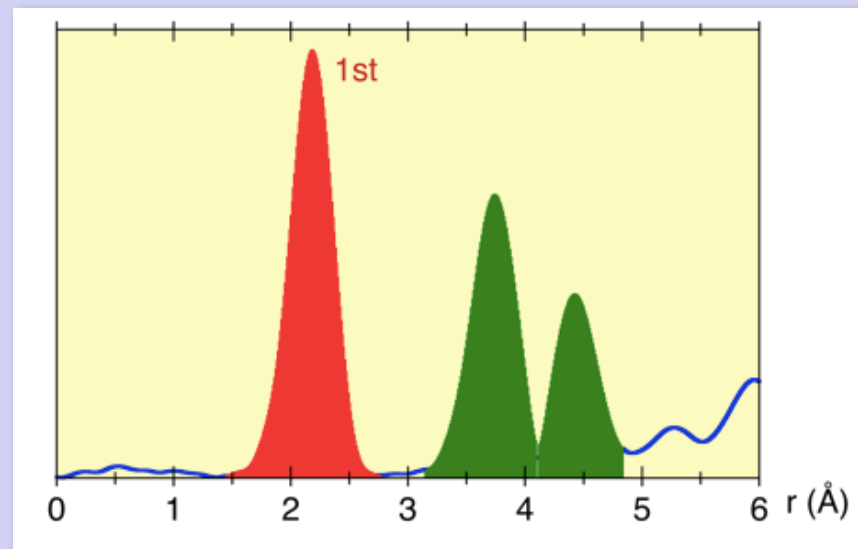
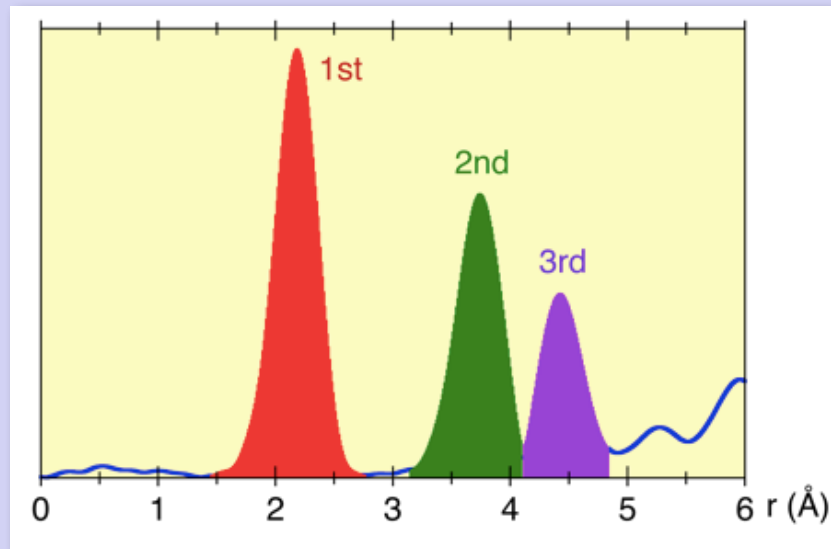
- 1st shell in bcc structure (2 distances)
 - Superposed outer shells
 - M.S. contributions

Depending on
sought accuracy

EXAFS data analysis

- ♠ Outer shells analysis

Analysis - Outer shells back-transform $r \rightarrow k$



$$\chi'(k) = (2/\pi) \int_{r_{min}}^{r_{max}} F(r) W(r) e^{-2ikr} dr$$

2nd shell

3rd shell

Joint analysis

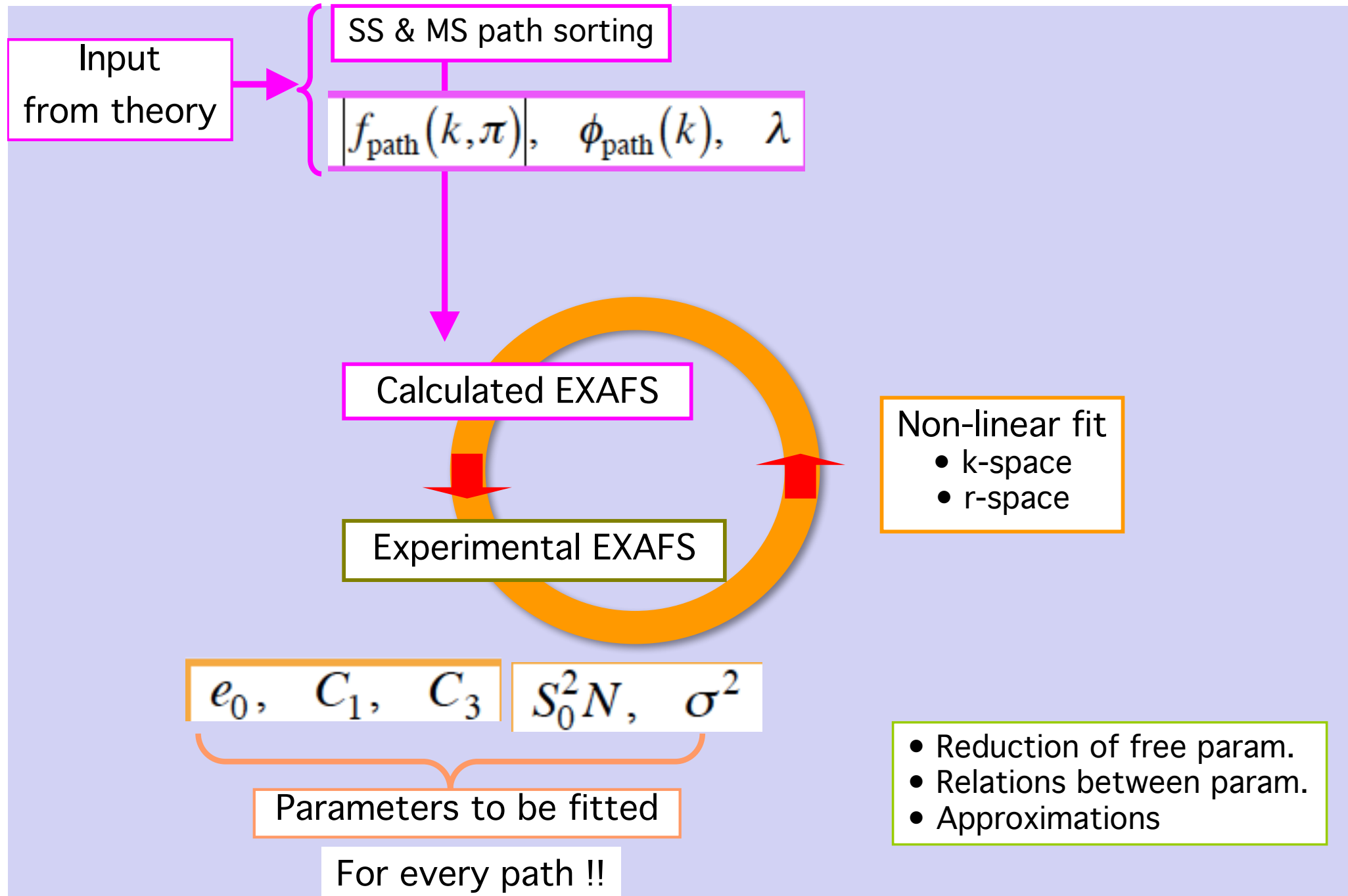


- Peak superposition
- Multiple Scattering
- (F.T. artefacts)

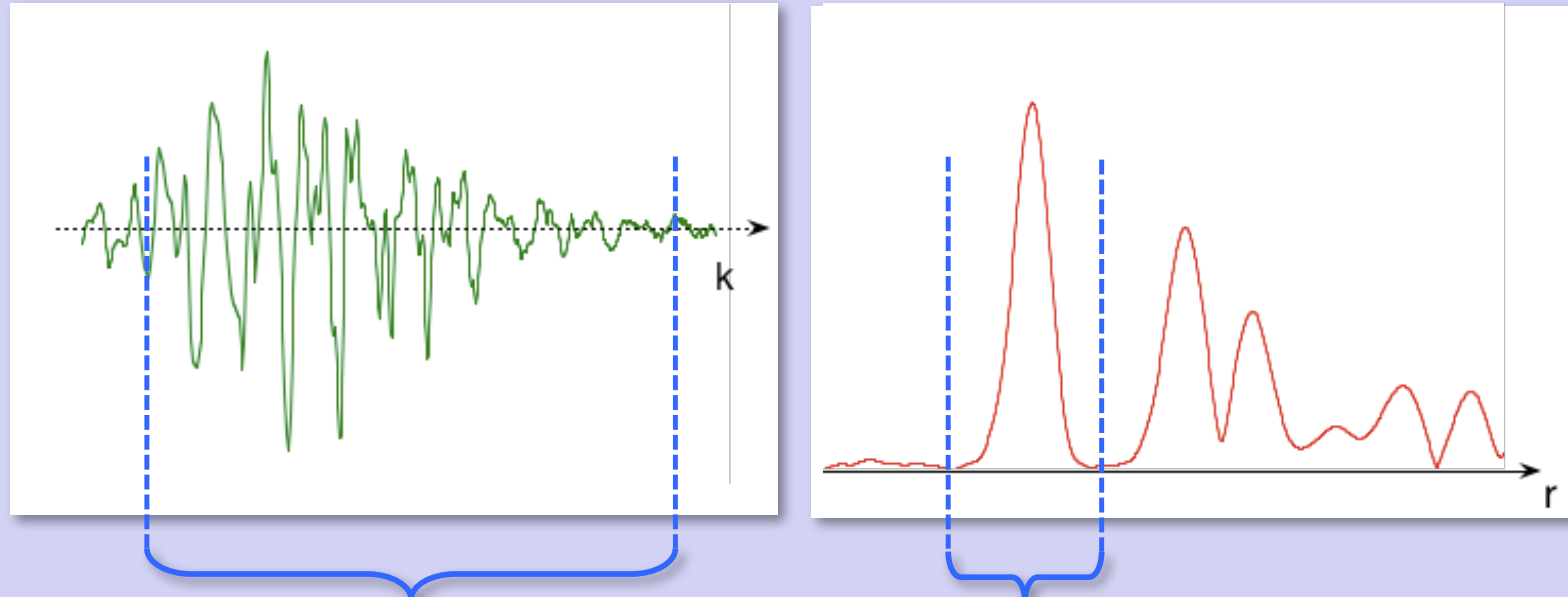


- No superposition problems
- Including M.S.
- (F.T. artefacts)

Analysis - non-linear fitting of outer shells



Analysis – Maximum available information



Δk

Δr

Maximum number
of independent
quantities
from an EXAFS spectrum

$$N_{\text{ind}} = \frac{2 \Delta k \Delta r}{\pi} + 1$$



- Signal quality
- Correlation effects

Analysis – Accuracy evaluation

$$\langle r \rangle = 2.85 \text{ \AA}$$

$$N = 12$$

$$\sigma^2 = 5.34 \times 10^{-3} \text{ \AA}^2$$



$$\langle r \rangle = (2.85 \pm 0.02) \text{ \AA}$$

$$N = 12 \pm 3$$

$$\sigma^2 = (5.34 \pm 0.2) \times 10^{-3} \text{ \AA}^2$$



$$X = X_0 \pm \delta X$$

Uncertainty

Random experimental fluctuations

Estimate of systematic errors

Statistical uncertainties of data analysis



Repeat
measurements !!

Quantitative uncertainty from experiment

Repeated measurements

- Same run, different data files
- Different beamlines, different times
- ...
- Different edges (signal contamination ?)

Indep. data
Gaussian distr.?

Quality of data

Ratio method, highly sensitive

Data analysis

- Background subtraction
- FT windows
- Fitting intervals
-

Non-indep.
data
Uniform distr.?

Definition
of phys. quantities

- Average .vs. crystallographic distance
- Debye temperature
-

Systematic errors

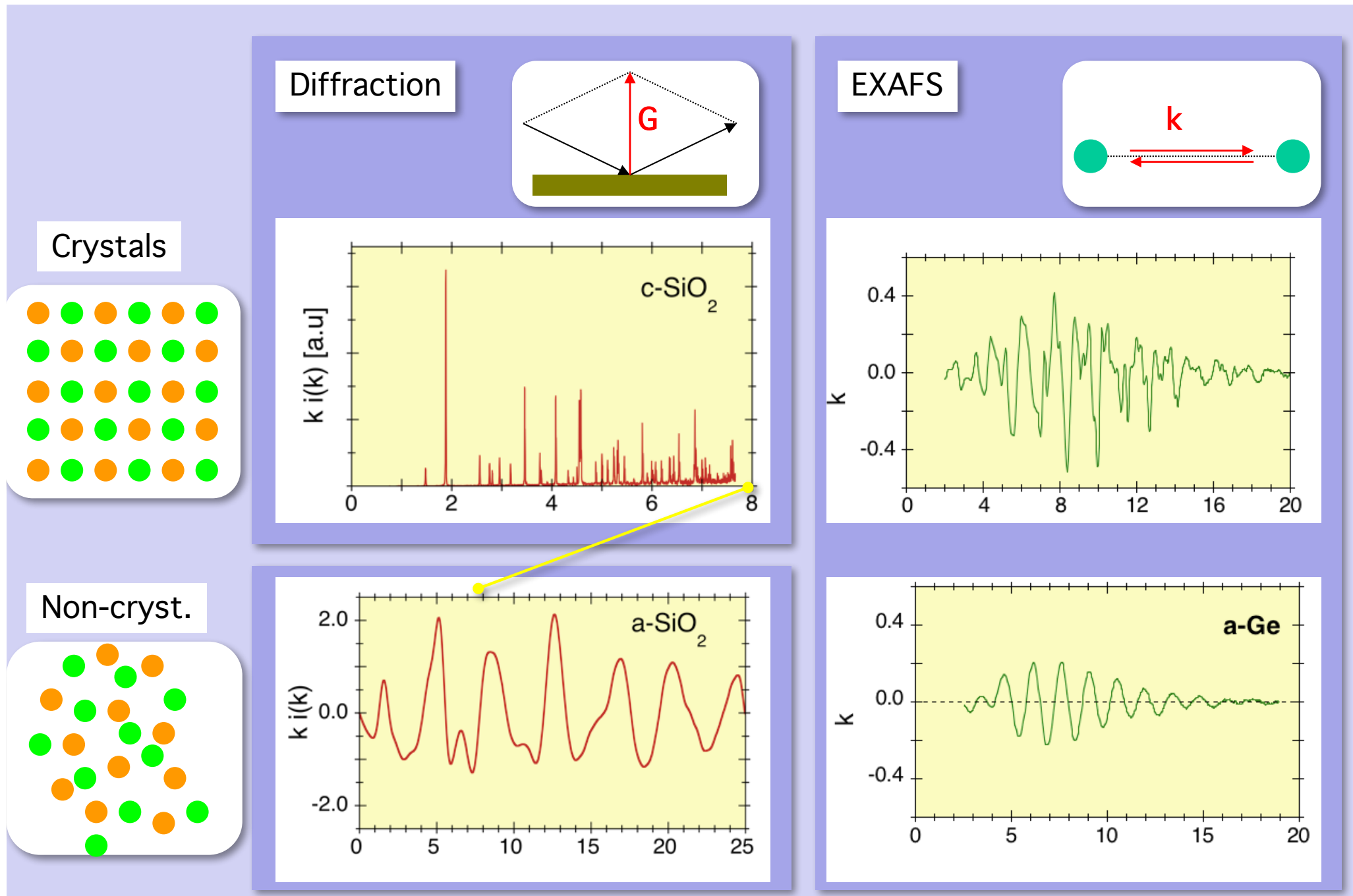
??

EXAFS data analysis

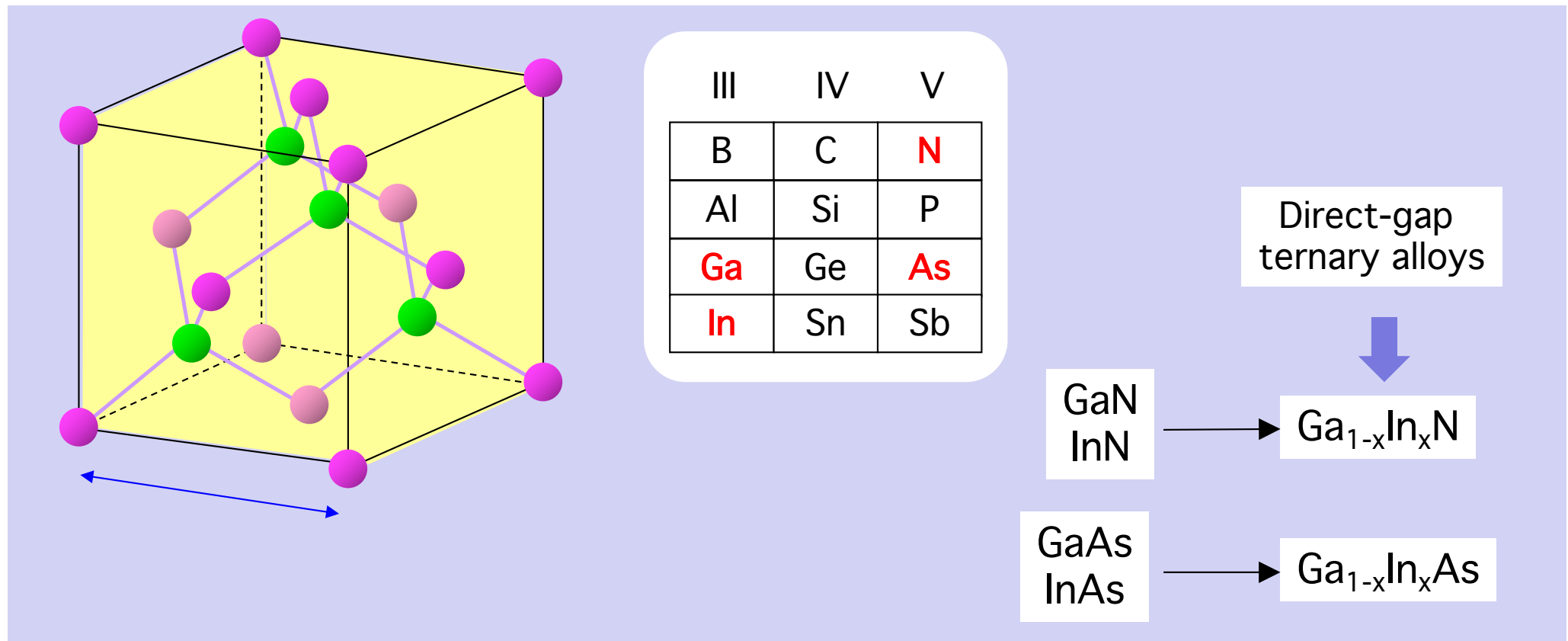
- ♠ Examples and interpretation of results

(comparison EXAFS-XRD)

Diffraction .vs. EXAFS



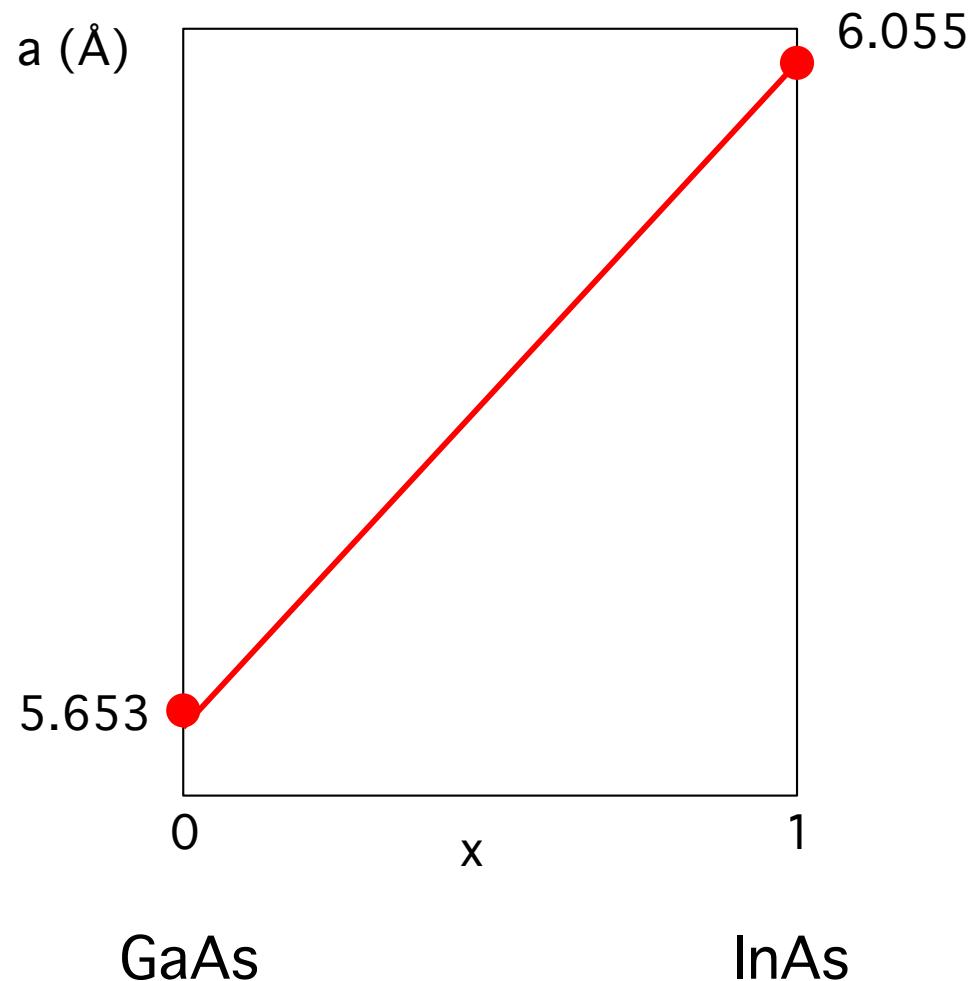
Random solid solutions (a)



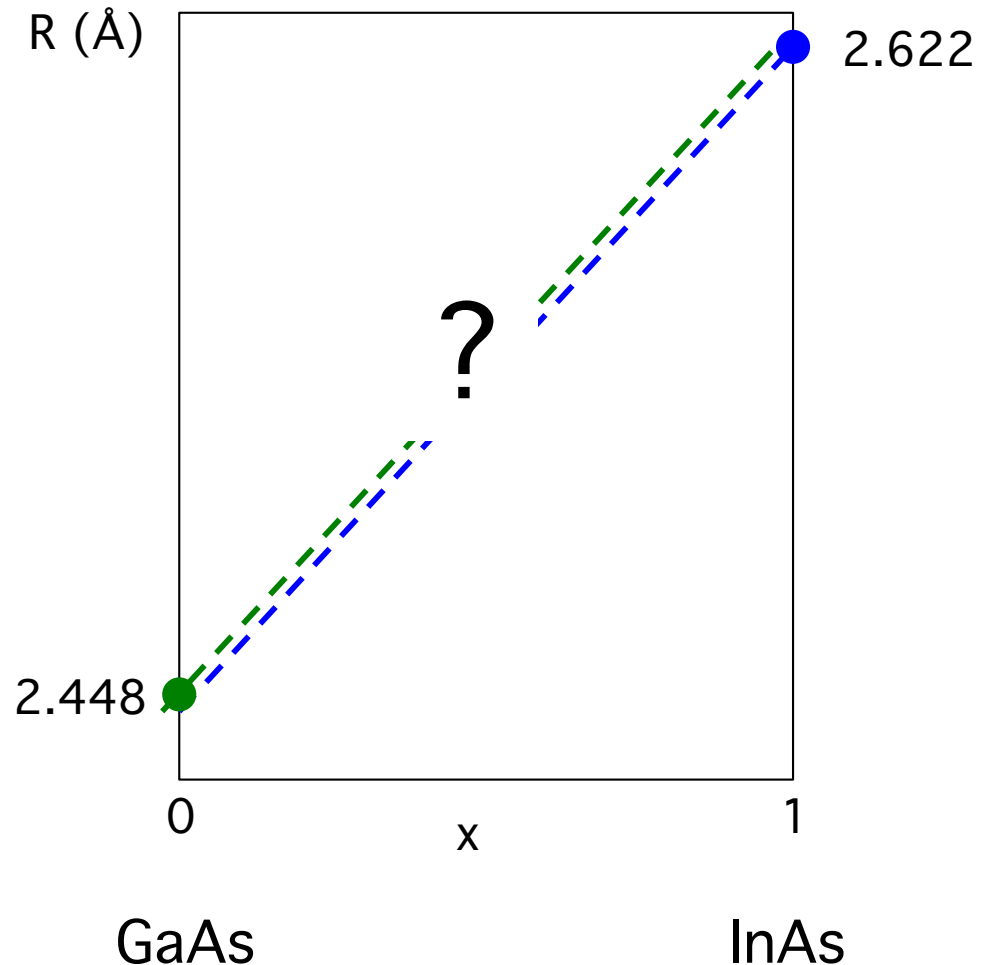
Lattice parameter (XRD)	a (Å)	GaAs	$\text{In}_x\text{Ga}_{1-x}\text{As}$	InAs
N-N distance (EXAFS)	r (Å)	5.653	6.055	6.055
Energy gap	E_g (eV)	2.448	2.622	2.622
		1.43	0.36	0.36

Random solid solutions (b)

Lattice parameter (from XRD)
Vegard's law

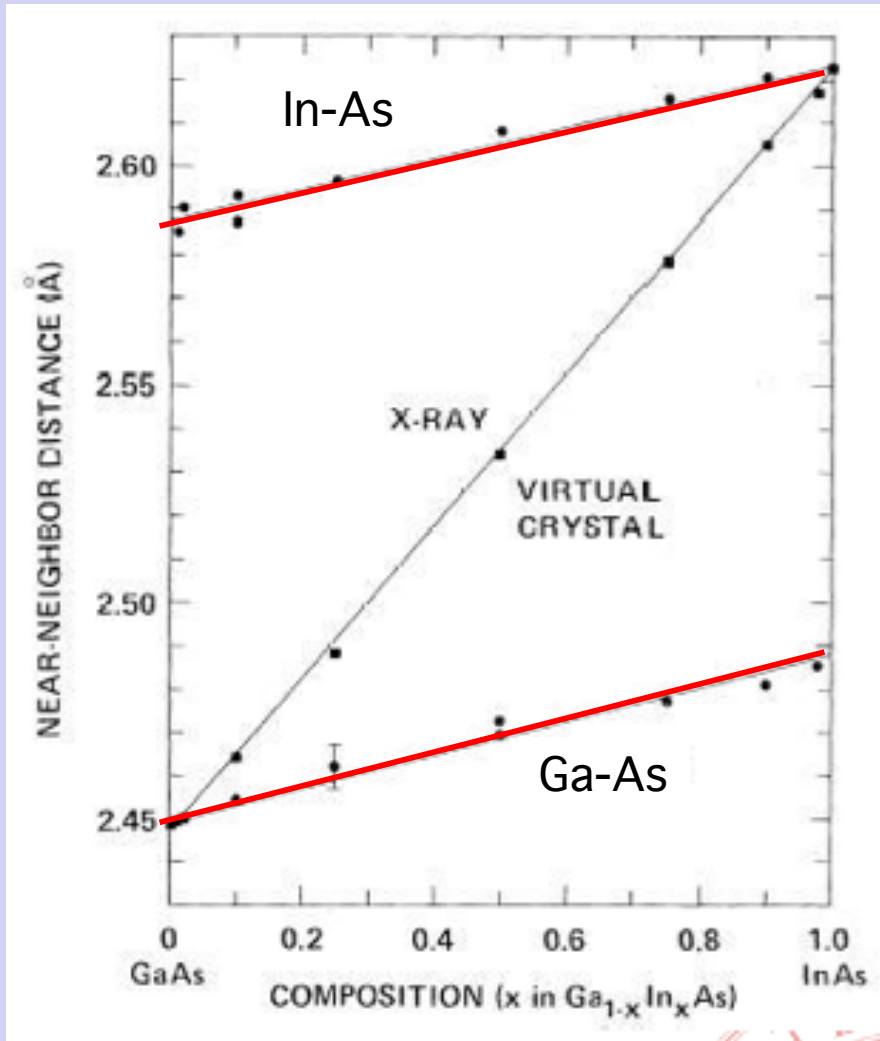


N-N distance
Virtual crystal approximation



Random solid solutions (c)

EXAFS: selectivity of atomic species



In K edge, 4 As NN

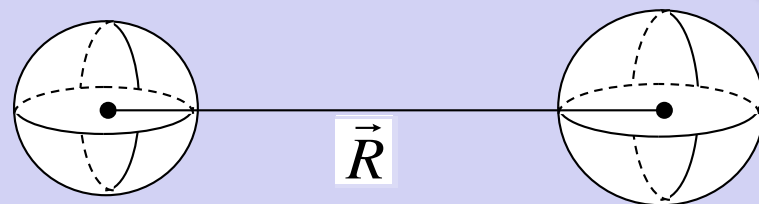
EXAFS results
for Nearest-Neighbours

Ga K edge, 4 As NN

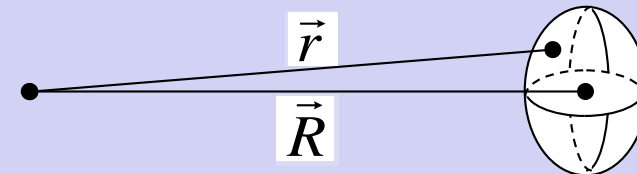
Distortion
of the virtual crystal

Effects of thermal vibrations in crystals

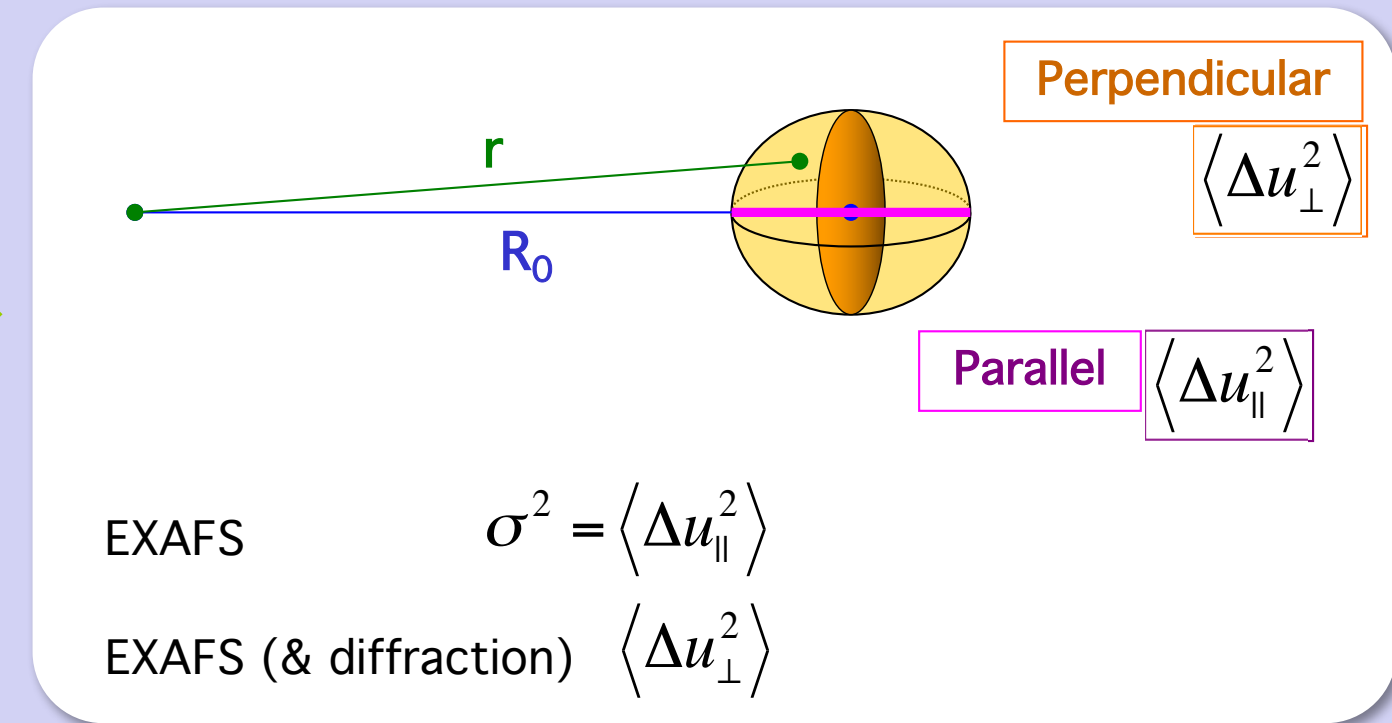
XRD → atomic thermal ellipsoids



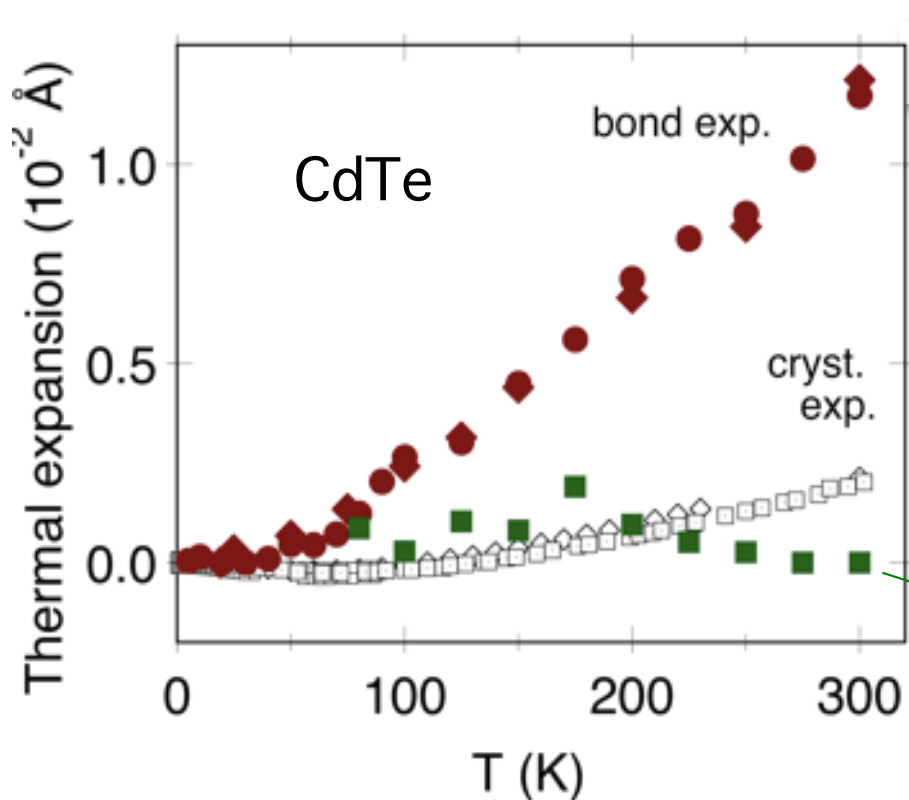
EXAFS → relative thermal ellipsoids



Relative
vibrations:
MSRDs



Bond distances in crystals



EXAFS

XRD

$$\langle \mathbf{r} \rangle = \left\langle \left| \vec{\mathbf{r}}_b - \vec{\mathbf{r}}_a \right| \right\rangle$$

$$\langle \mathbf{r} \rangle \approx R + \frac{\langle \Delta u_{\perp}^2 \rangle}{2R}$$

$$R = \left| \langle \vec{\mathbf{r}}_b \rangle - \langle \vec{\mathbf{r}}_a \rangle \right|$$

EXAFS
neglecting 3rd cumulant

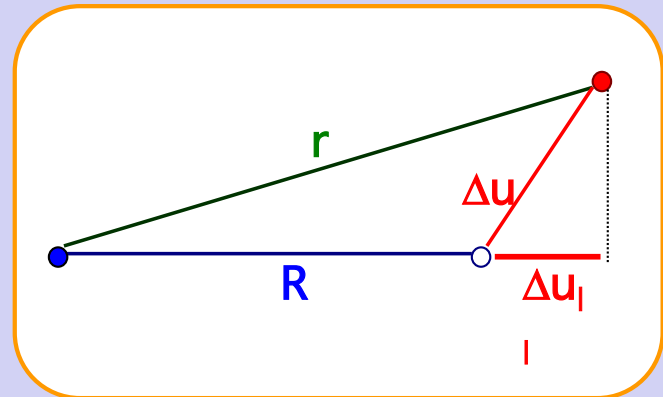
Difference (Å)

T (K)	Cu	Ge	CdTe
5	1.3×10^{-3}	1.5×10^{-3}	1×10^{-3}
300	4×10^{-3}	8×10^{-3}	11×10^{-3}

EXAFS Debye-Waller factor

Paolo
Fornasini
Univ. Trento

$$\begin{aligned}\sigma^2 \approx MSRD &= \langle \Delta u_{\parallel}^2 \rangle = \left\langle [\hat{R} \cdot (\vec{u}_b - \vec{u}_a)]^2 \right\rangle \\ &= \left\langle (\hat{R} \cdot \vec{u}_b)^2 \right\rangle + \left\langle (\hat{R} \cdot \vec{u}_a)^2 \right\rangle - 2 \left\langle (\hat{R} \cdot \vec{u}_b)(\hat{R} \cdot \vec{u}_a) \right\rangle\end{aligned}$$



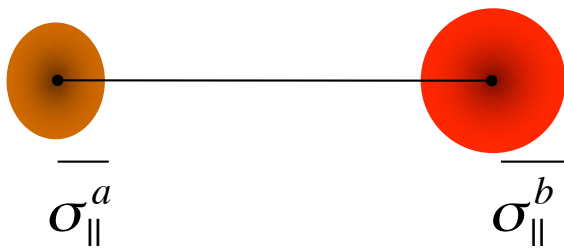
MSD
Mean Square
Displacements

DCF
Displacement
Correlation Function

Thermal factors from Bragg diffraction:

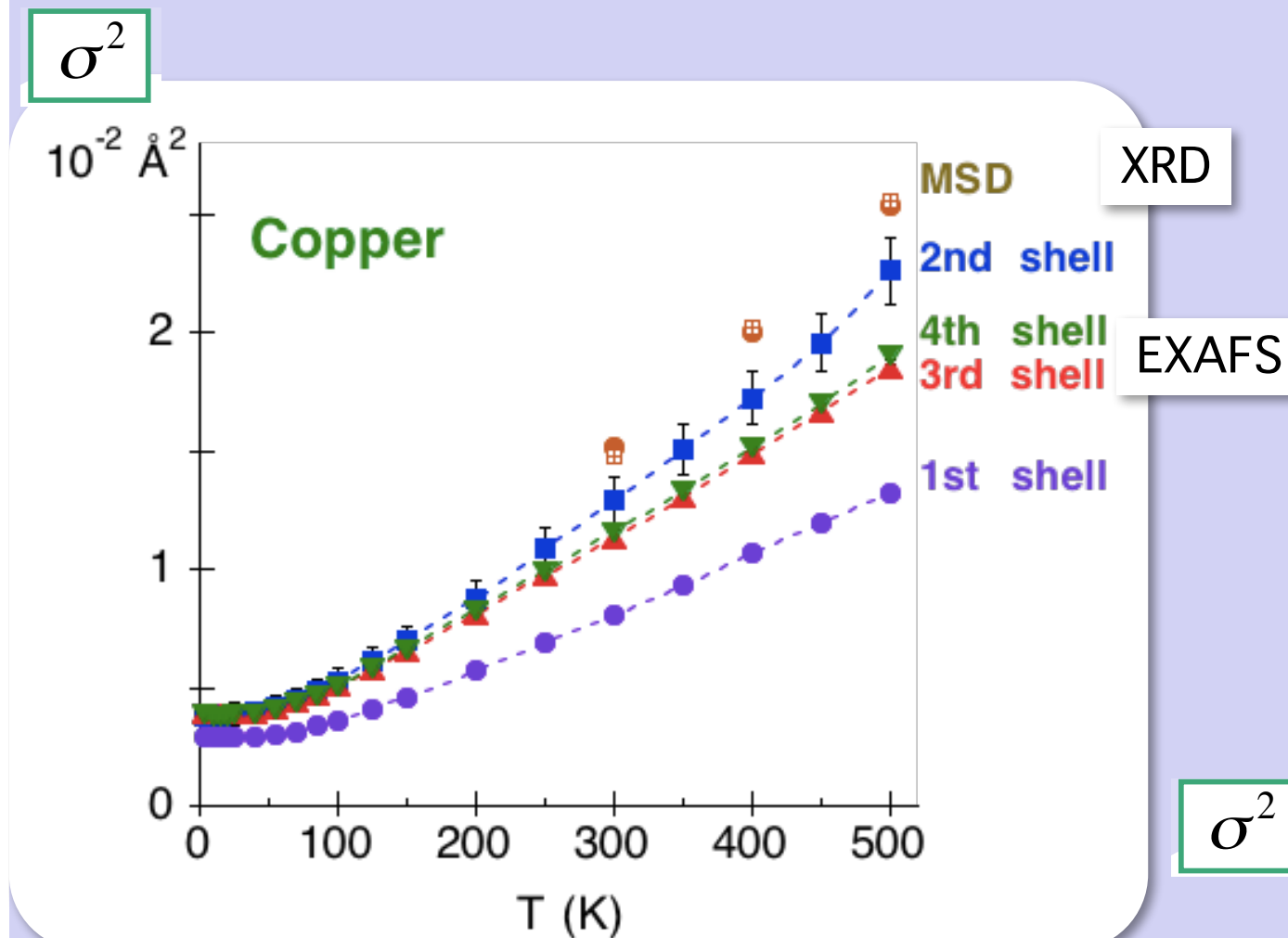
$$U_{\parallel}^a = \left\langle (\hat{R} \cdot \vec{u}_a)^2 \right\rangle = (\sigma_{\parallel}^a)^2$$

$$U_{\parallel}^b = \left\langle (\hat{R} \cdot \vec{u}_b)^2 \right\rangle = (\sigma_{\parallel}^b)^2$$



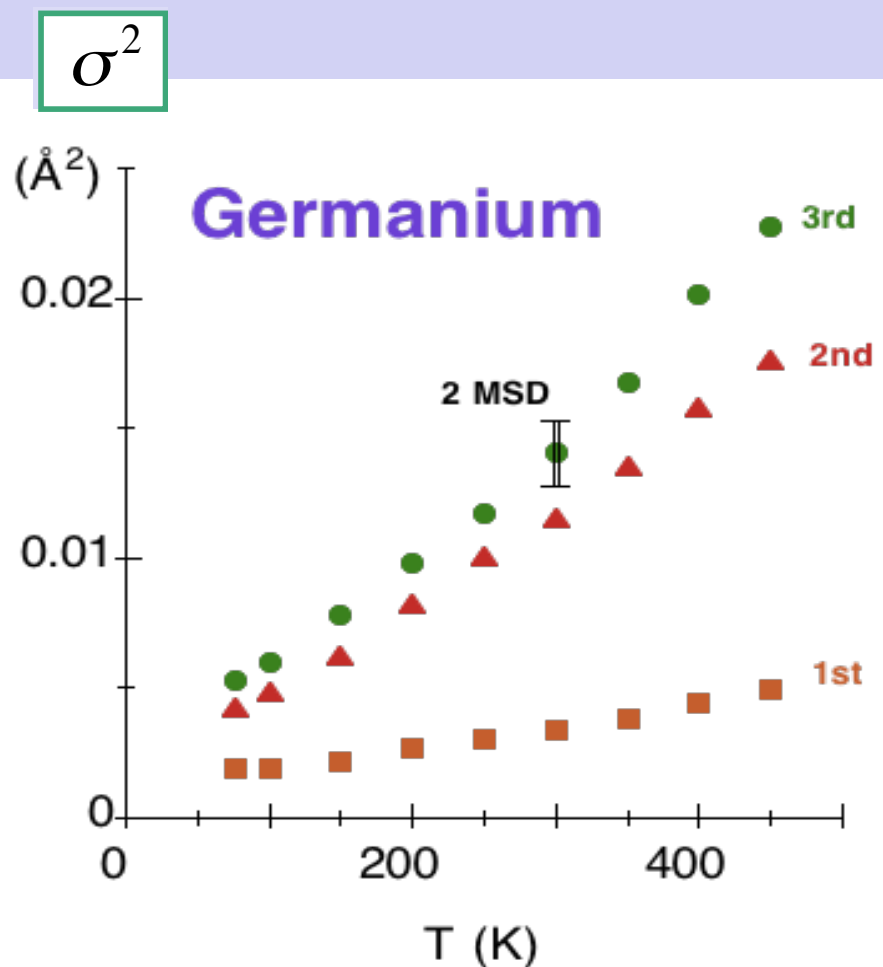
Debye-Waller factor – Debye model

$$\sigma^2 = \frac{3\hbar}{2\omega_D^3 \mu} \int_0^{\omega_D} \omega \coth \frac{\hbar\omega}{2k_B T} \left[1 - \frac{\sin(\omega q_D R)}{\omega q_D R} \right] d\omega$$



Debye-Waller factor – Einstein model

$$\sigma^2 = \frac{\hbar}{2\mu\omega_E} \coth\left(\frac{\hbar\omega_E}{2kT}\right)$$



Non-Bravais crystal

Debye temperatures

$$\begin{aligned}\theta_D &= 354 \text{ K} \\ \theta_M &= 290 \text{ K} \\ \theta_3 &= 290 \text{ K} \\ \theta_2 &= 299 \text{ K} \\ \theta_1 &= 460 \text{ K}\end{aligned}$$

Einstein frequency force const.

$$\begin{aligned}\nu &= \omega/2\pi & k &= \mu\omega^2 \\ & (\text{THz}) & & (\text{eV}/\text{\AA}^2) \\ \nu_3 &= 3.95 & k_3 &= 2.18 \\ \nu_2 &= 4.21 & k_2 &= 2.48 \\ \nu_1 &= 7.55 & k_1 &= 8.15\end{aligned}$$

The end



Basic bibliography

- G.S. Brown and S. Doniach: *The principles of X-ray Absorption Spectroscopy*, in *Synchrotron Radiation research*, ed. by E. Winick and S. Doniach, Plenum (New York, 1980) [A general introduction to X-Ray absorption]
- P.A. Lee, P.H. Citrin, P. Eisenberger, and B.M. Kincaid, Rev. Mod. Phys. 53, 769 (1981) [Review paper on EXAFS]
- T.M. Hayes and J. B. Boyce, Solid State Physics 27, 173 (1982) [Review paper on EXAFS]
- B.K. Teo: *EXAFS, basic principles and data analysis*, Springer (Berlin, 1986) [Introductory book on EXAFS]
- D.C. Koningsberger and R. Prins eds.: *X-ray Absorption: principles and application techniques of EXAFS, SEXAFS and XANES*, J. Wiley (New York, 1988) [Introductory book on XAFS]
- M. Benfatto, C.R. Natoli, and A. Filippioni, Phys. Rev. B 40, 926 (1989) [Paper on multiple scattering calculations]
- J. Stöhr: *NEXAFS spectroscopy*, Springer (Berlin, 1996) [Book on XANES]
- J.J. Rehr and R.C. Albers, Rev. Mod. Phys. 72, 621 (2000) [Review paper on EXAFS]
- P. Fornasini, J. Phys.: Condens. Matter 13, 7859 (2001) [EXAFS and lattice dynamics]
- G. Bunker: *Introduction to XAFS*, Cambridge U.P. (2010) [Introductory book on XAFS]
- S. Kalvin: *EXAFS for everyone*, CRC Press (2013) [Handbook for experimentalists]
- J.A.van Bokhoven and C. Lamberti eds.: *X-ray absorption and X-ray emission spectroscopy: theory and applications*, Wiley (2016)